NTNU
Norwegian University of
Science and Technology

Muhammad Umar Khan

2022

Master's thesis

NTNU
Norwegian University of
Science and Technology
Faculty of Engineering
Department of Energy and Process Engineering

Master's thesis

Muhammad Umar Khan

Design and analysis of freeze concentrator for processing of fish protein hydrolysates

June 2022

NTNU
Norwegian University of
Science and Technology

NTNU
Norwegian University of
Science and Technology

Design and analysis of freeze concentrator for processing of fish protein hydrolysates

Muhammad Umar Khan

Sustainable Energy (Heat pumping process and system)
Submission date: June 2022
Supervisor: Armin Hafner
Co-supervisor: Ignat Tolstorebrov

Norwegian University of Science and Technology
Department of Energy and Process Engineering

Preface

This report summarizes my master's thesis work during the spring semester 2022 at the Norwegian university of science and technology, Department of Energy and Process Engineering. The project work is in collaboration with SINTEF ocean. The topic of this project is unique and formulated on the challenges of hydrolysation process and drying process especially freeze concentration process.

I warmly express my gratitude and wishes to Professor Dr. Armin Hafner and Dr. Ignat Tolstorebrov for their guidance and encouragement. Working with my these experienced and learned professors have been a steep learning curve for me. They polished my research skills and provided me an opportunity to do my thesis project practically in labs with full results. Thanks to Muhammad Zahid Saeed for his assistance and technical support in regards with Dymola software.

Finally, I deeply extend my thanks and gratitude to my parents for their prayers and full support throughout my thesis writing.

Summary

Efficient utilization of rest raw materials from fish processing (RRM) is a significant challenge for the fish processing industry. This will increase the level of sustainability for food production. One of the ways of RRMs utilization is the processing towards fish protein hydrolysates with subsequent production of food-grade powders. Drying of raw fish protein hydrolysates (FPH) is energy intensive process. The energy demand for industrial spray drying is 3183 kJ/kg, when drying FPH with solid content of 7%. The more energy efficient way to dewater fish protein hydrolysates is freeze concentration, which provide high quality of concentrate, energy efficiency (60% energy saving) and sustainability of the hydrolysate production.

The aim of this work was to develop simulations and lab scale setup for freeze concentration process for fish protein hydrolysates. The study investigates the important aspects which includes the crystallization of water in fish protein hydrolysates, dynamic refrigeration load during crystallization and separation of the ice from concentrate. The processes were modelled using Modelica tools, Engineering equation solver (EES) and MATLAB. The models were validated via experiments and literature review. The influence of the given factors was considered which includes refrigeration temperature, fluid flow, concentration of solids and ice fraction.

Results include the process of hydrolysation for 1 ton rest raw material, the dynamic modelling of batch and steady state freeze concentration process and wash column. Results contains the dynamic simulations of trans-critical CO_2 refrigeration system for batch and steady state process with COP of 1.37. Refrigeration system was able to maintain the evaporation temperature of - 40℃ while heating the hydrolysates through gas coolers to 50℃ and 90℃. Heat was recovered by melting ice from desuperheater and storing the sensible heat released by hydrolysates when cooled down to 4℃. Economic analysis was carried out to check the profitably of the project. Life cycle of project is 15 years which includes the payback time of 2 years and 8 months.

Sammendrag

Effektiv utnyttelse av restråstoff fra fiskeforedling (RRM) er en betydelig utfordring for fiskeforedlingsindustrien, og vil bidra til å øke bærekraftsnivået for matproduksjon av fisk. En av måtene å bruke RRM på er prosessering av fiskeproteinhydrolysater (FPH) med påfølgende produksjon av matvarepulver. Tørking av rå FPH er en energikrevende prosess. Energibehovet for industriell spraytørking er 3183 kJ/kg, ved tørking av FPH med faststoffinnhold på 7 %. Den mer energieffektive måten å avvanne FPH på er frysekonsentrasjon, som gir høy kvalitet på konsentrat, energieffektivitet (60 % energisparing) og bærekraftig hydrolysatproduksjon.

Målet med dette arbeidet var å utvikle simuleringer og laboratorieskalaoppsett for frysekonsentrasjonsprosessen for FPH. Studien undersøker viktige aspekter som inkluderer krystallisering av vann i FPH, dynamisk kjølebelastning under krystallisering og separasjon av isen fra konsentratet. Prosessene ble modellert ved hjelp av Modelica-verktøy, Engineering equation solver (EES) og MATLAB. Modellene ble validert via eksperimenter og litteraturstudie. Påvirkningen av faktorer som ble vurdert inkluderer kjøletemperatur, væskestrøm, konsentrasjon av faste stoffer og is fraksjon. Resultatene inkluderer prosessen med hydrolysering for 1 tonn restråmateriale, dynamisk modellering av batch- og steady state frysekonsentrasjonsprosess og is-separeringskolonnen.

Resultatene inneholder dynamiske simuleringer av transkritisk CO_2-kjølesystem for batch- og steady state-prosesser med COP på 1,37. Kjølesystemet var i stand til å opprettholde fordampningstemperaturen på -40 ℃ mens hydrolysatet varmes opp gjennom gasskjølere fra 50 ℃ til 90 ℃. Varme ble gjenvunnet ved å smelte is fra de-superheater og benytte varmen frigjort av hydrolysater når den ble avkjølt til 4 ℃. Økonomisk analyse ble utført for å sjekke lønnsomheten til prosjektet. Prosjektets livssyklus er 15 år som inkluderer tilbakebetalingstid på 2 år og 8 måneder.

Table of Contents

List of Tables

List of Figures

Abbreviations and Symbols

HCFC	Hydrochlorofluorocarbon
HFC	Hydrofluorocarbon
GWP	Global warming potential
HT	High temperature
LT	Low temperature
PH	Pressure enthalpy
TH	Temperature enthalpy
COP	Coefficient of performance
COP_{COM}	COP combine
COP_{Cac}	COP Carnot cooling
COP_{Cah}	COP Carnot heating
HTC	High temperature circuit
LTC	Low temperature circuit
REF	Refrigeration
Ph	Pressure enthalpy
Ts	Temperature entropy
VHC	Volumetric heating capacity
VRC	Volumetric cooling capacity
HX	Heat exchanger
η_{is}	Isentropic efficiency
Q_o	Evaporator load
Q_c	Condenser load
a	Exponent in ice growth equation
a_i	Activity of component i
b	Exponent in nucleation equation
c	Concentration
c_b	Bulk Temperature of solute
$(dc/dt)_{eq}$	Slope of phase diagram
d_e	Effective crystal diameter
D	Diffusion Coefficient

G	Gibbs free energy (Jenkelunas & Li-Chan)
k_g	Growth rate constant
k_n	Nucleation constant
L	Characteristic length
m	mass (kg)
R	Universal gas constant (J/mol.k)
T	Temperature (K or ℃)
T_b	Bulk temperature (K or ℃)
T_{fp}	Freezing point of solution (K or ℃)
T_∞	Surface Temperature of evaporator tube
U	Total heat transfer coefficient (W/m^2k)
v_{ice}	Ice velocity (linear ice growth rate) (m/s)
V	Volume (m^3)
V_{ice}	Molar volume of Ice (mol/m^3)
w_{ice}	Molar fraction of ice (m/s)
x	Mole fraction
α	Heat transfer coefficient (W/m^2k)
β	Mass transfer coefficient (m/s)
$\Delta_f H$	Heat of freezing (J/mol)
ΔT_b	Bulk total supercooling (K or ℃)
λ_{ice}	Thermal conductivity of ice (W/m.k)
λ	Thermal conductivity of solution (W/m.k)
μ_i	Chemical potential of component i (J/mol)
μ	Dynamic viscosity (kg/m.s)
ρ	Density (kg/m^3)
σ	Surface tension for ice particles in solution (J/m^2)
A_c	''Open'' cross-sectional area of the wash column (m^2)
B	Permeability (m^2)
C_l	Solidification rate at the wash front (wash liquid) (m^3/s)
C_s	Solidification rate at the wash front (solid) (m^3/s)
Cp	Specific heat capacity (kJ/kg.K)

ΔH_m	Heat of fusion (kJ/kg)
$L_{filtrations}$	Length of the filtration section (m)
L_{washs}	Length of the wash section (m)
L_{beds}	Total length of crystal bed (m)
v_l	Liquid velocity (m/s)
v_s	Solid velocity (m/s)
α_1	Crystal fraction in the feed slurry (m^3/m^3)
α_2	Crystal fraction in the slurry section (m^3/m^3)
ε	Porosity in the filtration and stagnant section
ε_w	Porosity in the wash section
η_l	Viscosity (Pa s)
$Ø_{feeds}$	Feed flow (m^3/s)
$Ø_{ml,\ filters}$	Mother liquor flow at the filters from top section (m^3/s)
$Ø_{ml,\ bottoms}$	Mother liquor flow at the filters from bottom, (m^3/s)
$Ø_{products}$	Product flow, (m^3/s)
$Ø_{residues}$	Residue flow, (m^3/s)
$Ø_{s,\ filters}$	Crystal flow at the filters, (m^3/s)
$Ø_{s\ knife}$	Crystal flow at the knife, (m^3/s)
$Ø_{steer}$	Steering flow, (m^3/s)
$Ø_{wl\ knife}$	Wash liquid flow at the knife, (m^3/s)
ρ_L	Density of the liquid (kg/m^3)
ρ_S	Density of the solid (kg/m^3)

Subscripts

cr	Crystals
top	Top section
slurry	Slurry section
filtrations	Filtration section
wash	Wash section
stagnant	Stagnant zone
filters	At the filters
eq	equilibrium

w	water
i	Interface between ice and solution
ice	Ice
l	Liquid
s	Solid
b	Bulk

Chapter 1

1 Introduction

Fish and marine products are one of the most used protein sources for human consumption. However, a big part of the catch is utilized for production of cheap by-products such as fish meal and oil. At the same time, a growing amount of fishery and, consequently, fishing waste demands efficient solutions for their utilization since they have good nutritional source, which is highly underestimated (Petrova et al., 2018).

Fish protein hydrolysates (FPH) are produced form hydrolysation technique which involves breakdown of proteins and fats present in internal tissues of fish into smaller parts (Damodaran et al., 2007). The reaction usually takes place in a controlled condition, enzymatic hydrolysis and chemical hydrolysis were found to be the widely used hydrolysation techniques. However the enzymatic hydrolysis is more sustainable process. (Slizyte R, 2010).

An improved functional properties was reported by (He et al., 2013; Kristinsson & Rasco, 2000) when comparing the FPH to the origin protein due to breakdown of larger proteins into finer ones. The other important properties like anti-oxidative, anti-hypertensive behaviour of FPH was found to be improved as reported in several studies (Chalamaiah et al., 2012; He et al., 2013; Sarmadi & Ismail, 2010).(Jenkelunas & Li-Chan, 2018) investigated and reported that FPH can be used in cryoprotectants application for fish products which are in frozen state.

Liquid FPH is a water mixture of hydrolysed proteins, the original product, which contains up to 95% of moisture. FPH in a liquid form is highly unstable moreover the transportation costs are high due to strict requirements of cold chain. Thus, dried FPH is preferable due to long shelf-life, cheap storage, and transportation. Nevertheless, at the same time, the removal of such a big amount of water from liquid FPH is a difficult and costly task, which is one of the challenges of dried FPH production (Petrova et al., 2018). Conventionally, spray dryers were widely used to remove the moisture content and convert it into final powder state. However, the industrial spray dryers are the major energy consumers of around 4 500 and 11 500 kJ/kg of moisture removed (Mujumdar, 2007).

As an alternative technique, freeze concentration and evaporation methods can be adopted before drying, which reduces the overall energy consumption rate. Freeze concentration technique is a novel method for dewatering of food products. Concentration is to stabilize the quality of food, increase shelf-life and decrease energy costs for further processing. The multistage evaporation of 1 kg of water requires energy less than 2,700 kJ/kg and for freeze concentrators ~ 330 kJ/kg of water as reported in studies by (Miyawaki et al., 2005). These dewatering methods can reduce the moisture content significantly down 50-70%. This makes drying methods like freeze drying applicable due to significant decreasing of raw product flow.

The aim of this thesis is to design an energy efficient freeze concentration process for fish protein hydrolysates and setup a lab scale freeze concentration process for validation of numerical results. Dynamic modelling of crystallizer and wash column was carried out in MATLAB while simulation of refrigeration system was carried out in Dymola and EES. Simulations were carried out to study the dynamic profile of solution's bulk temperature, diameter of crystals, ice fraction, propagation of ice, bulk cooling, calculation of gas coolers, desuperheater and evaporator capacity and heat recovery.

Chapter 2

2 literature review

2.1 Refrigeration history:

Natural ice was the only source of cooling in the ancient time. Ice collected from glaciers and frozen lakes etc. were stored in unique underground spaces. In the mid-19th century, first mechanical refrigeration system invented and patented by Jacob Perkins. The system had a condenser, hand-operated compressor, and expansion device. Natural working fluids like ammonia, CO_2 and isobutene, etc. were utilized at that time. With the advent of synthetic working fluids in 1930, natural fluids phased out due to better operating conditions of their counterparts. Later, the artificial fluids found to be harmful to the Ozone layer and the environment. After the Montreal protocol in 1987, there was a strong emphasis to phase out the high GWP (Global warming potential) refrigerants and increase research on natural working fluids like Ammonia and CO_2 (Eikevik, 2021a).

2.2 Refrigeration principles

Refrigeration is the process to extract heat from low pressure side (LT) and discharge at high pressure side with the help of some external work. The process runs with the working fluid named as refrigerant. The refrigerant absorbs heat from low pressure side and evaporator should have lower temperature for possible heat. After evaporation the refrigerant is in gas form which is compressed till condenser pressure. Refrigerant condenses while rejecting the heat to ambient and condenser temperature is higher than ambient for required heat transfer. The refrigerant temperature and pressure are reduced until evaporator using throttling valve. A simple refrigeration system is shown below with state points from 1 to 4.

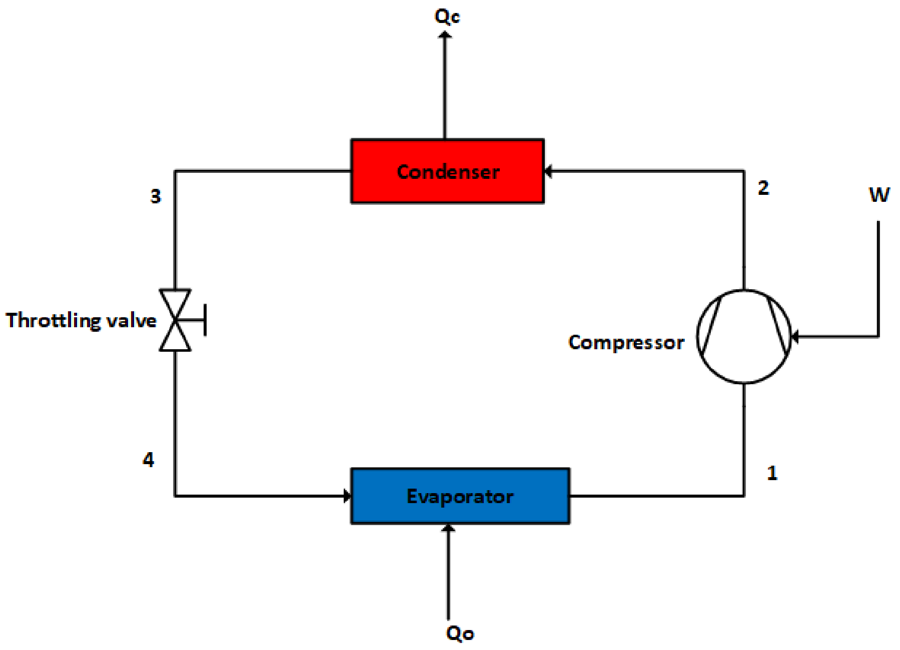

Figure 2.1 Simple refrigeration cycle

Thermodynamic process and state points are given below

1-2: Isentropic compression. The ideal work done by the compressor is given as $W_{is} = m_R(h_{2s} - h_1)$, actual work can be calculated by dividing the W_{is} by isentropic efficiency.

$$W = \frac{W_{is}}{\eta_{is}}\ (kW) \tag{2.1}$$

2-3: Isobaric rejection. The heat is rejected to ambient by condenser which is the sum of evaporation heat and compressor work.

$$Q_c = Q_o + W = m_R(h_2 - h_3)\ (kW) \tag{2.2}$$

3-4: Isenthalpic expansion. Temperature and pressure of refrigerant is reduced by expansion valve and process has constant enthalpy h_3=h_4.

4-1: Isobaric heat absorption. Heat absorbed by the evaporator surrounding is evaporator load of the system. Which can be expressed as:

$$Q_o = m_R(h_1 - h_4)\ (kW) \tag{2.3}$$

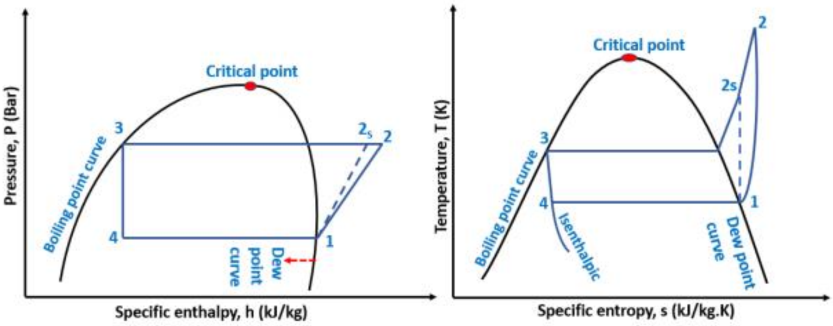

Figure 2.2 Ph and Ts diagrams of refrigeration cycle (Saeed, 2019).

The performance of a system is expressed by a dimensionless number named as coefficient of performance COP, which is the ratio of output divided by input power.

$$COP_{ref} = \frac{Q_o}{W} \tag{2.4}$$

$$COP_{hp} = \frac{Q_c}{W} \tag{2.5}$$

$$COP_{comb} = \frac{Q_c + Q_o}{W} \tag{2.6}$$

The reverse Carnot cycle is the ideal refrigeration process which operates between high and low temperatures. Efficiency of Carnot process is the ratio between real and Carnot COP, the Carnot COP for heating and cooling process is given below:

$$COP_{Cac} = \frac{T_L}{T_H - T_L} \tag{2.7}$$

$$COP_{Cac} = \frac{T_H}{T_H - T_L} \tag{2.8}$$

$$\eta_{Ca} = \frac{COP}{COP_{ca}} \tag{2.9}$$

2.3 Refrigerants

Refrigerants are the fluids that transfer heat from low temperature side to the high temperature side of the refrigeration system. With the advent of the refrigeration systems by Jacob Perkins in 1834, ethyl ether (R-610) was used as first refrigerant. It's use restricted shortly due to safety concerns and new fluids ammonia (R-717), carbon dioxide (R-744), sulphur dioxide (R-764) and air (R-729) etc. came into operation. In 1930, a new class of refrigerants chlorofluorocarbons (CFCs) introduced, succeeded by hydrochlorofluorocarbons (HCFCs) in 1950, with a slogan of environmental concern, better operating and safety conditions. In fact, many accidents happened with their handling and adverse effect on the ozone layer soon realized (Dincer, 2017).

In 1987, Montreal protocol initially signed by 26 countries to regulate the use and production of chemicals that contribute to the Ozone layer depletion. The treaty defined time frame to ban the use of these chemicals. In developed countries, CFCs phased out in 1996 and HCFCs are due until 2030. In comparison developing countries phased out CFCs in 2010 and are expecting to phase out HCFCs in 2040 (Britannica, 2021) In the late 1980s after Montreal protocol, hydrofluorocarbons (HFCs) utilization increased due to no effect on Ozone layer but they do contribute to greenhouse effect. In 1997, Kyoto protocol signed to control global warming by reducing emissions of HCFCs. Latest regulations are the EU F-Gas 2015 and Kigali amendment 2016, the later came into effect by January 2019. Kigali amendment aim is to target 80% reduction in HFCs consumption by 2047 (UNIDO, 2016). Hydro fluoro olefins (HFOs) are the latest successor of HCFCs after the adoption of European Directive 2006. HFOs series come with a label of no effect on ozone depletion, less GWP and better safety, but issues are reported concerning flammability and formation of dangerous acid (Makhnatch, 2019).

2.3.1 Ammonia

Ammonia is a natural refrigerant with good thermophysical properties. The critical temperature and pressure of ammonia is 132.4 ℃ and 112.8 bar, respectively. It has no GWP and ozone layer impact. It is a prominent working fluid in industrial applications. The amount of ammonia charge in the refrigeration systems vary from 300-1100 kg. Ammonia has a high specific enthalpy of condensation and evaporation, relatively high volumetric cooling capacity, average 20% higher COP than other working fluids. Ammonia systems having moisture content initiate the corrosion of copper and its alloys. The fluid is poisoning, flammable in a volume concentration of 15-28% with air, irritating to skin and eyes. It has stinking odour which may create panic, but this gives an early warning of leakage (5-10 ppm) (Widell, 2016).

Additional safety measures are necessary for ammonia systems, which includes the low working fluid charge, gas-tight machinery room, leak detectors, independent ventilation system with scrubber systems and emergency exits with self-closing doors. However, ammonia system with a required safety measures is a reasonable choice (Eikevik, 2021a).

2.3.2 Carbon dioxide

In 1988, Professor Gustav Lorentzen at NTNU reintroduced the CO_2 working fluid. The fluid has marvellous properties. It is nontoxic, no flammability and is not harmful to atmosphere. CO_2 is not produced directly as a refrigerant; it is a by-product of many industrial processes. The critical temperature and pressure are 31.1 ℃ and 73.8 bar respectively. High energy density due to high pressure results in high volumetric heating capacity (VHC). High VHC reduce the compressor volumes, and size for CO_2 compressors are normally 5-6 times smaller than for ammonia. Pipes and valves etc. dimensions would also reduce but need more strength and durability due to high pressure in the system (Eikevik, 2021a).

CO_2 has a low critical temperature. Condensing temperature near 28°C reduce the COP to a greater extent. To be able to work in higher heat rejection temperatures, the system operates in a transcritical process. It is a process, which works at a pressure higher than critical pressure, heat absorption at constant temperature but heat rejection at gliding temperature. There is not any liquid formation above critical pressure due to presence of fluid in the supercritical region. So, the condenser is replaced by a gas cooler. Expansion loss would be high near the critical point, and it is necessary to optimize the high-pressure side for better COP factor. In real systems, there are many benefits of using CO_2. The compressor works at high isentropic efficiency and low-pressure ratio. High heat transfer and low pressure drops results in higher COP of CO_2 systems (Eikevik, 2021a). CO_2 is a long-term environment friendly refrigerant. A large number of CO_2 systems are working in EU. Due to latest modifications of parallel compression and ejector technology, it is possible to utilize these systems in high ambient temperatures with high COP. CO_2 is expecting to become a standard refrigerant in the EU supermarkets in future (Gullo et al., 2017).

Properties	**units**	**R717**	**R744**
Molecular weight	g/mol	17.03	44.01
Evaporation heat	kJ/kg	1261.7	232.0
Thermal conductivity, liquid	W/m.K	0.5455	0.1110
Thermal conductivity, gas	W/m.K	0.0260	0.0187
Specific volume, liquid	dm^3/kg	1.566	1.073
Specific volume, gas	dm^3/kg	289.39	10.20
Ignition temperature	°C	630	ND
Density(liquid) at 0°C	kg/m^3	639	928
Density(gas) at 0°C	kg/m^3	4	98
Boiling point at 1 bar	°C	-33.33	-78.03
Critical temperature	°C	132.3	31.1
Critical pressure	Bar	113.3	73.8
Flammability	-	No	No
Toxic	-	Yes	No
GWP	-	0	1

Table 2.1 Properties of R717 and R744 (Eikevik, 2021a).

2.4 Hydrolysis

There are several methods used to produce FPH, including chemical hydrolysis (acid and alkaline hydrolysis), autolysis, bacterial fermentation, and enzymatic hydrolysis. Among them, enzymatic hydrolysis and chemical hydrolysis are the most commonly used methods due to a number of advantages. The chemical hydrolysis process is low cost, is rapid and results in a high protein recovery;

however, there is little control over the consistency of the hydrolysed products, with large variations in free amino acid profile due to the non-specific breakdown of peptide bonds (Celus et al., 2007).

The hydrolysation process starts with the mincing of rest raw material, after the mincing process, the minced RRM is pumped to a tank. In the tank the required amount of water and enzymes are added usually 50 % of water and 0.1% of enzymes are added. The tank is heated to 50 ℃ and this temperature is maintained for 1 hour, which is the ideal temperature for enzymes to breakdown minced RRM to smaller peptides and amino acids. After the hydrolysation process the tank is maintained at 90 ℃ to terminate all enzyme activities. At the end the filtration process is carried out to separate FPH from ash and slug. This approach was used to produce 600 kg of hydrolysates at Myre Norway with the help of SINTEF ocean during the process different samples were taken which will be analysed in Lab for further study. **Figure 2.3** Shows the systematic diagram of hydrolysation process and **Appendix D** contains the field pictures taken at different steps in hydrolysation process.

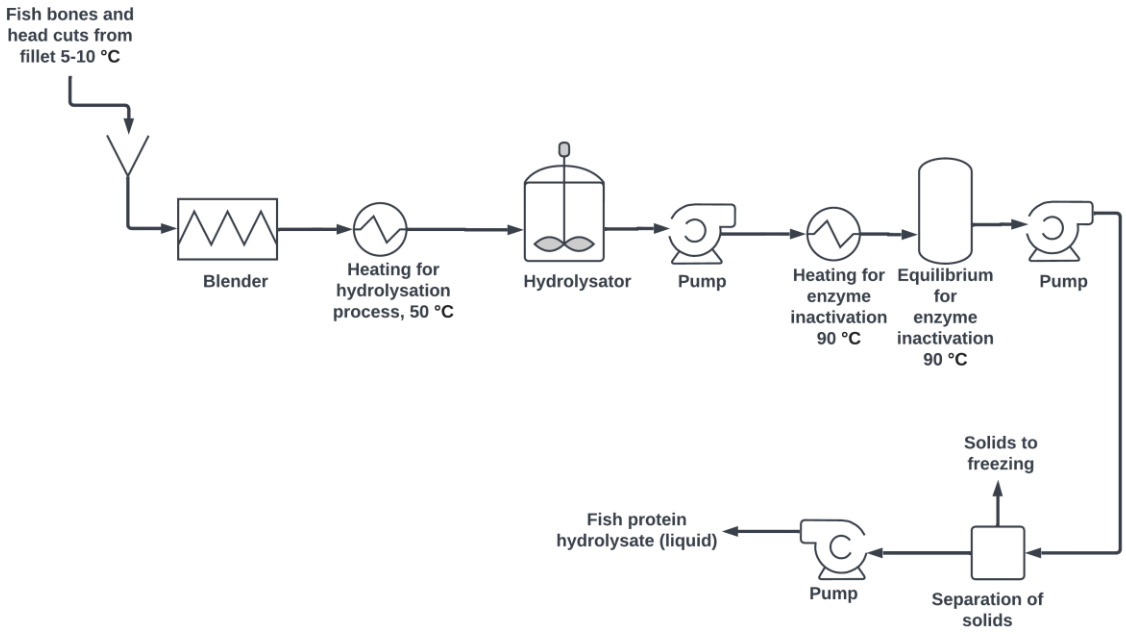

Figure 2.3 Schematic diagram of hydrolysis process

FPH is produced in its liquid form which is unstable which need freezing and dewatering to make a stable product. Freeze drying and dewatering techniques can be used to increase shelf life. Energy demand of different processes for 1 ton rest raw material were calculated by (Sherman, 2022), which are shown in **Table 2.2**.

Drying method used	Freeze concentration	Three effect evaporators	Mechanical vapor recompression	Direct drying
Spray drying	1245.3	1182	629	3183
Drum drying	1124.3	1158	606	2958
Vacuum freeze-drying	1230	1163	611	3315

Table 2.2 Summary of overall energy demands when processing 1-ton RRM (kWh per kg) (Sherman, 2022).

Introduction of freeze concentration can result in 60% energy saving compared to conventional spray drying. An overview of different conservation techniques is given below:

1) Evaporation
2) Concentration by reverse osmosis and osmotic evaporation
3) Vacuum freeze drying
4) Freeze Concentrator

2.4.1 Evaporation:

Evaporation is defined as the vaporization by boiling of a volatile solvent (water, in our case) to increase the concentration of a solution or a suspension (Berk, 2013).

- Evaporation is the thermal process, and the solution is heated to its boiling point. Thermal damage of quality is expected in this process.
- The viscosity of the solution increases as the concentration of solute increases.

2.4.1.1 Multiple effect evaporation

Multiple-effect evaporation is evaporation in stages, whereby the vapors generated in one stage serve as the heating medium in the next stage. Thus, the first stage acts as a “steam generator” for the second, which acts as a condenser to the fist and so on. The number of “effects” is the number of stages thus arranged in the chain. The fist effect is heated with boiler steam. The vapors from the last effect is sent to the condenser (**Figure 2.4**). In the multieffect evaporator shown in **Figure 2.4**, the liquid and the vapors advance in the same direction (Berk, 2013).

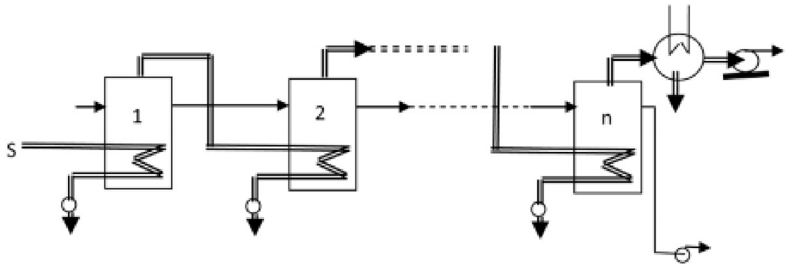

Figure 2.4 Schema of feed-forward multi effect evaporation (Berk, 2013).

2.4.1.2 Vapor recompression

Raising the pressure of the vapor generated by evaporation increases its saturation temperature and therefore its usefulness as a source of heat. The principle of vapor recompression is schematically represented in **Figure 2.5** for a hypothetical single-stage evaporator.

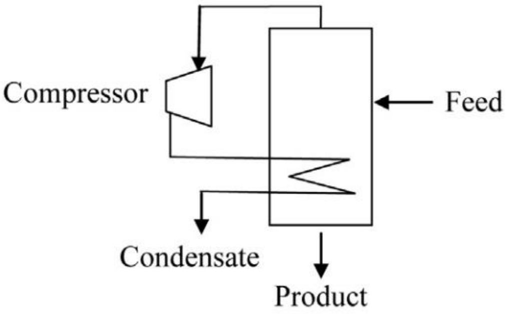

Figure 2.5 Principle of vapor recompression in single effect evaporation (Berk, 2013).

Vapor recompression can work in single-stage evaporation as shown, but it is usually applied in combination with multieffect evaporation. Two methods of vapor recompression are used:

2. Mechanical recompression: because of the large volumes of vapor to be handled, rotating compressors (turbo-compressors, centrifugal compressors, and blowers) are used. The main shortcoming of mechanical recompression is the high rate of wear, accelerated greatly by the presence of water droplets in the vapors (Berk, 2016).
3. Thermo-recompression: the low-pressure vapors from the evaporator can be compressed with the help of a small amount of high-pressure live steam, using a steam ejector. A schema of a double-effect evaporator comprising thermo-recompression is shown in **Figure 2.6** (Berk, 2016).

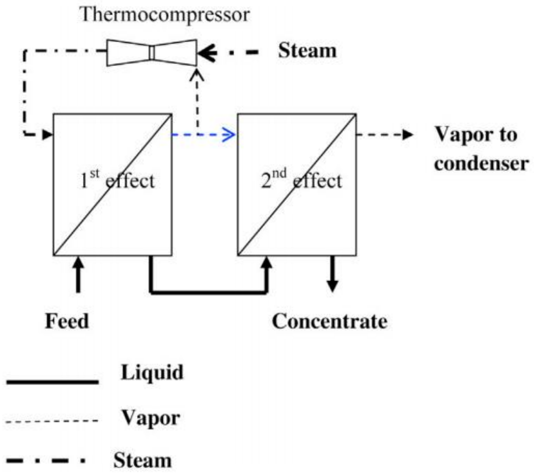

Figure 2.6 Double effect evaporator with thermocompression of vapors (Berk, 2016).

Ejectors being relatively inexpensive and of low maintenance cost, thermo recompression is usually preferred over mechanical recompression. Due to the very high velocities of gas flow attained at the nozzle, ejectors usually emit a disturbing high-pitch noise, requiring appropriate acoustic insulation (Berk, 2016).

2.4.2 Concentration by reverse osmosis and osmotic evaporation

Reverse osmosis is a membrane process. "Osmosis" means the spontaneous transfer of water from a more dilute into a more concentrated solution through a membrane. To prevent osmotic transfer of water into a solution, a certain pressure, called osmotic pressure, must be applied in the direction opposite to that of the transfer. If a pressure stronger than the osmotic pressure is applied, the direction of water transfer is reversed, and water passes from the more concentrated to the less concentrated medium (Berk, 2016). The processes of osmosis and reverse osmosis are compared in **Figure 2.7**.

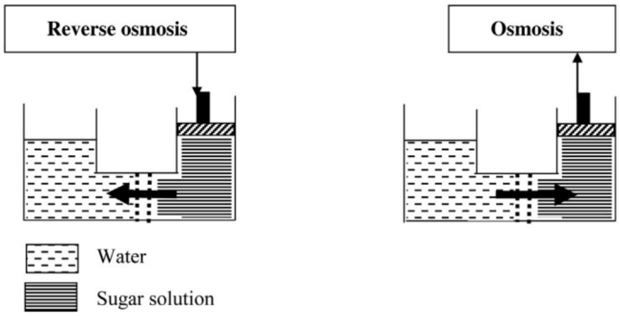

Figure 2.7 Principle of osmosis and reverse osmosis (Berk, 2016).

2.4.3 Vacuum freeze drying

Vacuum Freeze-drying is another dewatering technique in which water is vaporized from frozen food under vacuum, without passing through the liquid phase. The heat for subliming the ice may be provided in a variety of ways but the most common is by radiation from shelves warmed by a heat-transfer fluid which has been heated by steam.

In theory, the heat for sublimation of the ice can be provided by microwave energy and, in fact, the use of microwaves should be expected to accelerate drying considerably. Substantial research has been performed on this application of microwave energy, but major physical problems remain to be resolved. A major problem is the glow discharge or corona effect which results at pressures between 0.1 and 5.0 Torr, which results in ionization of gases in the chamber and undesirable changes in food quality (Corp, 1987).

2.4.4 Freeze Concentration

Freeze concentration is a separation process for liquid mixtures (solvents). It separates liquid mixtures by removing heat from the mixture until one or more components solidifies or forms a crystalline phase and then physically separating the crystals from the mixture by mechanical methods. The separated crystals are usually very pure, except for minor contamination from the liquid layer adhering to the crystal surface. The crystals are usually melted with heat recovered from precooling the mixture (Corp, 1987).

Freeze concentration is the gentle technology to remove water while freezing the water in solution. There are generally two principles in freeze concentration suspension and layer crystallization.

2.4.4.1 Suspension Crystallization:

Freeze concentration consists of ice nucleation and growth, followed by separation. The most common method includes crystallization of ice particles in the solution, ice suspension crystallizers, and washing of ice crystals in a separate washing column (Thijssen, 1975).

2.4.4.2 Layer Crystallization:

In layer crystallization a layer of ice is frozen on a cooled surface. This process is used for purifying chemicals, but not for large-scale freeze concentration. One reason for that is probably that solute inclusion is hard to avoid during the growth process (Scholz, 1993).

2.4.4.3 Melt Crystallization

Melt crystallization systems remove heat and cool the liquid to create a driving force for the formation and growth of crystals. Melt crystallization provides an economic and energy-efficient alternative purification step in cases where standard distillation is unsuitable due to close boiling isomers, azeotropic systems, products that tend to polymerize, heat sensitive products, or explosive substances. The suspension-based process provides slow growth rates that allow pure crystal formation even in relatively impure melts. By combining this extremely selective crystallization system with our proven washing column technology that separates the crystal from the mother liquor, an ultra-pure product can often be obtained after one step (GEA).

Suspension crystallization process is ideal for continuous process, so this sub chapter contains all the theory needed to design a batch freeze concentrator. The aim of the modelling is to predict how the size distribution develops with time under different process conditions, and to develop strategies to narrow the size distribution. Also, the ripening phenomena has been studied by population balances (Huige, 1972; Smith, 1985).

2.4.4.4 Calculation of freezing point

The freezing point variation with concentration for an aqueous solution is an important parameter. It gives the operation condition for the refrigerator because the refrigeration evaporation temperature must be lower than the freezing point of the solution. As water is frozen out the freezing point is lowered, and for a batch process the temperature must be adjusted, or the kept constant lower than the end freezing point (Flesland).

The freezing point for solution can be calculated by applying the equilibrium condition for water and ice in solution:

$$\mu_w{}^s = \mu_w{}^l \qquad 2.10$$

Chemical potential of ice is assumed to be equal to the chemical potential for pure ice as the solubility of different particles in ice is negligible.

The chemical potential for water in solution is given by:

$$\mu_w{}^l = \mu_w{}^{0.1} + RT\ln a_w \qquad 2.11$$

Here $\mu_w{}^{0.1}$ is the chemical potential for water at a reference state, R is the gas constant, T is the temperature and a_w is the water activity in the solution.

$$dT_{fp} = \frac{RT_{fp}{}^2}{\Delta_f H x_w} dx_w \qquad 2.12$$

where it is assumed that the activity coefficient is constant in a small temperature interval. This equation is transformed to moment form and used in a model together with the moment equations, to calculate the freezing point change as the solution becomes concentrated (Flesland).

2.4.4.5 Nucleation and ice growth

In crystallization, nucleation describes the development of new particles, which is necessary to control if the size of the particles is important. Primary nucleation is happening only in pure water and demands high supercooling. Since the solutions which are to be freeze concentrated contains foreign particles, the dominating nucleation mechanism is secondary nucleation. In suspension crystallizers the ice crystals grow in a slightly supercooled solution, shown schematically in **Figure 2.8** The bulk supercooling is defined the difference between the bulk temperature (T_b) and the actual equilibrium temperature, the freezing point corresponding to the bulk concentration (Flesland) :

$$\Delta T_b = T_{fp}(c_b) - T_b \qquad 2.13$$

The bulk supercooling necessary for ice growth consists of different parts due to growth resistances. They are mass transfer resistance, curvature effect, inbuilding kinetics and heat transfer resistance (see equation (2.16)) below. In equation (2.16) the curvature effect is neglected. The nucleation intensity, B^0, and the ice growth rate, vice, are both dependent on the level of supercooling, given by (Flesland) :

$$B^0 = k_n * (\Delta T_b)^b \qquad 2.14$$

$$v_{ice} = \frac{\partial L}{\partial t} = k_v * (\Delta T_b)^a \qquad 2.15$$

were B^0 is the nucleation in (particles pr. volume and time), Vice is the linear ice growth rate. k_n, k_v, a and b are coefficients that most often must be determined by experiments. An overview of experimental results is given by (Hartel, 1987).

In this study, in order to reduce the variables, some of the parameters are taken from literature; the growth exponent a = 1 (Wey, 1970), the nucleation exponent: b = 1.25 for supercooling $0.25 < \Delta Tb$, <1.0 and 2.1 for $0.01 < \Delta Tb < 0.2$ (Hartel, 1987). The ice growth rate is assumed linearly dependent on the supercooling. This is proved experimentally for crystals larger than 0.1mm (Huige, 1972; Wey, 1970). For smaller crystals surface effects must be accounted for. The ice growth may also be derived from heat and mass correlations. It is common to treat the effects that limits ice growth as a series of resistances (Dennis R Heldman & Daryl B. Lund, 1992; Wey, 1970). Heat and mass transfer are then connected by assuming equilibrium at the ice surface. When the solute concentration gradient is regarded as the driving force, the ice growth is expressed by (Wey, 1970):

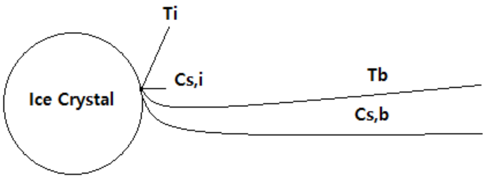

Figure 2.8 Ice particle in supercooled solution

$$v_{ice} = \frac{1}{\left[\left(\frac{c_i}{\rho_{ice}\beta}\right) + \frac{1}{k_i} - \left(\frac{dc}{dT}\right)_{eq} * \left(\frac{\Delta_f H}{\alpha}\right)\right]} (c_i(T_b) - c_b) \qquad 2.16$$

Where ρ_{ice} is the density of the solution, $c_i(T_b)$ is the solute concentration at the ice-liquid interface, c_b is the bulk concentration, ρ_{ice} is the density of pure ice, ß is the mass transfer coefficient, k_i is a kinetic parameter, $(dc/dT)_{eq}$ is the slope of the equilibrium line in the phase diagram and α is the heat transfer coefficient. The concentration at the interface is assumed equal to the equilibrium concentration at the bulk-temperature. Equation (2.16) was developed for ice particles growing in a supercooled solution, and it is assumed that the ice growth is linearly dependent on the concentration difference or similarly the bulk supercooling. The linear dependence has been verified by experiments for crystals of size, d > 0.1mm (Wey, 1970).

From equation (2.16), one would expect size dependent ice growth since both the heat and mass transfer coefficients depends on the particle size. This is not always the case, but rather growth rate dispersion caused by local changes of the growth conditions (Flesland).

2.4.4.6 Population balance

In general, all particulate processes may be described by population balances (M.A., 1988). In ice crystallization, crystals are created (nucleation) and grow to a certain size, depending on the conditions. At the same time breakage or dissolution of crystals of a certain size may occur. A population balance is a balance of the number of crystals within ranges of sizes dL. In the present study only nucleation and growth are considered.

Breakage is neglected. For a batch-crystallizer the population balance reduces to:

$$\frac{\partial \mathrm{n}}{\partial \mathrm{t}} = -\frac{\partial(\mathrm{n} * \mathrm{v}_{\mathrm{ice}})}{\partial \mathrm{L}} \tag{2.17}$$

were L is a characteristic length of the crystals, t is time, n = n(t,L) is a size distribution and V_{ice} is the linear growth rate of the crystals. This equation is connected to a heat balance for the crystallizer. To solve the partial differential equation for the population balance coupled to the heat balance, which is an ordinary differential equation, the population balance is transformed to moment equations. Then we get a set of ordinary differential equations to be solved. In freeze concentration it is important to control the nucleation and growth to decrease the spread in size and get large enough crystals that can be easily separated from the concentrate. In the process of Niro Process Technology, the crystals are grown to a size of 0.5mm before washing (Flesland).

2.4.4.6.1 Moment equations

The moments of a size distribution function are defined by

$$\mu_{\mathrm{i}} = \int_0^{\infty} \mathrm{n}\mathrm{L}^{\mathrm{i}}\mathrm{d}\mathrm{L} \tag{2.18}$$

The first four moments which are used in this study, describes total number crystals, total length of crystals, total area, and total volume of crystallized material. Density multiplied by the third moment gives the total mass of crystalized material per volume of the suspension. We multiply equation (2.18) with $L^{i}dL$ and integrate from 0 to ∞ (M.A., 1988). This gives a set of coupled ordinary differential equations that can be combined with heat and mass balances.

$$\frac{\partial \mu_0}{\partial \mathrm{t}} = \mathrm{B}^0 * \mathrm{V} \tag{2.19}$$

$$\frac{\partial \mu_1}{\partial \mathrm{t}} = \mu_0 * \mathrm{v}_{\mathrm{ice}} \tag{2.20}$$

$$\frac{\partial \mu_2}{\partial \mathrm{t}} = 2\mu_1 * \mathrm{v}_{\mathrm{ice}} \tag{2.21}$$

$$\frac{\partial \mu_3}{\partial \mathrm{t}} = 2\mu_2 * \mathrm{v}_{\mathrm{ice}} \tag{2.22}$$

where nucleation B^0 and linear ice growth rate v_{Ice} is empirically given by

$$\mathrm{B}^0 = \mathrm{k_n} * (\Delta \mathrm{T_b})^{\mathrm{b}} \tag{2.23}$$

$$\mathrm{v}_{\mathrm{ice}} = \frac{\partial \mathrm{L}}{\partial \mathrm{t}} = \mathrm{k_v} * (\Delta \mathrm{T_b})^{\mathrm{a}} \tag{2.24}$$

The coefficients must be determined by experiments or appropriate correlations for heat and mass transfer coefficients, and in some cases kinetic effects. Nucleation B° is given in (number /s- volume) and ice growth rate v_{ice} is given in (m/s).

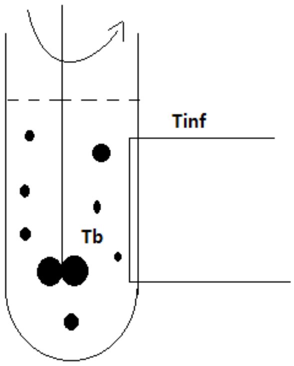

Figure 2.9 The batch crystallizer model

2.4.4.6.2 Heat balance

A heat balance for a batch crystallizer gives

$$-U * A(T_\infty - T_b) = \frac{\partial}{\partial t}\left(m_l * Cp_l * (T_b - T_{ref})\right) + \frac{\partial}{\partial t}\left(m_{ice} * Cp_{ice} * (T_{ice} - T_{ref})\right) - \frac{\partial}{\partial t}(m_{ice} * h_{ice}) \quad 2.25$$

Here it is assumed that T_{ice} is equal to the bulk temperature (T_b), and that the reference temperature T_{ref} is equal to 0°C or 273K. The total heat transfer is assumed constant but different correlation for variable heat transfer with ice formation or viscosity can easily be included in the program that was developed.

Equation (2.25) must then be transformed into moment form. The third moment is equal to the volume fraction of ice:

$$\mu_3 = \frac{V_{ice}}{V} \quad 2.26$$

and the mass of ice in the crystallizer is:

$$m_{ice} = \rho_{ice} * V * k_v * \mu_3 \quad 2.27$$

and then the mass of the separated concentrate is:

$$m_l = \rho_l * V * (1 - k_v * \mu_3) \quad 2.28$$

were the volume form factor k_v for spheres is 4/3π when L is radius.

The equation (2.25), (2.27) and (2.28) gives

$$\frac{U * A(T_b - T_\infty)}{V} = \frac{\partial}{\partial t}(\rho_l * Cp_l * (1 - k_v * \mu_3)T_b) + \frac{\partial}{\partial t}((\rho_{ice} * k_v * \mu_3) * Cp_{ice} * T_b) - \frac{\partial}{\partial t}(\rho_{ice} * h_{ice} * k_v * \mu_3) \quad 2.29$$

V, ρ_{ice}, h_{ice}, Cp_{ice}, ρ_l and Cp,l are assumed constant. By using the product rule and solving for $\frac{\partial T_b}{\partial t}$ one gets

$$\frac{\partial T_b}{\partial t} = -\frac{U * A(T_b - T_\infty)}{V * [\rho_l * Cp_l + (\rho_{ice} * Cp_{ice} - \rho_l * Cp_l) * k_v * \mu_3]} - \frac{\partial \mu_3}{\partial t}\frac{[(\rho_{ice} * Cp_{ice} - \rho_l * Cp_l) * k_v * T_b - \rho_{ice} * h_{ice} * k_v]}{\rho_l * Cp_l + (\rho_{ice} * Cp_{ice} - \rho_l * Cp_l) * k_v * \mu_3} \quad 2.30$$

The moment form of the freezing point depression becomes:

$$\frac{\partial T_{fp}}{\partial t} = \frac{R * (T_{fp} + 273.15)^2}{\Delta_f H x_w} * \frac{\partial x_w}{\partial t} \quad 2.31$$

$$= \frac{RT^2}{\Delta_f H} * \frac{-\frac{m_{s0}}{M_S} * \frac{\rho_{ice} * k_v * V}{M_W}}{\left(1 - \frac{\rho_{ice} * k_v * \mu_3}{M_W}\right) * \left(\frac{m_{w0}}{M_W} - \frac{\rho_{ice} * k_v * \mu_3}{M_W}\right)} * \frac{\partial \mu_3}{\partial t} \quad 2.32$$

The moments and the temperatures are assumed only variable with time. The equations (2.19), (2.20), (2.21), (2.22), (2.30) and (2.32) are solved simultaneously by Euler method with 0.0001s time step. A MATLAB program (**Appendix A**) was developed to solve all the equations numerically.

The initial conditions are the moments of the size distribution of the seeds, the initial bulk temperature, and the initial freezing point. It is assumed that the seeds are of size zero which means that the moments μ_1 ,μ_2 and μ_3= 0.

2.4.4.7 Crystallizer Types

This section deals with the different types of crystallizers and which crystallizer is ideal to use for freeze concentration process.

2.4.4.7.1 Forced circulation crystallizer

The forced circulation (FC) crystallizer is the most common type of crystallizer. Simple in design and easy to operate, it is usually employed in evaporative crystallization of relatively flat or inverse solubility products, in rather viscous media and when scaling is a major issue. Its high mechanical energy input and high secondary nucleation rate make it best solution when large crystals are not required (average size <1 mm) (GEA).

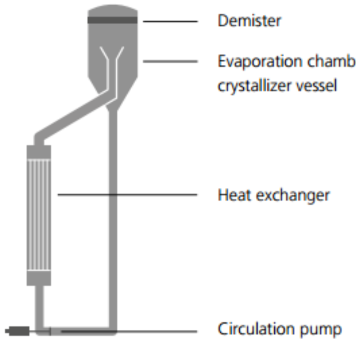

Figure 2.10 Forced circulation crystallizer (GEA).

The FC evaporates solvent, thus increasing the supersaturation in the process liquor, and causing crystallization. Slurry from the crystallizer vessel is circulated through the heat exchanger, and returned to the crystallizer vessel, where its supersaturation is relieved by deposition of material on the crystals present in the slurry. The supersaturation is controlled, to avoid spontaneous nucleation, by sufficient circulation capacity. Most conventional FC units operate under vacuum, or slightly over atmospheric pressure (GEA).

2.4.4.7.2 Draft tube baffle crystallizer

The draft tube baff (DTB) crystallizer is specially designed to produce coarse crystals with narrow size distribution. According to process requirements it can be used for evaporative, cooling, or reactive crystallization, always providing steady operation under the whole capacity range due to its ability to operate at optimal supersaturation and to control crystal population inside the system. The DTB can produce large particles (up to 3 mm) because it gently agitates growing crystals. It has a controlled residence time for optimal growth and a long operating cycle with limited encrustations. The DTB was given this name because it provides two discharge streams: the slurry that contains the product crystals, and the mother liquor (saturated solvent) with a small amount of fines (GEA).

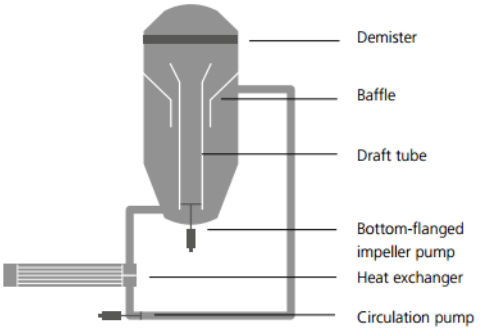

Figure 2.11 Draft tube baffle crystallizer (GEA).

Most conventional DTB crystallizers operate under vacuum, or slightly over atmospheric pressure. DTB crystallizers have been studied widely in crystallization theory and can be modelled with accuracy. Its distinct zones of growth and clarified mother liquor make it possible to define in terms of kinetic parameters, and thus growth and nucleation rates can be determined. These features make the DTB crystallizer very suitable to mathematical description, and thus subject to good operating control (GEA).

2.4.4.7.3 OSLO crystallizer

This crystallizer type is also referred to as flid-bed-crystallizer. GEA is the premier designer of OSLO crystallizers in the world. The primary advantage of the OSLO crystallizer is the ability to grow crystals in a fluidized bed, which is not subject to mechanical circulation methods (GEA).

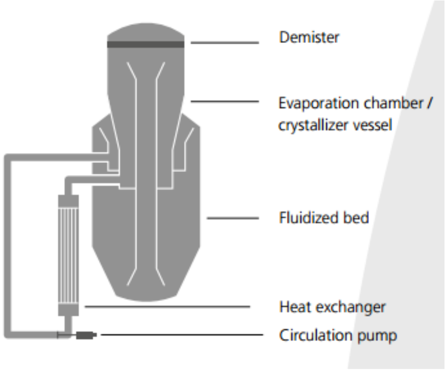

Figure 2.12 OSLO crystallizer (GEA).

Compared to other crystallizers, an OSLO crystallizer will grow the largest crystals. The slurry is then removed from the crystallizer's fluidized bed and sent to be separated (GEA).

2.4.5 Wash Column:

After the crystallization process in the crystallizer the next step is to separate solid ice from the solution, this can be achieved by wash column. There are three wash columns based on the transport mechanism of solids named as gravitational, mechanical, and hydraulic.

2.4.5.1 Gravity wash column

In gravity wash column gravitational forces are responsible for the downward transport of the particles through the column. The slurry is fed at the top of the column and the crystals form a loose bed of particles. The mother liquor leaves the column via an overflow. At the bottom of the column the crystals are molten, and part of the pure melt is used as reflux, which provides a counter current washing action. Gravity wash columns use agitators at low rotational speed to prevent channelling in the bed and agglomeration of the particles (Oord-Knol, 2000).

2.4.5.2 Hydraulic wash column

Slurry coming from crystallizer bed compaction with slurry pump (2) generating drag force on crystals. Transport of compact ice bed to scraper (3) with suspension and melting of ice in melt circuit (4). Extra force on bed with circulation of filtered liquid by steering pump (5) filter (6) in filter tubes part of filtrate (7) return to crystallizer for further concentration Part of filtrate (8) to next stage or product tank Control of wash front with light cell (9). Bed porosity around 40% Existing applications up to 50 mm $^{2}s^{-1}$ (van Beek, 2018).

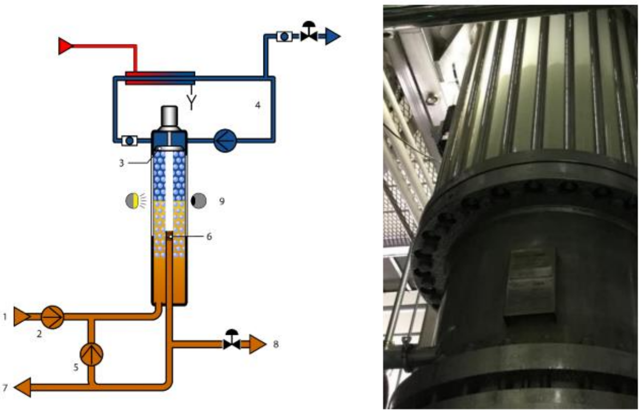

Figure 2.13 Schematic (left) and industrial scale(right) Hydraulic wash column (van Beek, 2018).

2.4.5.3 Piston wash column

Slurry inlet from crystallizer (1) bed compaction by piston with sieve plate (2) on top. After bed compaction ice transport to scraper (3) with suspension and melting of ice in melt circuit (4). Piston also functions as plunger pump (5) that takes in slurry and pushes out filtrate. Part of filtrate (6) return to crystallizer for further concentration and part of filtrate (8) to next stage or product tank wash front detection by light cell (7) or conductivity measurement in produced water Bed porosity around 20% existing applications up to 200 mm $^{2}s^{-1}$ (in multi stage configuration) (van Beek, 2018).

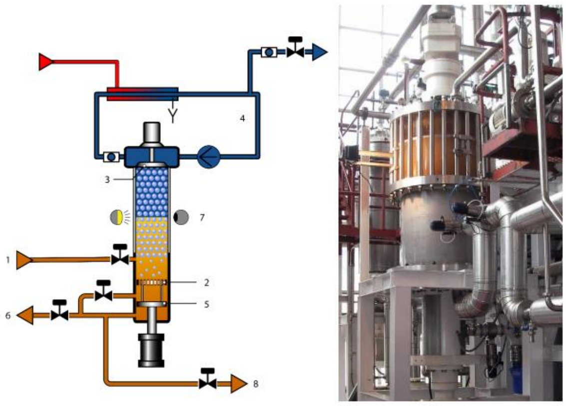

Figure 2.14 Schematic (left) and industrial scale(right) Piston wash column (van Beek, 2018).

2.4.5.4 Filter in Production Vessel

Scraped surface wire mesh filter (1) no bed but circulation in draft tube with screw pump (2). Forced circulation along filter. Existing applications up to 300 mm $^{2}s^{-1}$ (van Beek, 2018).

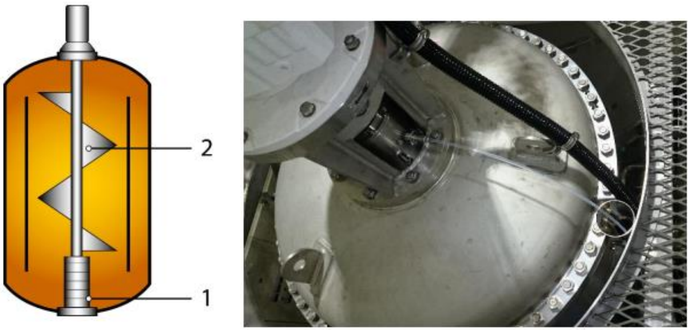

Figure 2.15 Schematic (left) and industrial scale(right) filter wash column (van Beek, 2018).

2.4.5.5 Dynamic behaviour of wash column

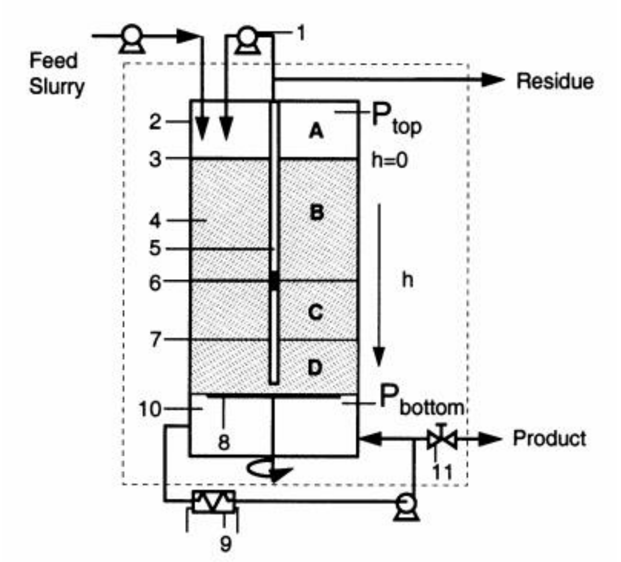

Figure 2.16 Principle of a hydraulic wash column (Oord-Knol, 2000).

1 = Steering pump; 2 = column wall; 3 = bed level; 4=moving packed bed; 5 = filter tube; 6 = filter; 7 = wash front level; 8 = rotating knife; 9 = melter; 10 = reslurry chamber; 11 = product valve. A = slurry section; B = filtration section; C = stagnant section; D s wash section.

Figure 2.16 is a drawing of the hydraulic wash column, where the chosen system boundary is shown by the dotted line. With this system boundary the inputs are the feed flow, the temperature and the crystal concentration in the feed, the steering flow, and the opening of the product valve. The output variables of the model are the total bed height and the position of the wash front, which should be controlled for proper operation. Additional outputs are the residue flow, the product flow, and the pressure at the top of the bed, P_{top}, and in the melting circuit, P_{bottom} (Oord-Knol, 2000).

To derive the model three main sections are defined: the top section, the bottom section, and the melting circuit. The top section stretches from the top of the wash column to the filters. It consists of the slurry section A, where a loose slurry is present, and the filtration section B, which is the part of the packed bed between the top of the bed and the filters. Since the position of the filters is fixed, the position of the crystal bed is determined by the length of the filtration section, $L_{filtration}$ (m) (Oord-Knol, 2000).

The bottom section stretches from the filters to the knife and is totally occupied by the packed bed. The bottom section is subdivided into the stagnant zone (c) and the wash section (D). The packed bed pores in the stagnant zone are filled with mother liquor, while the pores in the wash section are filled with wash liquid. The position of the wash front therefore corresponds to the length of the wash section. The melting circuit consists of several parts: the re-slurry chamber 10, the circulation pump, the smelter, and all tubing between these pieces of equipment and the product valve (Oord-Knol, 2000).

2.4.5.5.1 Volume balances for the top section

In the top section there are two phases present, crystals, and mother liquor. An overall volume balance for the top section gives:

$$\text{Ø}_{\mathrm{feed}} + \text{Ø}_{\mathrm{steer}} = \text{Ø}_{\mathrm{s,filters}} + \text{Ø}_{\mathrm{ml,filters}} \qquad 2.33$$

where $Ø_{\mathrm{s,filters}}$ is the amount of solid material that leaves the top section to enter the bottom section at the filters, and $Ø_{\mathrm{ml,filters}}$is the mother liquor flow from the top section that leaves the column via the filters. The length of the filtration section is calculated with help of the solids balance in the top section:

$$\frac{dV_{\mathrm{cr,top}}}{dt} = \alpha_1 Ø_{\mathrm{feed}} - Ø_{\mathrm{s,filters}} \tag{2.34}$$

The total amount of solid material in the top section is distributed over the slurry section and the filtration section:

$$V_{\mathrm{cr,top}} = A_c * ((1-\varepsilon)l_{\mathrm{filtration}} + \alpha_2 L_{\mathrm{slurry}} \tag{2.35}$$

The required parameters are the porosity of the crystal bed, ε, and the concentration of the crystals in the slurry section, α_2. It is assumed that the crystal concentration in the slurry section equals the crystal concentration in the stream, which enters the wash column after mixing the crystal-free steering flow with the feed flow, having crystal concentration α_1. Since the total length of the top section is constant, the length of the filtration section is calculated by combining Equation (2.34) and 2.35) (Oord-Knol, 2000).

$$\frac{dL_{\mathrm{filtration}}}{dt} = \frac{1}{A_c * (1-\varepsilon)} * (\alpha_1 Ø_{\mathrm{feed}} - Ø_{\mathrm{s,filters}}) \tag{2.36}$$

2.4.5.5.2 Bottom section: Overall balance and two liquid balances

In the bottom section one solid phase, the crystals, and two liquid phases, wash liquid and mother liquor, are present. The total volume of the bottom section is constant; therefore, an overall volume balance for the bottom section combines the flows entering and leaving with the volume of the solid material that is created by crystallization C_s and the volume of the wash liquid that disappears C_l due to the same crystallization:

$$Ø_{\mathrm{s,filters}} + C_s + Ø_{\mathrm{wl,knife}} = Ø_{\mathrm{ml,bottom}} + Ø_{\mathrm{s,knife}} + C_l \tag{2.37}$$

Due to the density difference between solid and liquid material, the volumes Cs and C_l are not equal. Since these volumes represent the same mass, the solid and the liquid densities are used to relate those volumes:

$$C_l = \frac{\rho_s}{\rho_l} * C_s \tag{2.38}$$

It is assumed that the total cooling capacity of the descending crystals is used to crystallize the ascending wash liquid. The amount of crystallized material can be calculated from a heat balance and the temperature difference between the feed slurry and the melt.

$$C_s = \frac{C_p(T_{\mathrm{melt}} - T_{\mathrm{feed}})}{\Delta H_m} * Ø_{\mathrm{s,filters}} \tag{2.39}$$

The volume of wash liquid in the wash column changes due to the wash-liquid flow entering at the knife, said to be positive, and by the wash liquid that crystallizes. It is assumed that the wash front does not reach the filters and therefore, there is no loss of wash liquid out of the column via the filters. The length of the wash section is directly related to the wash liquid volume; therefore:

$$\varepsilon_w * A_c * \frac{dL_{wash}}{dt} = \emptyset_{wl,knife} - C_l \qquad 2.40$$

The porosity in the wash section is calculated from a simple heat balance and the porosity in the top section:

$$\varepsilon_w = \varepsilon - (1 - \varepsilon) * \frac{C_p * (T_{melt} - T_{feed})}{\Delta H_m} \qquad 2.41$$

When the length of the wash section changes, mother liquor will flow into or out of the bottom section. Defining a mother-liquor flow out of the section positive gives:

$$A_c * \varepsilon * \frac{dL_{wash}}{dt} = \emptyset_{ml,bottom} \qquad 2.42$$

Both the mother liquor from the top section and the bottom sections leaves the column via the filter tubes to split again into the steering flow and the residue flow. So the residue flow, which is an output variable, can be calculated as follows (Oord-Knol, 2000).

$$\emptyset_{residue} = \emptyset_{ml,bottom+}\emptyset_{ml,filters} - \emptyset_{ml,steer} \qquad 2.43$$

2.4.5.5.3 Melting circuit

The crystals from the packed bed leave the bottom section via the knife. All crystals must be melted, as the product is a liquid. Assuming that the crystals are molten at the moment they enter the melting circuit, the following mass balance holds, where a correction is needed for the density difference between solid and liquid (Oord-Knol, 2000).

$$\frac{\rho_s}{\rho_l} * \emptyset_{s,knife} = \emptyset_{wl,knife} + \emptyset_{product} \qquad 2.44$$

2.5 Thermal Energy Storage

Energy demand on the fishing vessels, industries and different sectors varies with respect to time. This energy fluctuations and demands can be optimized with the thermal energy storage (TES). A complete TES process contains three steps, charging, storing, and discharging. A TES system stores energy by heating, cooling, melting, or vaporizing a solution/material. Reverse of this process energy can be used for heating and cooling applications.

In the mid-19th century, chemical storage batteries were common to supply power for signal lighting, telegraphs, and other electrical devices. In 1896, an inventor from Toledo, Homer T. Yaryan established a thermal storage system to utilize the excess heat for hot water district heating plant in that city at the time of peak electric demand. Steam storage in other plants were not as successful as his plant. Other TES methods in the 1890s were compressed air and hot water flashing into steam to drive the engines of cars (Dincer I 2010).

2.5.1 Sensible TES

Sensible TES is the storage of energy by either increasing or decreasing the temperature of the material without any phase change. The efficacious of energy storage depends on the specific heat capacity and density of the material. The heat stored in a material in a unit time can be expressed as:

$$Q_{sensible} = \frac{mC_p\Delta T}{3600s} = \frac{\rho VC_p\Delta T}{3600s} \qquad 2.45$$

There is a wide range of materials for storing energy, but the selection of the medium is highly dependent on the application and temperature range. Each storage medium has its own pros and cons. Some materials for the sensible heat storage are oil, air, sand, soil, and bricks. One important consideration during selection of storage medium is the heat transfer rate, the rate at which the energy can be stored and extracted. The main components in TES are storage tank, medium and charging/discharging device. The storage tank must be able to hold the thermal storage material, avert the heat losses and maintain thermal gradient. High thermal losses mean the tank can't hold the desired temperature for a longer period (Dincer I 2010).

For sensible heat storage, water is the most popular choice. The reason to select water are obvious as it is inexpensive, high specific heat capacity, easily available and no safety hazards. Water makes it easy to pump and transfer thermal energy at different rates by pumping, however the application is limited due to freezing and boiling point of water.

2.5.2 Latent TES

Latent TES is the storage of energy with phase change material (PCM). PCM store energy during conversion (liquid to solid) and released in the reverse process (solid to liquid). For example, water conversion to ice at 0°C stores a latent heat of 333 kJ/kg and the same amount of energy release in the reverse process (Dincer I 2010). The TES equation is given below:

$$Q_{Latent} = m\Delta h_L \qquad 2.46$$

2.5.3 TES in hydrolysation process

Hot water thermal energy storage system was used to store the sensible heat released when hydrolysates was cooled down to 4°C. Several well insulted cylinders attached in series and TES system was charged when hydrolysates were cooled down. TES was discharged to avoid the fluctuations in demand. Diffusers were used in the tank to avoid the mixing in tank to avoid the thermal loss. **Figure 3.13** shows how to use sensible heat released by hydrolysates to heat up water and store it.

Chapter 3

3 System Design

This chapter describes the study and assumptions for the freeze concentration, refrigeration loads and heat recovery, which is the basis for the software simulation and result analysis.

3.1 System description

The system consists of three parts named as crystallizer, wash column and refrigeration system. The configuration for crystallizer features a wall cooled drum crystallizer in which an anchor mixer is fitted equipped with scrapers to keep the walls ice-free and with internals for enhanced bulk mixing attached to the arms of the anchors (van Beek, 2018).

The wash columns separate the ice by making a compressed bed of ice which is forced from bottom to top through a column. The bed is continuously fed from the bottom and scraped of at the top. As it moves at relatively slow speed from bottom to top, wash water is pressed into the bed from top to bottom to provide an intensive washing of the ice. The ice bed transport is generated by hydraulic forces of a slurry pump (HWC) or the direct mechanical action of a piston (PWC). The liquid leaves the column via a filter which is integrated in filter tubes in the column or in an annual ring around the column (HWC) or via a filter plate which is mounted on top of the piston (PWC). The typical filter width is 150 mm (van Beek, 2018).

The hydraulic and piston wash column have a typical limit for trouble free operation with water production around 30–50 mm^2s^{-1} viscosity (D. Verdoes, 2003). To overcome this limitation a multiple stage step can be used in which ice flows to the most dilute stage and concentrated solution flows to the most concentrated stage (van Beek, 2018).

A trans-critical CO_2 system was developed with an evaporator pressure of 10 bar while the intermediate and high side pressures were 35 bar and 100 bar respectively. Two cases were studied with and without ejector. To enhance the heat recovery a thermal energy storage was also included.

Refrigeration process begins with evaporation of CO_2 at -40°C which keeps the crystallizer in desired temperature while desuperheater is used to cool down CO_2 to saturated gas and all this superheat is used to melt down the ice in ice slurry and excessive water obtained by this process is used in hydrolysation process. Saturated liquid at 35 bar is throttled down to evaporator at 10 bar while the saturated gas is preheated with internal gas heat exchanger and compressed to 100 bar. Two gas coolers cool down the CO_2 till 30°C while heating hydrolysate to 50°C and 90°C. After Internal gas heat exchanger, the CO_2 is throttled down to 35 bar in separator and this process repeats itself. **Figure 3.1** shows the complete schematic of proposed CO_2 system.

3.2 System Sketch

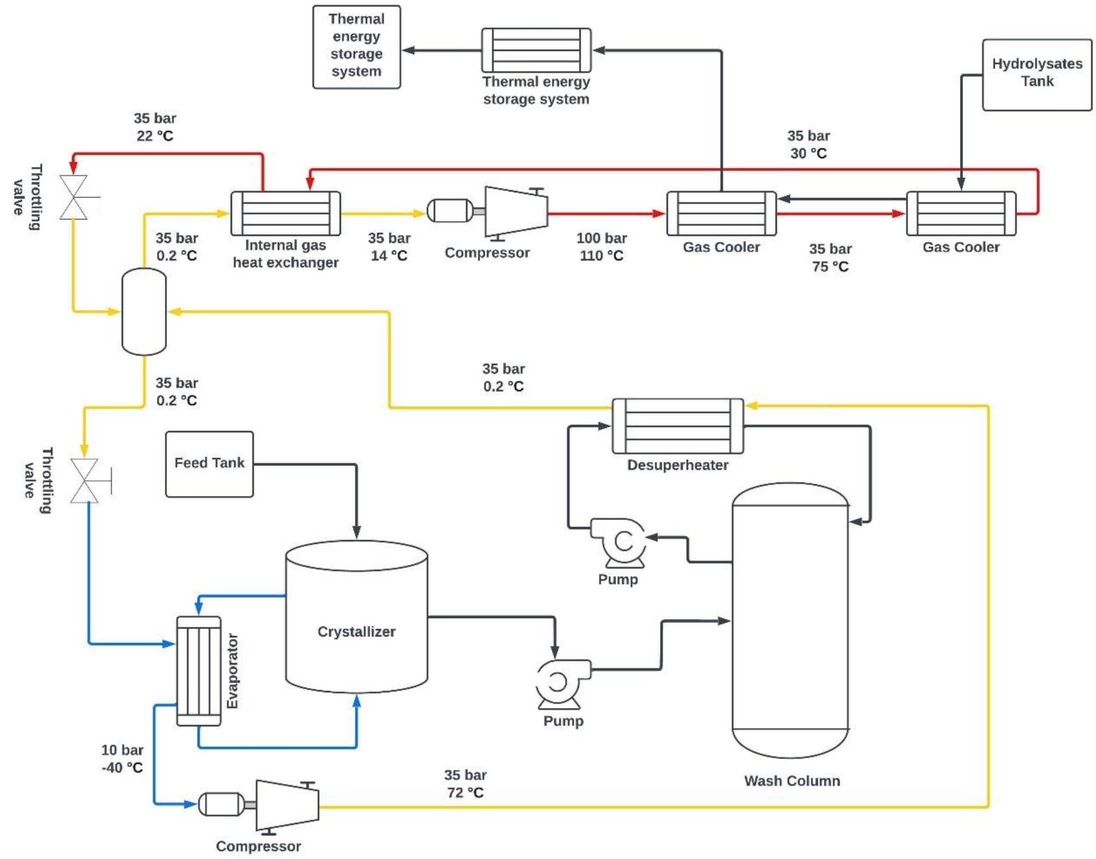

Figure 3.1 Schematic diagram of CO_2 system

Two case studies were adopted for freeze concentration. One deals with batch flows and other deals with steady state flow. The freeze concentration process also contains two equipment's named as crystallizer and wash column. The description of both processes is given below:

3.2.1 Batch Process:

The working of system starts with feeding liquid hydrolysates into crystallizer in batches. In this study, 1741 kg of hydrolysates is considered as one batch. The crystallizer forms a liquid slurry which contains ice crystals and concentrated solution. With the help of pump, this liquid slurry is transported to wash column and due to difference in densities between ice and concentration solution both are separated using a filtration column inside a wash column. The evaporator is used to keep crystallizer at desired temperature of -40 ℃ and desuperheater heat is used to melt the ice. The water recovered in this process is stored in tank which can be used in hydrolysation process. In this process the desired concentration of hydrolysates is achieved in one go.

3.2.2 Steady State Process:

The working of system starts with feeding liquid hydrolysates into crystallizer continuously. 15 percent of ice is formed in crystallizer which is pumped to wash column for separation. The concentrate solution is collected in receiver. The concentrated solution is pumped back to crystallizer and same process is repeated until the desired concentration is achieved. After the desired concentration is achieved with the help of 3 side valve concentrated solution is collected without disturbing the process cycle. **Figure 3.2** shows the steady state process.

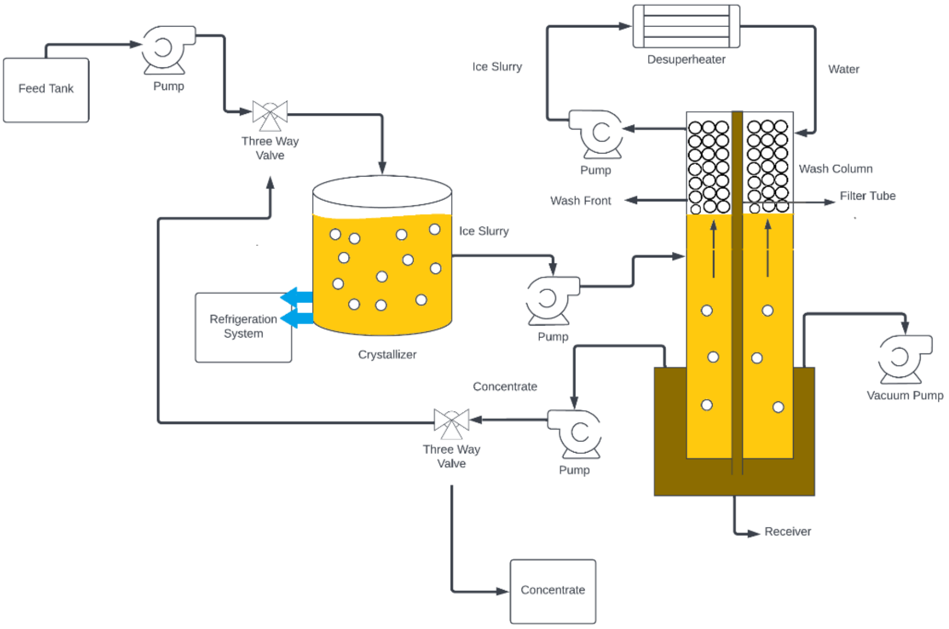

Figure 3.2 Schematic diagram of steady state process

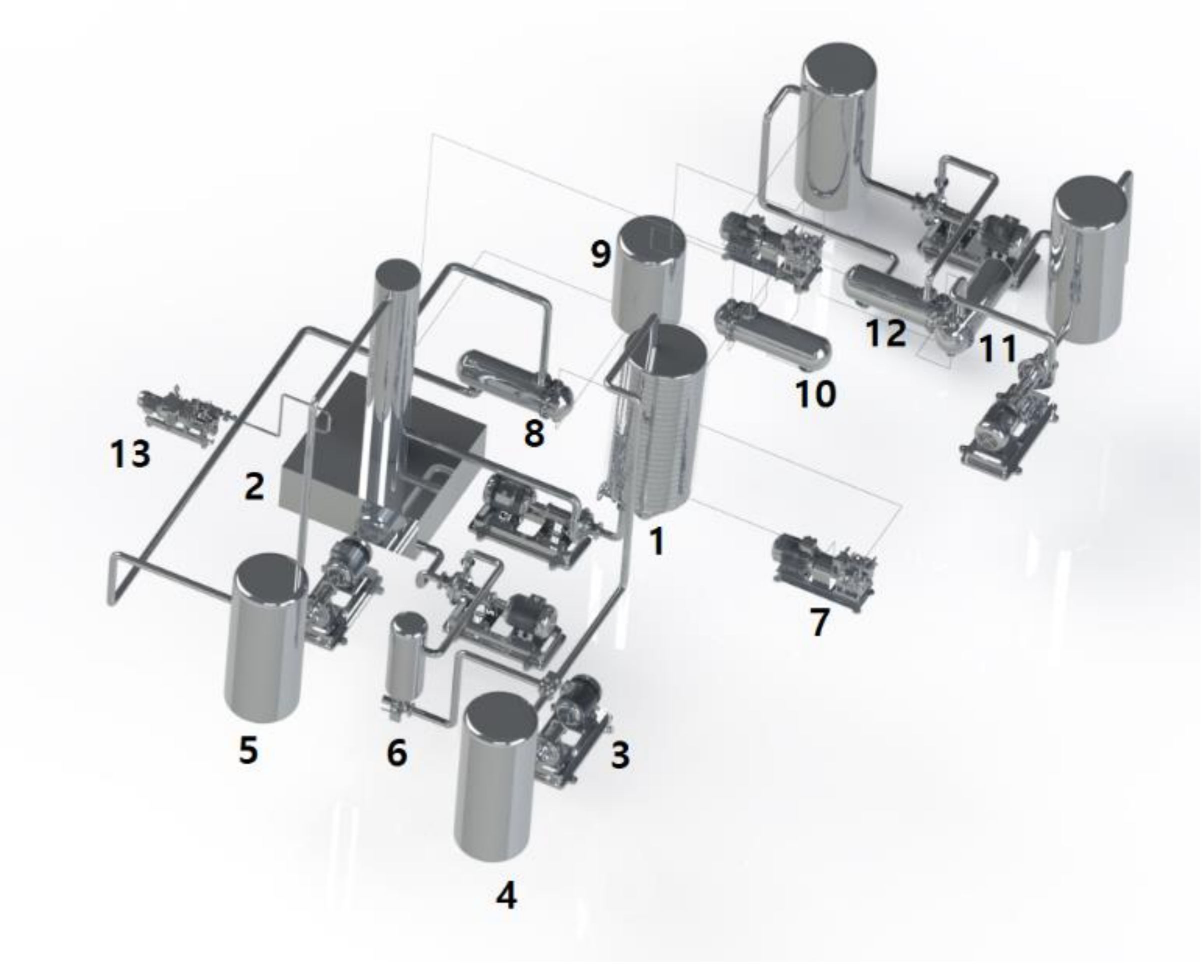

Figure 3.3 3d model of CO_2 refrigeration system with crystallizer and wash column

1)Crystallizer 2) Wash column 3) Pump 4) Hydrolysate storage tank 5) Water storage tank 6) Concentrate storage tank 7) Compressor 8) Desuperheater 9) Separator 10) Internal heat exchanger 11) 1st Gas Cooler 12) 2nd Gas Cooler 13) Vacuum pump

Ice slurry is formed in crystallizer (1) which is pumped to wash column (2). Ice and concentrated solution are separated in wash column. Concentrated solution is pumped to tank (6) for storage. If desired concentration is not achieved the concentration solution is pumped back to crystallizer. Crystallizer also works as an evaporator; CO_2 evaporates while cooling down the hydrolysates. Compressor (7) compresses the CO_2 to 35 bar and superheat is used to melt the ice with the help of desuperheater (8). Saturated gas and liquid are collected in separator, throttling valve is used to reduce the pressure of saturated liquid to 10 bar which is transported to crystallizer to cool down hydrolysates. Internal gas heat exchanger (10) is used to increase the COP of system. After internal gas heat exchanger CO_2 is compressed to 100 bar, two gas cooler (11 and 12) are used to heat up the hydrolysates to 90℃ and 50℃.

3.3 Fish Protein Hydrolysates

Fish protein hydrolysate (FPH) is a breakdown product of fish proteins containing smaller peptides and amino acids. FPH is obtained by treatment of fish meat with trypsin, alcalase, chymotrypsin, pepsin, or other enzymes under controlled conditions of pH and temperatures. Most FPHs are amorphous powders, hygroscopic in nature, containing 81–93% protein, less than 5% fat and 3–8% ash and 1–8% moisture (Venugopal, 2016).

Fish protein hydrolysates comprise of 93% of water,6.3% of protein, 0.35% of fat and 0.35% of ash. The estimation of solution was carried out to predict the properties of FPH and will be validated by experiments.

3.4 Specific heat

Specific heat, Cp is the amount of energy, which is necessary to increase temperature of 1 kg of product by one Kelvin (J $kg^{-1}K^{-1}$). Specific heat of food materials is taken usually at atmospheric pressure. Water has the highest Cp among other food compounds. Thus, the specific heat capacity of products cannot be higher than the value of the specific heat of water: approx. 4.18 kJ kg^{-1} K^{-1}. Heat capacity of foods is calculated as a sum of the heat capacities of its compounds (Cp,i) multiplied by its mass shear (xi) in the product (Eikevik, 2021b).

$$C_p = \sum x_i C_{p,i} \tag{3.1}$$

most of the food compounds have the heat capacity in the range between 1.0 and 2.2 kJ kg^{-1} K^{-1}. Only water has heat capacity of 4.18 KJ $kg^{-1}K^{-1}$ at normal conditions (temperature of 25°C and atmospheric pressure). All the food compounds, except of water, show increasing of the heat capacity with the increasing of the temperature. Water shows opposite trend.

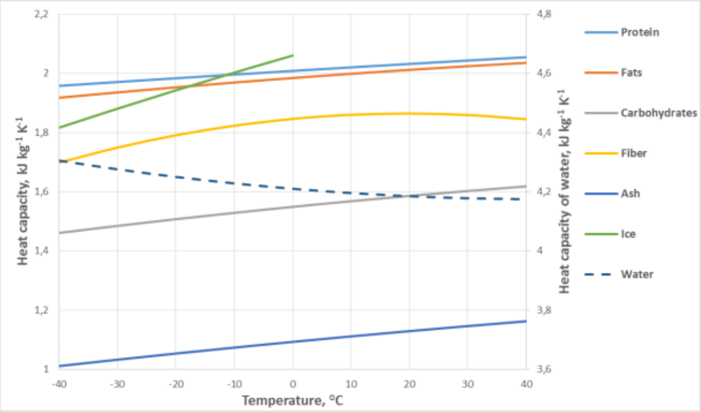

Figure 3.4 Heat capacities of food compounds (Eikevik, 2021b).

3.5 Density

Density (kgm^{-3}) is the important transport property for calculation of heat and mass transfer phenomena in food. It reflects the ratio of mass to volume of a product. The influence of temperature and pressure on density of basic compounds of foods is relatively small due to their low compressibility and low thermal expansion. The density of ash, proteins, fats, ice and carbohydrates are increasing with increasing of the temperature and pressure. The increasing can be described by quasi-linear trend-line in the temperature range between -40.0 and +40.0 °C. However, water shows some deviation from this trend. The density of pure (fresh) water increases between its melting point (0.0 °C) and 4.0 °C. The density of air is strongly affected by pressure and temperature (Eikevik, 2021b).

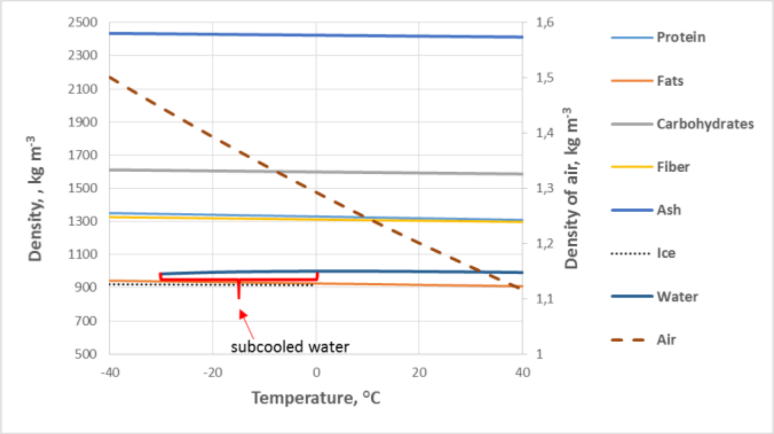

Figure 3.5 Density of food compounds with respect to temperature (Eikevik, 2021b).

3.6 Freezing Load:

The freezing load of hydrolysates in crystallizer is estimated by CpΔT. This is the heat which should be removed by evaporator. Fish protein Hydrolysates contain proteins, fats and ash. It reduces the freezing point of solution due to the dissolved solutes in water. The initial freezing point of the hydrolysates was experimentally determined by DSC which was -0.61℃. When ice forms, it doesn't contain any solutes molecules and the concentration of solutes increases in the rest, which prevent the full crystallization of hydrolysates at initial freezing point.

Hydrolysate's freezing is a transient process some of water freezes at the initial freezing point that changes the thermal properties of solution. This phenomenon of freezing point depression continues until final freezing temperature. The process up to required freezing point is the combination of sensible and latent heat.

The calculation of freezing load was done in following way. First calculate the fraction of ice based on initial freezing point and final freezing temperature.

$$\mathrm{x_{ice,T}} = \left(1 - \frac{\mathrm{T_f}}{\mathrm{T}}\right)\left(\mathrm{x_w} - \mathrm{x_{un,w}}\right) \qquad 3.2$$

Latent heat of water for final freezing temperature

$$\mathrm{L_{w,T}} = \mathrm{L} * \mathrm{x_{ice,T}} \qquad 3.3$$

Sensible heat to cool solids and fats from $\mathrm{T_o}$ to T

$$\Delta \mathrm{h_s} = (\mathrm{x_p Cp_p} + \mathrm{x_{ash} Cp_{ash}} + \mathrm{x_{fats} Cp_{fats}})(\mathrm{T_o} - \mathrm{T}) \qquad 3.4$$

Sensible heat to cool down unfreezable water from $\mathrm{T_o}$ to T

$$\Delta \mathrm{h_s} = \mathrm{x_{un,w} Cp_w}(\mathrm{T_o} - \mathrm{T}) \qquad 3.5$$

Sensible heat to cool freezable water to freezing point

$$\Delta \mathrm{h_{freezable,w}} = \mathrm{x_{liq} Cp_{ice}}(\mathrm{T_o} - \mathrm{T_f}) \qquad 3.6$$

Sensible heat to cool ice:

$$\Delta \mathrm{h_{ice}} = \mathrm{x_{ice} Cp_{ice}}(\mathrm{T_f} - \mathrm{T}) \qquad 3.7$$

Sensible heat to cool water, which is still unfrozen at Temperature 'T' (except for unfreezable water, which is calculated earlier, otherwise the unfreezable water should be included into the amount of liquid water):

$$\mathrm{x_{liq,w}} = \mathrm{x_w} - \mathrm{x_{ice}} - \mathrm{x_{un,w}} \qquad 3.8$$

$$\Delta \mathrm{h_{liq,w}} = \mathrm{x_{liq,w} Cp_w}(\mathrm{T_f} - \mathrm{T}) \qquad 3.9$$

Total freezing load will be

$$\mathrm{Q_f} = \dot{\mathrm{m}}(\mathrm{L_{w,T}} + \textstyle\sum_{\mathrm{i}=1}^{\mathrm{m}} \Delta \mathrm{h_i}) \qquad 3.10$$

Final Freezing Temperature (°C)	Ice content	$\mathrm{Q_f}$ (kW)
-2	0.6116	113.31
-5	0.7726	143.72
-10	0.8263	158.45
-20	0.8532	174.4
-40	0.8666	199.7

Table 3.1 Freezing temperature vs ice content and $\mathrm{Q_f}$

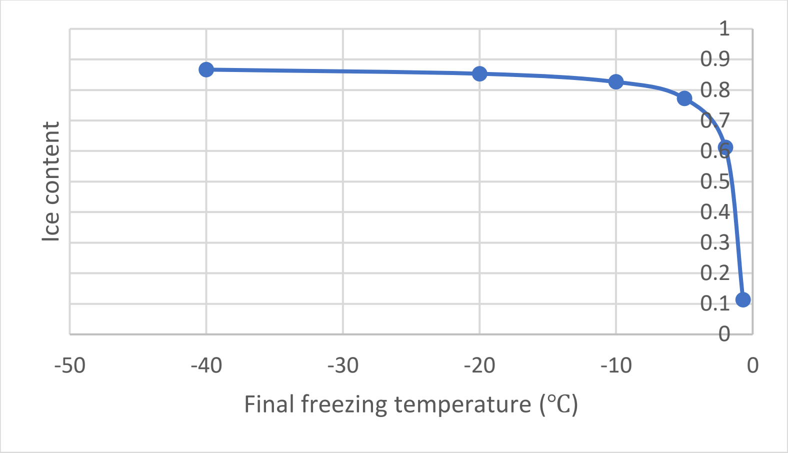

Figure 3.6 Ice content vs final freezing temperature

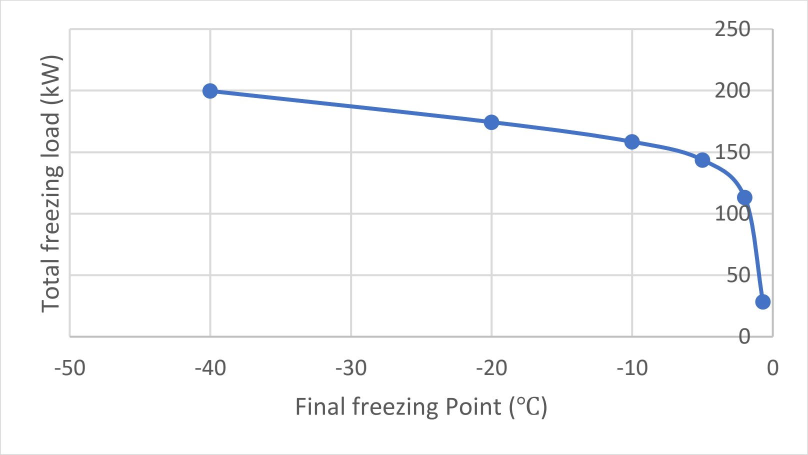

Figure 3.7 Total freezing load vs Final freezing point

For the batch process the desired concentration is achieved in one go in crystallizer and batch is pumped to wash column so the freezing load will vary with time. The freezing load contains two parts one subcooling till freezing point and other part contains the removal of latent heat.

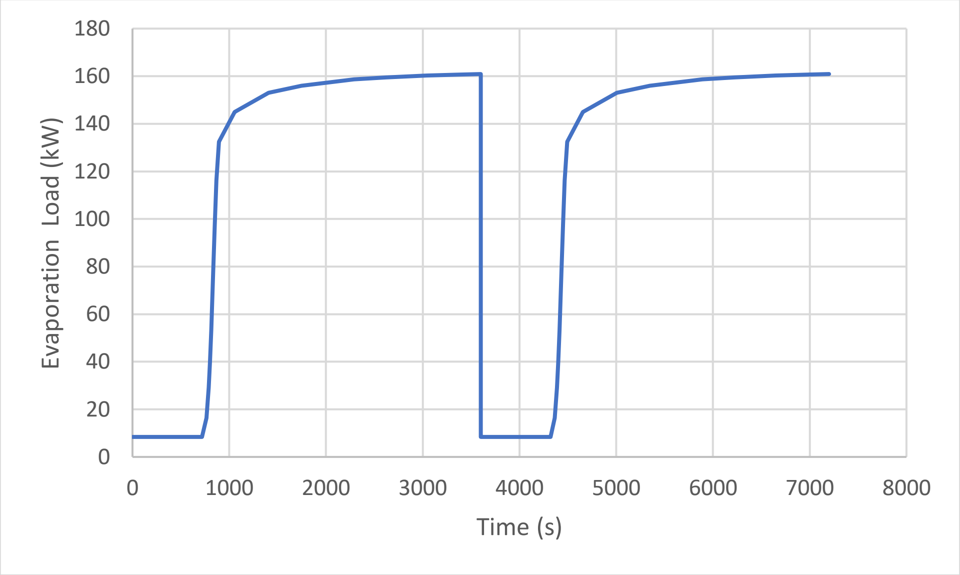

Figure 3.8 Batch Process Evaporation Load Vs Time

For steady state process the system is warmed up to achieve the desired concentration. Freezing load varies with respect to time and after the desired concentration is achieved the freezing load is constant. The freezing load can be divided into two parts, first part shows the cooling duty from 4℃ to initial freezing point and second part depicts the removal of latent heat (15 % as only 15 percentage of ice is formed).

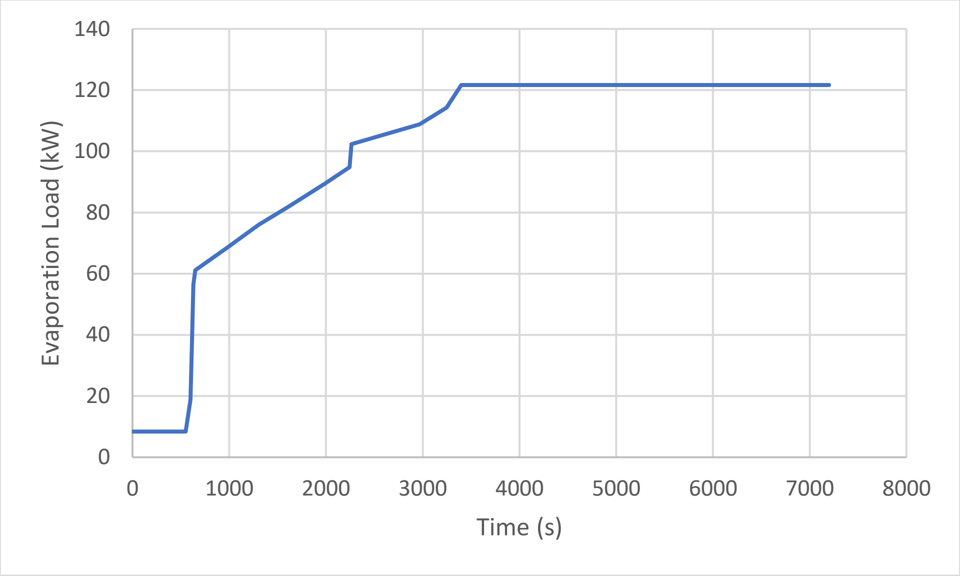

Figure 3.9 Steady State Process Evaporation Load Vs Time

3.7 Wash Column:

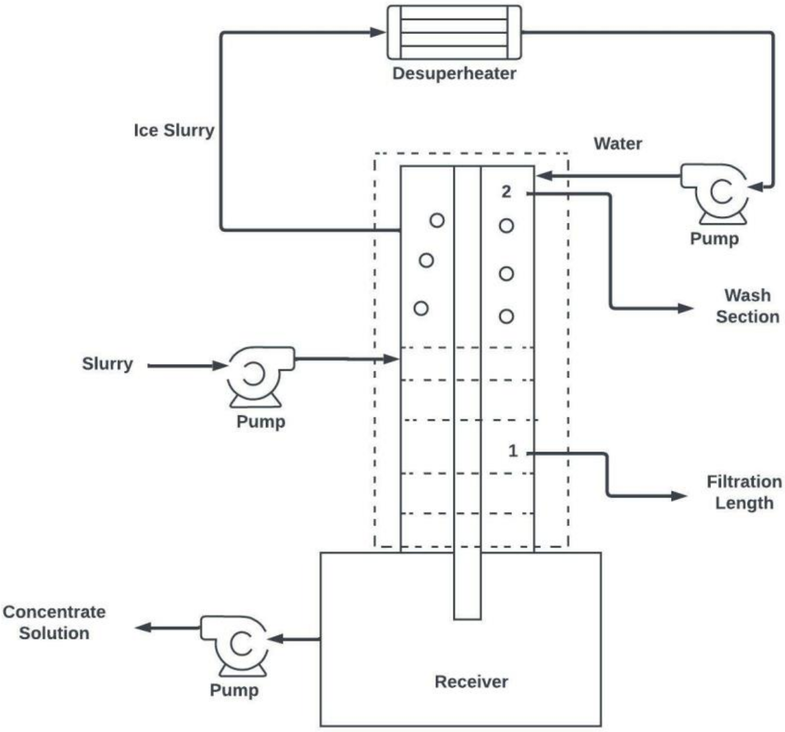

Figure 3.10 Schematic diagram of wash column

To derive this system three main sections are defined which are bottom section, top section and melting circuit. The bottom section stretches from the bottom of wash column to the filters. It contains filtration section (1) which is the part of the packed bed between the top of the bed and the filters. The position of filter is fixed, and the top of the crystal bed is determined by the length of the filtration section L filtration (m).

The top section stretches from filters till washing front (2), due to the difference in densities the ice moves to wash front while the mother liquor drops down and is collected from the receiver of the wash column.

The melting circuit consists of three components, the circulating pump, condenser and desuperheater which melts the ice. The dotted lines on the **Figure 3.10** shows our control volume.

3.7.1 Assumptions

The assumptions used to derive the dynamic model are:

- The column is totally filled with liquid and crystals.
- Both liquid and crystals are incompressible.
- Water is used as wash liquid.
- The column is one dimensional and there is only flow in axial direction.
- The porosity and permeability in the defined section are constant.
- The melting circuit applies enough heat to melt ice crystals.
- Wash liquid doesn't reach the filters.

3.7.2 Volume Balance

3.7.2.1 Bottom Section

In bottom section there are two phases present crystals and mother liquor

$$\text{Ø}_{\mathrm{feed}} = \text{Ø}_{\mathrm{s}} + \text{Ø}_{\mathrm{ml,filters}} \tag{3.11}$$

Ø_s (m^3/s) is the amount of ice that moves at the top of wash column while $\text{Ø}_{ml,filters}$ (m^3/s) is the mother liquor that leaves the column via filters.

The length of the filtration section is calculated with the help of solid mass balance at the bottom section:

$$\frac{dV_{\mathrm{cr,bottom}}}{dt} = \text{Ø}_{\mathrm{feed}} - \text{Ø}_{\mathrm{ml,filters}} \tag{3.12}$$

The total amount of crystals in the bottom section will be:

$$V_{\mathrm{cr,bottom}} = A_c * ((1-\varepsilon) l_{\mathrm{filtration}} + l_{\mathrm{slurry}}) \tag{3.13}$$

As the length of bottom section is constant so, the length of filtration is calculated by combination of equation (3.12) and (3.13) which gives:

$$\frac{dL_{\mathrm{filtration}}}{dt} = \frac{\text{Ø}_{\mathrm{feed}} - \text{Ø}_{\mathrm{ml,filters}}}{A_c(1-\varepsilon)} - \frac{dL_{\mathrm{slurry}}}{dt} \tag{3.14}$$

Required parameters are ε and A_c, where ε is the porosity of the crystal bed while A_c is the cross-sectional area of wash column. Bernoulli equation was used to calculate the volume flow rate of mother liquor. **Figure 3.11** shows the state points used in Bernoulli equation. The Bernoulli equation is given below:

$$P_1 + \rho g h_1 + {}^1\!/_2\, \rho {v_1}^2 = P_2 + \rho g h_2 + {}^1\!/_2\, \rho {v_2}^2 \tag{3.15}$$

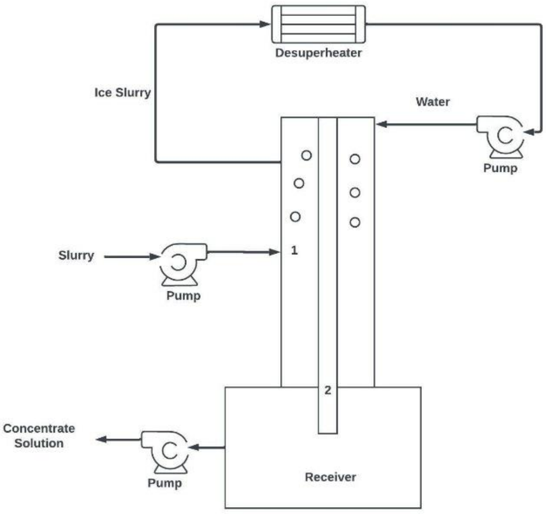

Figure 3.11 State points for Bernoulli equation

h₁ and v₁ are zero because point one is the reference point to measure height and v₁ is zero because of stagnation in wash column so the Bernoulli equation will be:

$$P_1 = P_2 + \rho g h_2 + {}^{1}/_{2}\,\rho {v_2}^2 \qquad 3.16$$

$$v_2 = \sqrt{\frac{2(P_1 - P_2)}{\rho} - 2gh_2} \qquad 3.17$$

$$\text{Ø}_{\text{ml,filters}} = v_2 A_c \qquad 3.18$$

Volume flowrate can be calculated by multiplying velocity with cross section area of filter holes in filter tube.

3.7.2.2 Top Section:

In the top section one solid phase, the crystals and two liquid phases are present, wash liquid and mother liquor. The total volume is constant therefore an overall volume balance for the top section combines the flow entering and leaving the control volume. The ice volume (C_s) and the volume of wash liquid (C_l):

$$\text{Ø}_{\text{ml,filters}} + C_l = \text{Ø}_s + C_s + \text{Ø}_{wl} \qquad 3.19$$

Due to the densities difference between liquid and solid material C_s and C_l are not equal but they can be related by their respective densities.

$$C_l = \frac{\rho_s}{\rho_l} * C_s \qquad 3.20$$

The heat required to melt the crystals can be calculated by heat balance and the temperature difference between temperature of feed and melting point of ice.

$$C_s = \frac{C_p(T_m - T_{feed})}{\Delta H_l} * \text{Ø}_s \qquad 3.21$$

It is assumed that wash liquid doesn't reach filters therefore there is no loss of wash liquid out of column via filters. The wash column length can be calculated by:

$$\varepsilon_w * A_c * \frac{dL_w}{dt} = \text{Ø}_{w,l} - C_l \qquad 3.22$$

The porosity in the wash section can easily be calculated from heat balance and porosity of bottom:

$$\varepsilon_w = \varepsilon - (1 - \varepsilon) * \frac{C_p * (T_m - T_{feed})}{\Delta H_l} \qquad 3.23$$

When the ice starts melting the mother liquor flows out of the bottom section:

$$A_c * \varepsilon * \frac{dL_w}{dt} = \emptyset_{ml,bottom} \qquad 3.24$$

So, the concentrated solution flowing out can be calculated by:

$$\emptyset_{conc} = \emptyset_{ml,bottom+}\emptyset_{ml,filters} \qquad 3.25$$

3.7.2.3 Melting Circuit

The packed ice at the top is melted using condenser and subcooler heat through wash liquid with the assumption that crystals start melting as they enter melting circuit, the following mass balance holds if the correction of densities between solid and liquid are considered.

$$\frac{\rho_s}{\rho_l} * \emptyset_s = \emptyset_{wl} + \emptyset_{ice,s} \qquad 3.26$$

A MATLAB program is developed to solve this dynamic model and (**Appendix B**) contains the skeleton file.

3.7.2.4 Exponential Approximation

Exponential approximation was used to calculate the required filtration length of the wash column, the approximation is given below:

$$X = \int Ce^{-aL} dL \qquad 3.27$$

Where,

X, C, a and L are the share of ice fraction, share of the concentrated solution, porosity of crystal bed and filtration length respectively and (**Appendix C**) contains the skeleton file.

3.8 Heat Recovery

Desuperheater heat can be used to melt the ice slurry which can be used in hydrolysation process. For heat recovery estimation of enthalpy values of CO_2 at different temperatures (CoolPack) were used. More heat can be recovered when hydrolysates are cooled down from 70°C to 4°C. Hydrolysates at 90°C can preheat upcoming hydrolysates from 2nd gas cooler to 70°C. The remaining heat can be stored in TES until hydrolysates are cooled down to 4°C

For heat recovery estimation enthalpy values of CO_2 at different temperatures (CoolPack) were used.

$$Q = \dot{m} * \Delta h \qquad 3.28$$

The heat recovery from the refrigeration system is dependent on the refrigeration load and operation conditions. Figure below elaborates the heat recovery scheme opted for this system.

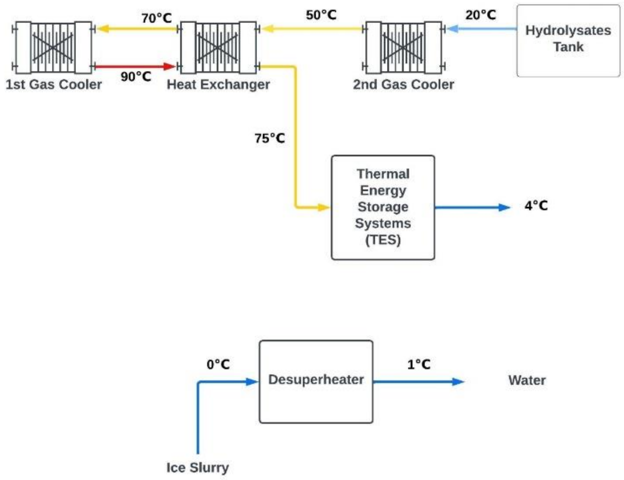

Figure 3.12 Heat recovery

3.9 Thermal Energy Storage System with water

To store the heat from hydrolysates that are cooled from 75℃ to 4 ℃ a TES system was used. Water was heated up to 60℃ and stored in well insulated tanks, this hot water can be used for domestic purposes. The proposed thermal energy storage system is given below:

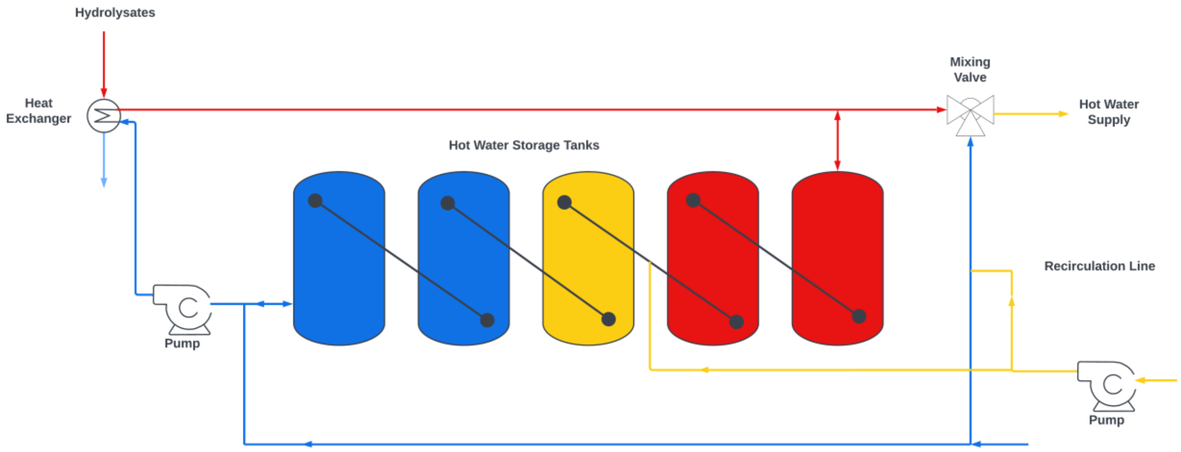

Figure 3.13 Thermal Energy Storage System.

Thermal stratification was employed to minimize the mixing effect in domestic hot water tank which minimized the thermal losses.

Chapter 4

This chapter contains the simulation model and the related assumptions. Batch crystallizer and wash column simulations were carried out in MATLAB while the refrigeration cycle simulation was carried out in Dymola.

4 Simulation Software

MATLAB stands for matrix laboratory is a proprietary multi-paradigm programming language and numeric computing environment developed by MathWorks. MATLAB allows matrix manipulations, plotting of functions and data, implementation of algorithms, creation of user interfaces, and interfacing with programs written in other languages.

Dymola software contains components and refrigerant libraries from TLK-Thermo GmbH which were used for dynamic simulations. Three libraries were used, TIL 3.90 for components such as compressors, heat exchanger and vales. TIL 3.90 was used for refrigerants and secondary fluid while TIL 3.9.2 to read and input refrigeration load files. Dave is a software from TLK which can be used to plot Dymola results. Ph and Ts diagrams can also be visualized with the help of TLK Dave. The software can read two inputs load formats MATLAB(.mat) and Excel(.csv). The software has a built-in control of different parameters and boundary conditions.

EES also known as Engineering equation solver can be used to solve thousands of coupled non-linear algebraic and differential equations. Software can also be used to solve differential and integral equations, perform linear and nonlinear regression, check unit consistency, and generate high quality graphs. A major feature if EES is the high accuracy of thermodynamic and transport properties database which can be used to calculations.

4.1 Time Discretization

To numerically solve a partial differential equation which is dependent on time one must discretize that partial differential equation in time. There are many numerical methods to solve time dependant partial differential equations named as Euler, TVD, Heun and classical Runge-Kutta method. The major difference between these methods is the stability of method which is determined by time step. Classical Euler discretization is given below:

$$\mathrm{U}^{\mathrm{n}+1} = \mathrm{U}^{\mathrm{n}} + \mathrm{dt} * \mathrm{R}(\mathrm{U}) \qquad 4.1$$

Where ,

$\mathrm{U}^{\mathrm{n}+1}$ represents solution at next time step

U^{n} shows solution at current time step

dt time step

R(U) Contant terms

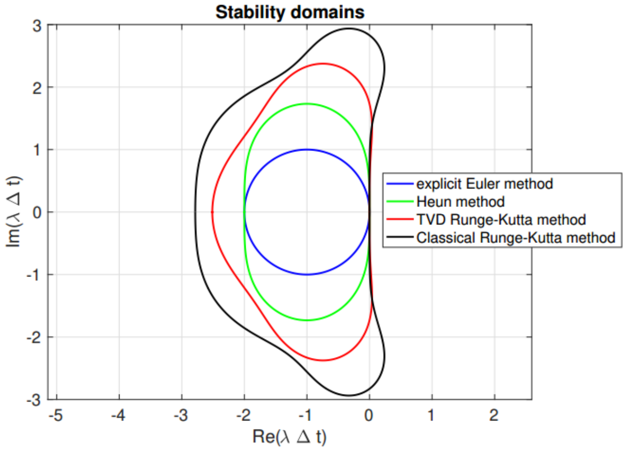

Figure 4.1 Stability domains of explicit Euler method, Heun's method, TVD Runge Kutta method, and classical fourth-order explicit Runge-Kutta method (Muller, 2020).

For this project Euler method was used for time Discretization.

4.2 Model Description

In this project three components were simulated named as crystallizer, wash column and refrigeration system. Simulation of crystallizer and wash column was carried out in MATLAB while simulation of refrigeration system was carried out in Dymola.

To simulate crystallizer, six coupled partial differential equations were solved and the time discretization of those PDE's is given below:

$$\mu_0{}^{n+1} = \mu_0{}^{n} + dt * (B_0 * V) \tag{4.2}$$

$$\mu_1{}^{n+1} = \mu_1{}^{n} + dt * (\mu_0{}^{n} * v_{ice}) \tag{4.3}$$

$$\mu_2{}^{n+1} = \mu_2{}^{n} + dt * (2 * \mu_1{}^{n} * v_{ice}) \tag{4.4}$$

$$\mu_3{}^{n+1} = \mu_3{}^{n} + dt * (3 * \mu_2{}^{n} * v_{ice}) \tag{4.5}$$

$$T_b{}^{n+1} = T_b{}^{n} + dt * \left(-\frac{U * A * (T_b - T_\infty)}{V * (\rho_l * Cp_l + (\rho_{ice} * Cp_{ice} - \rho_l * Cp_l) * k_v * \mu_3{}^{n})} - \frac{\mu_3{}^{n+1} - \mu_3{}^{n}}{dt} * \frac{((\rho_{ice} * Cp_{ice} - \rho_l * Cp_l) * k_v * T_b - \rho_{ice} * h_{ice} * k_v))}{\rho_l * Cp_l + (\rho_{ice} * Cp_{ice} - \rho_l * Cp_l) * k_v * \mu_3{}^{n}}\right) \tag{4.6}$$

$$T_f{}^{n+1} = T_f{}^{n} + dt * \left(\frac{R * T^2}{\Delta_f * H} * \frac{-\frac{m_{s,0}}{M_s} * \frac{\rho_{ice} * k_v * V}{M_w}}{\left(\frac{m_{s,0}}{M_s} + \frac{m_{w,0}}{M_w} - \frac{\rho_{ice} * k_v * V * \mu_3{}^{n}}{M_w}\right) * \left(\frac{m_{w,0}}{M_w} - \frac{\rho_{ice} * k_v * V * \mu_3{}^{n}}{M_w}\right)} * \frac{\mu_3{}^{n+1} - \mu_3{}^{n}}{dt}\right) \tag{4.7}$$

$$v_{ice} = k_v * (T_f{}^{n} - T_b{}^{n})^a \tag{4.8}$$

$$B_0 = k_n * (T_f{}^{n} - T_b{}^{n})^b \tag{4.9}$$

All these six equations were solved simultaneously in one time step. The simulation was run for 3600 seconds with a time step of 0.0001 seconds. To increase the stability domain of simulations and decrease the time step RK method 4 was also implemented. General form of RK method 4 is given below:

$$\frac{dy}{dt} = f(t, y), y(t_0) = y_0 \tag{4.10}$$

Here y is the unknown function of time t and $\frac{dy}{dt}$ should be approximated numerically to find out the value of unknown function with respect to time. At time t_0 the initial values will be used which are given in **Table 4.2**. RK method 4 discretization is given below:

$$y^{n+1} = y^n + \frac{1}{dt} * (k_1 + 2k_2 + 2k_3 + k_4) \tag{4.11}$$

$$t^{n+1} = t^n + dt \tag{4.12}$$

$$k_1 = f(t^n, y^n) \tag{4.13}$$

$$k_2 = f\left(t^n + \frac{h}{2}, y^n + h\frac{k_1}{2}\right) \tag{4.14}$$

$$k_3 = f\left(t^n + \frac{h}{2}, y^n + h\frac{k_2}{2}\right) \tag{4.15}$$

$$k_4 = f(t^n + h, y^n + hk_3) \tag{4.16}$$

k_1 is the slope at the beginning of the interval, using (Euler's method).

k_2 is the slope at the midpoint of the interval, using y and k_1.

k_3 is the slope at the midpoint of the interval, using y and k_2.

k_4 is the slope at the midpoint of the interval, using y and k_3.

The constant values used in calculation are given in **Table 4.1**

	Unit	Value
a	-	1
K_n	-	1*10^10
K_v	-	1*10^-6
Cp_{sol}	kJ/kg.k	4
U	W/m^2K	150
m	kg	1741
Ms	Kg/mole	342*10^-3
Mw	Kg/mole	18*10^-3
b	-	1.25

Table 4.1 Constant Terms to solve crystallizer PDE’s

K_n, K_v, a and b are coefficients that are generally determined experimentally. For now, these parameters were taken from literature. Similarly, it goes of molar weight of protein but for this project molar weight of sucrose was used.

Initial condition to solve equation (4.2), (4.3), (4.4), (4.5), (4.6) and (4.7) are given in **Table 4.2**.

	Unit	Value
μ_0	-	0
μ_1	-	0
μ_2	-	0
μ_3	-	0
T_f	℃	-0.61
T_b	℃	4

Table 4.2 Initial values to solve crystallizer PDE's

Two different approaches were used to calculate the filtration length of the wash column and the simulation to find the length was carried out in MATLAB. The time discretization of those PDE's is given below:

$$L_f^{n+1} = L_f^{n} + dt * ((\frac{\emptyset_{feed} - \emptyset_s}{A_c * (1 - \varepsilon)} + \frac{1}{(1 - \varepsilon)} * \frac{L_s^{n+1} - L_s^{n}}{dt}) \quad 4.17$$

$$X^{n+1} = X^{n} + dl * C * e^{-a*L} \quad 4.18$$

$$L_w^{n+1} = L_w^{n} + dt * \left(\frac{\emptyset_{w,l} - C_l}{\varepsilon_w * A_c}\right) \quad 4.19$$

$$\emptyset_{ml,bottom} = A_c * \varepsilon * \left(\frac{L_w^{n+1} - L_w^{n}}{dt}\right) \quad 4.20$$

The constant terms used in simulation are given in **Table 4.3**.

	Unit	Value
$\emptyset_{feed}$	m^3/s	0.0005
d	m	0.5
α	-	0.8
ρ_{ice}	Kg/m^3	917
ρ_{water}	Kg/m^3	1000
$\rho_{c,sol}$	Kg/m^3	1132
ε	-	0.2
$\emptyset_{wl}$	m^3/s	0.000034

Table 4.3 Constant Terms to solve wash column PDE's

Initial condition to solve equation (4.17), (4.18), (4.19) and (4.20) are given in **Table 4.4**.

	Unit	Value
L_f	m	0
L_w	m	0
$\emptyset_{ml,bottom}$	m^3/s	0
$\emptyset_{conc}$	m^3/s	0
$\emptyset_w$	m^3/s	0

Table 4.4 Initial values to solve wash column PDE's

The first PDE depends on time, so the simulation time was set 200 second while other PDE depend upon filtration length. Through hit and trial method, a filtration length was selected which gave 100 percent share of ice.

The refrigeration system was simulated using Dymola software with some simplifications, few of them are explained in pervious chapters and rest will be discussed in this chapter. A trans critical CO_2 system was developed to increase the COP ejector solution was also considered. Plate heat exchangers were used for all the heat exchangers. Heat exchanger coefficients are shown in **Table 4.5**.

Heat Exchanger	**Coefficient, W/m^2K**
Desuperheater	1000
Internal Gas Heat Exchanger	1000
1st Gas Cooler	1000
2nd Gas Cooler	3000

Table 4.5 Heat transfer coefficients of heat exchangers

A tube was used instead of a heat exchanger for evaporator. Heat boundary was used to give evaporation load as input and was attached to tube. Evaporation load was stored in csv file and was run using Dymola file reader. 7 PI controllers were used in the simulations the first two were used to control the frequency of efficient compressor (compressor type in Dymola) to maintain 10 and 35 bar suction pressure. Last two were used to control the opening of throttling valve which senses the high pressure which was fixed 100 bar while the other maintains 5K superheat for the low-pressure compressor.

Outlet temperature from the desuperheater was controlled by the mass flow of pump with PI controller, which took outlet temperature of desuperheater as input. Inlet and outlet temperature of hydrolysates from desuperheater was fixed to 0℃ and 25℃ respectively. The outlet temperature of desuperheater was controlled by adjusting the water flow in condenser with PI controller. To remove the desuperheater heat, ice, and water slurry at 0℃ was used.

Outlet temperature from the 1st gas cooler was controlled by the mass flow of pump with PI controller, which took outlet temperature of 1st gas cooler as input. Inlet and outlet temperature of hydrolysates from 1st gas cooler was fixed to 70℃ and 90℃ respectively. The last PI controller was used to cool down the CO2 to 30℃ while heating up the hydrolysates to 50℃.

Isentropic efficiency of compressor was fixed to 70%. Dymola doesn't contain any crystallizer library, so to visualize this tube named as "evaporator" was used which cooled down hydrolysates to desired temperature. Due to limitation of Dymola water was used instead of hydrolysates, ice, and water slurry. The complete simulation model is shown in **Figure 4.2**:

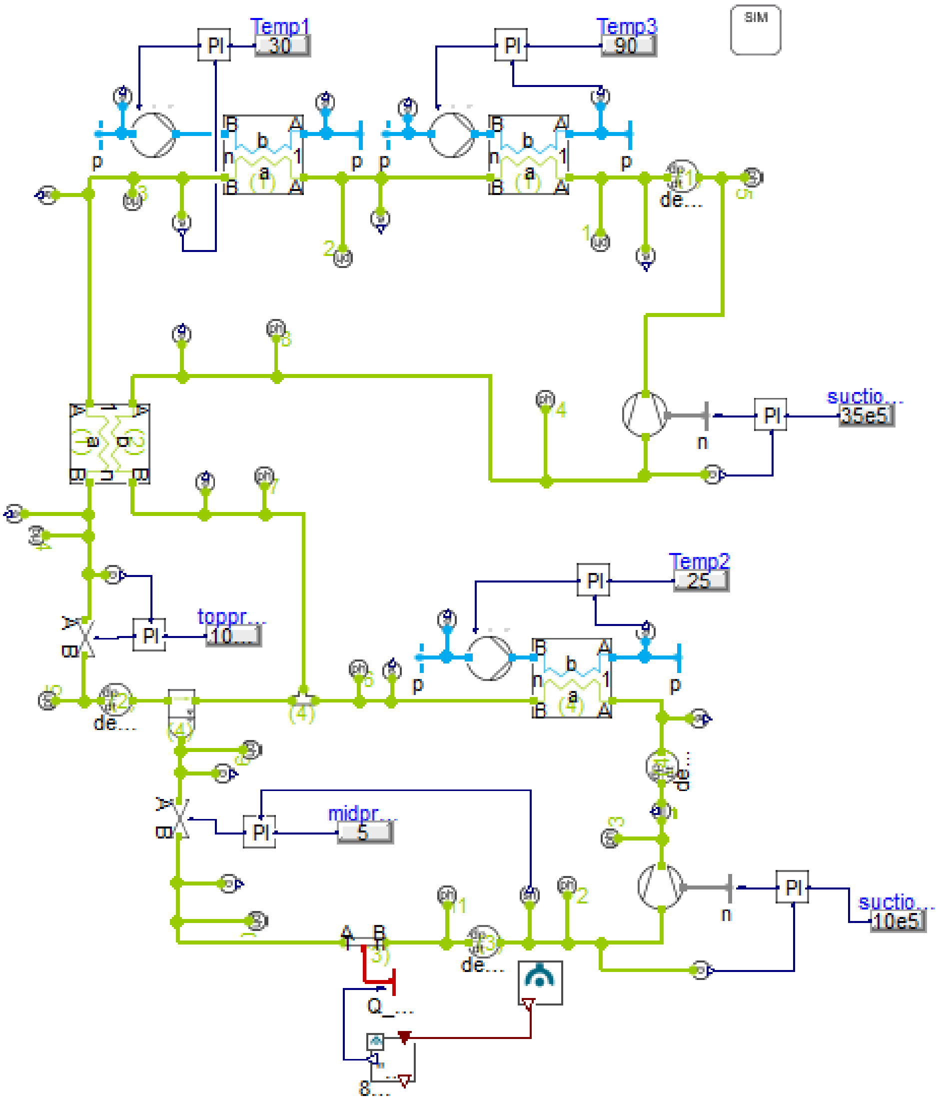

Figure 4.2 Simulation model Dymola

Chapter 5

5 Experiment Setup

Freeze concentration process setup was constructed to validate and further understand the practical challenges of the process. Freeze concentration process contains three major components refrigeration, crystallizer, and wash column system.

Varmeteknisk lab had a 12 liters crystallizer (slush machine) which was used for experiments. The crystallizer contained the refrigeration system in bottom while two compartments at top where the solution can be poured. A cylinder was attached at the bottom of compartments which contained the evaporator coils and scrubber surrounding the cylinder was attached to remove ice formation at the top of cylinder. **Figure 5.1** shows the crystallizer (slush machine).

Figure 5.1 Crystallizer (Slush machine)

1 scrubber and 2 cylinder containing evaporator coils

Wash column was constructed using Plexiglas pipe with an outer diameter of 0.1m and inner diameter of 0.09m. The 2-meter pipe was divided in two parts with equal length of 1 meter to create filtration and wash section. Filter tube holding was 3d printed and filter tubes with pore diameter of 25 µm was bought from the market. **Figure 5.2** and **Figure 5.4** shows filter tube housing, filter tube and wash column respectively.

Figure 5.2 Filter tube housing (right) and filter tube(left)

One meter filter tube wasn't available in market so 0.25m filter tube was used, and these filter tubes were stacked upon each other. Cylinder thread and nut was 3d printed to reduce the gap between filter tubes. Figure below shows cylinder threads and nut.

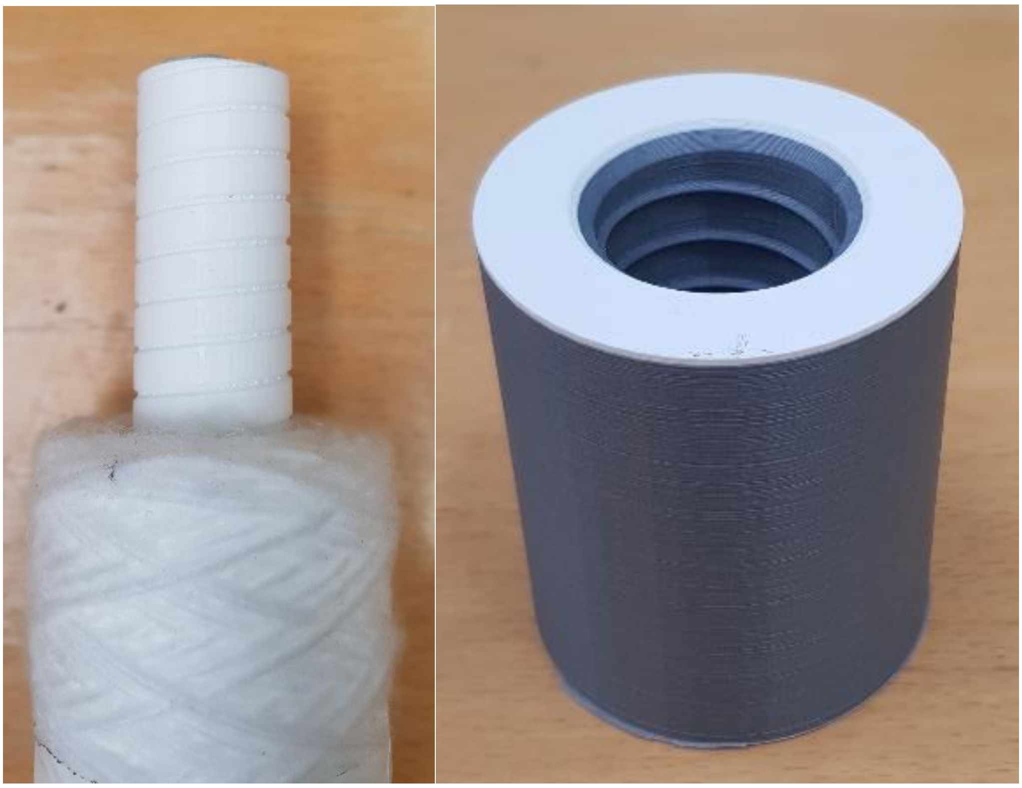

Figure 5.3 Threads with cylinder (left) and nut(right)

Figure 5.4 Wash Column

1)Wash column 2) Filtration section 3) wash section

A Plexiglas hollow cylinder was used as a receiver a hole was drilled at the centre where the bottom part of filter tube housing was glued. A vacuum pump and pressure sensor was connected at the top of receiver to maintain and measure 0.5 bar pressure all time. The main purpose of receiver was to collect the concentrated solution and pump in back to crystallizer for further processing.

Figure 5.5 Receiver

PVC pipes were used to connect the whole system together. Working principle of system as follows, crystallizer formed an ice slurry (approximately contained 15% of ice) which was pumped to wash column due to pressure difference between filtration section and receiver the concentrated fluid was collected in receiver. Concentrated solution was pumped back to crystallizer and this process was repeated until desired concentration was achieved. Cold water at the top of wash column was used to create an ice slurry which was collected in a tank. No pump was used for the transportation of water because pressurized water (7 bar) was used. **Figure 5.6** shows lab scale freeze concentration experimental setup. To maintain sub-zero temperature insulation was used on pipes and wash column.

Figure 5.6 Lab scale freeze concentration

1) Slush machine (Crystallizer) 2,7) Pump 3) Wash column 4) Filter Tube 5) Wash Front 6) Receiver 8) Vacuum Pump

Temperature probe provided by the RS pro was used to measure the temperature. The temperature measurement from temperature probe was recorded in data logger memory through USB port. Then readings from data logger was transferred to computer for further processing. The following figure shows the complete setup of temperature sensor and data logger.

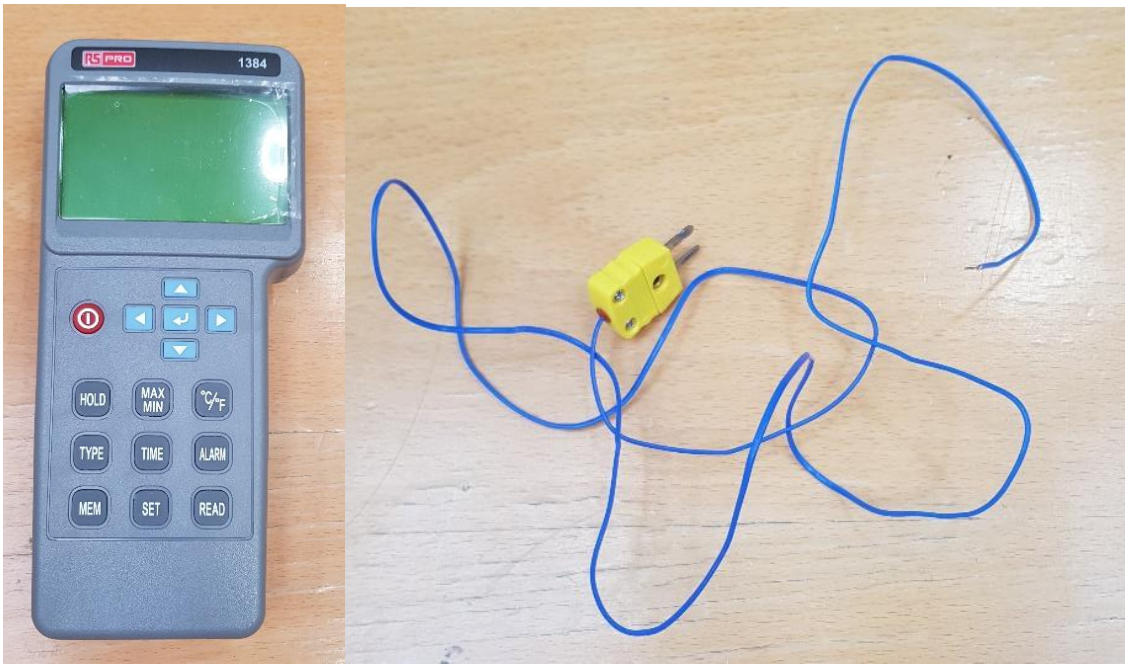

Figure 5.7 Data logger (left) and Temperature Probe (right)

Chapter 6

6 Results

This chapter describe the results and discussion of the simulated and calculated results from three different simulations. A result comparison of different parameters for solution bulk temperature, diameter of crystals, ice fraction, propagation of ice, bulk supercooling, calculation of freezing capacity and heat recovery from refrigeration system are presented and discussed in this chapter. The power and COP calculation in the results are only accounted for compressor work and heat removed by desuperheater and gas coolers. This chapter first contains the results from Dymola simulation followed by crystallizer and wash column simulations.

6.1 Design of simulation model

The refrigeration simulation model was built with assumptions and simplifications. The compressor efficiencies were fixed constant throughout the simulation time which reflects some deviation from the actual scenario. High, intermediate, and low pressures of system were controlled with the PI controller but still there were some fluctuations when the evaporation load changes with time. Two different design loads based on crystallizer function were considered (batch and steady state process). To observe the improvement in COP, ejector was also included in Dymola simulation.

The results obtained for Dymola simulation such as average wall temperature of heat exchanger, surface area of heat exchanger and capacity of evaporator were used in crystallizer and wash column dynamic simulations. Dynamic simulation of refrigeration and crystallizer system were run for two hours while the wash column simulation was run till 200 second.

6.2 Evaporation load

Two evaporation loads based on crystallizer function were studied. The first evaporator load depends upon batch process meaning a complete one batch of hydrolysates comes to crystallizer and ice is formed until the desired concentration is achieved and whole batch is pumped out to wash column where ice and concentrated solution are separated. Batch process evaporation load can be divided into two parts one cooling load (cooling down hydrolysates to initial freezing point) and second removal of latent heat fusion (formation of ice releases heat). Second evaporation load depends on steady state process in which only 15 percentage of ice is formed. Initially, this load is transient because of the warming up of the system until desired concentration. The steady state load contains the cooling duty (cooling down hydrolysates to initial freezing point), removal of 15% latent heat of fusion and additional cooling duty as the freezing point depresses. **Figure 6.1** shows both the loads for the refrigeration system:

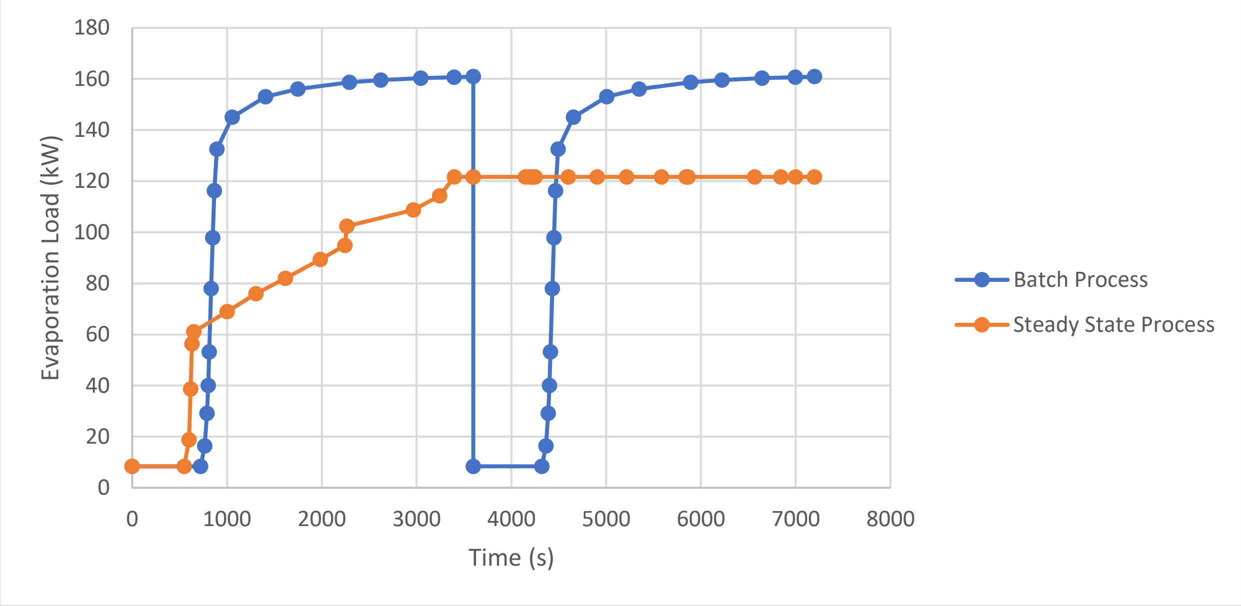

Figure 6.1 Evaporation Load Vs Time

Evaporation load for both batch and steady state process starts from 8.4 kW. For batch process it goes till 160 kW which drops to 8.4 kW after one hour and again reaches the same load as 160 kW and this loop continues until the crystallizer is run. For steady state operation the load increases till 121 kW and this load remains constant until the crystallizer process is run. The reason for low load in steady state process is 15% ice production which reduces the removal of latent heat of fusion.

6.3 Heat Recovery:

Desuperheater was used to melt the ice slurry and water obtained from this process was further used in hydrolysation process. Batch and steady state heat recovery is presented in the **Figure 6.2**.

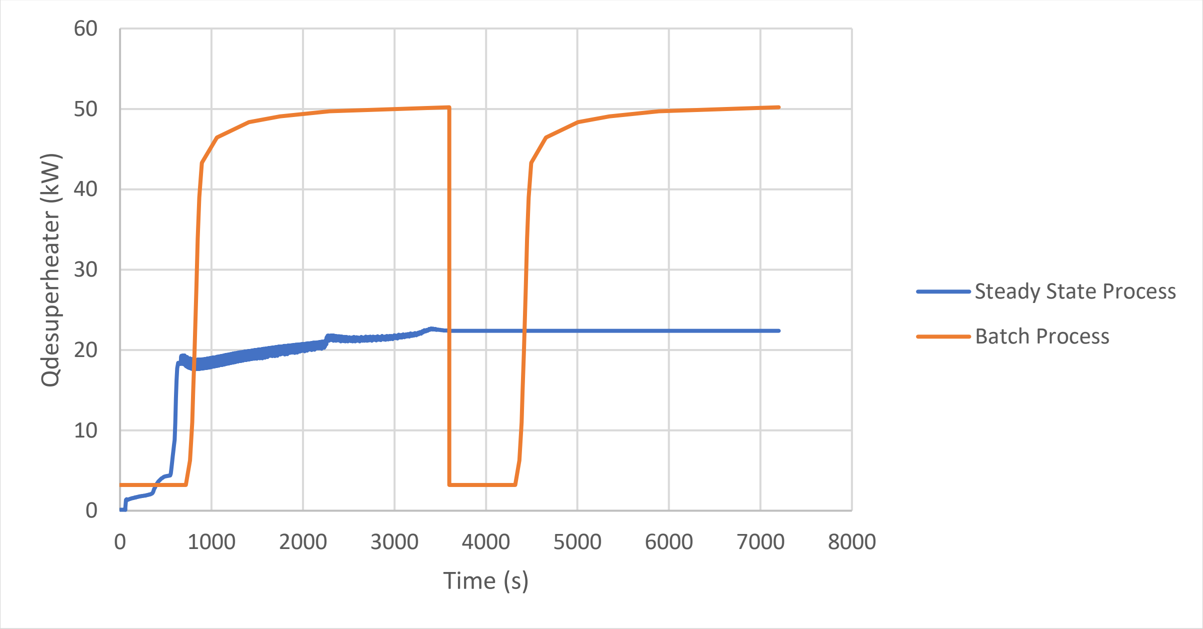

Figure 6.2 Heat Recovery Vs Time

Due to densities difference in the solution, ice comes at top in wash column which depicts the wash section. Water enters the wash section and forms an ice slurry; this ice slurry is pumped to a desuperheater where the ice in slurry is melted. Height of wash section can be controlled by pressure and mass flowrate of water supplied and it depends upon desuperheater capacity. Desuperheater capacity for batch process is more meaning more ice can be melted but due to batch process there will be more ice in wash section which might increase the size of wash column. The highest capacity for batch process is 50 kW while for steady state process is 22.4 kW.

6.4 Gas Cooler

Two gas coolers were used in the process, the first gas cooler heats up the hydrolysates to 90°C while the other gas cooler cools down the CO_2 to 30°C while achieving the 50°C for hydrolysation process. The heat capacities for both of Gas coolers are given below:

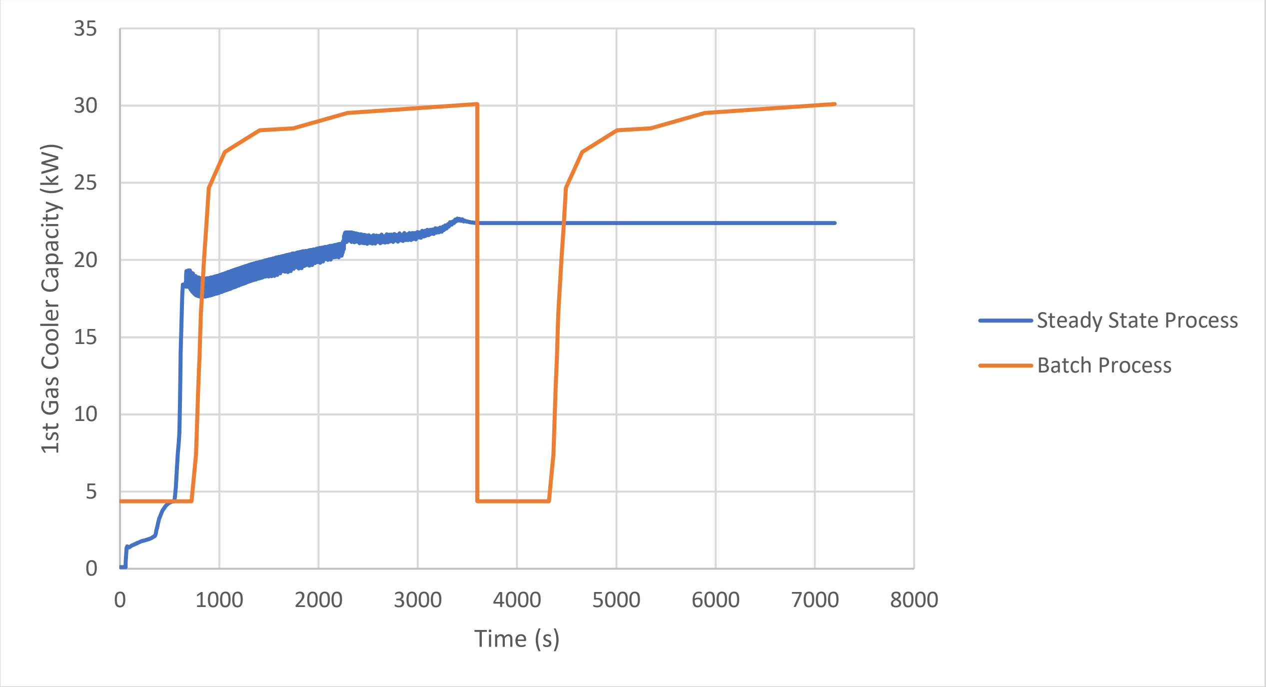

Figure 6.3 1st Gas Cooler Capacity Vs Time

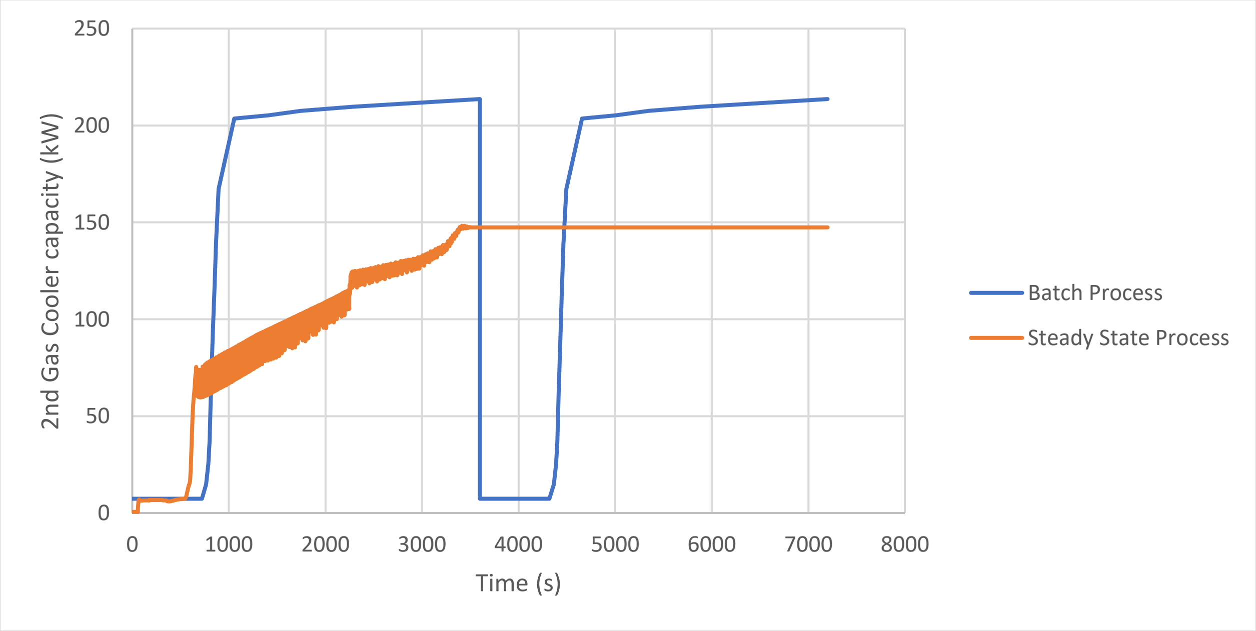

Figure 6.4 2nd Gas Cooler Capacity Vs Time

Heated hydrolysates were stored in insulated tanks for smooth operation of hydrolysation process. The fluctuations in the graphs are because of PI controller as it couldn't accurately control the outlet temperature from gas coolers as the load changes which kept fluctuating between 29℃ and 30℃.

6.5 TES system

The sensible heat released from hydrolytes when they are cooled down from 75℃ to 4℃ was used to heat up the water which was stored in insulated tanks. The tanks were charged with hot water when the system reaches maximum capacity and discharged when the system capacity is at its lowest. Multiple well insulated tanks in series with a combine volume of 1m^3 were used to store the sensible heat released from hydrolysates when they are cooled down to 4℃. **Figure 6.5** represents the how much sensible heat was absorbed by water and how much time it takes to fill up the desired volume.

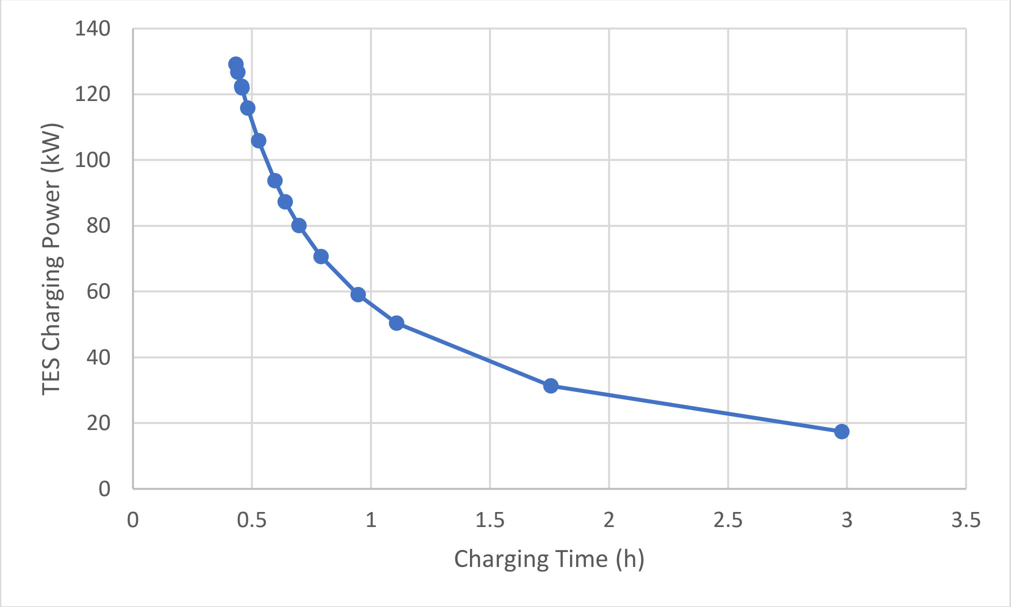

Figure 6.5 TES charging power Vs Time

6.6 Coefficient of Performance

The COP$_R$ was calculated by the evaporation load and due to constant pressures maintained during the simulation by PI controller which resulted in Constant COP$_R$ of 1.37. Ejector solution was also incorporated but only 3% COP improvement was observed. Evaporation temperature is dependent on how much concentration is required from freeze concentration process; suitable selection of desired concentration can increase the COP as shown in **Figure 6.7**.

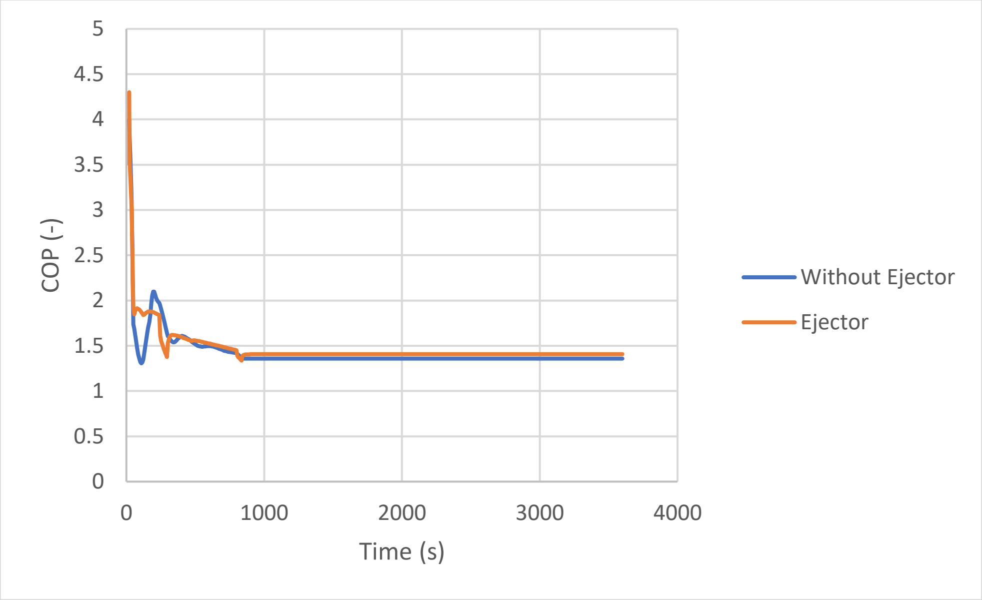

Figure 6.6 Coefficient of Performance of Refrigeration system

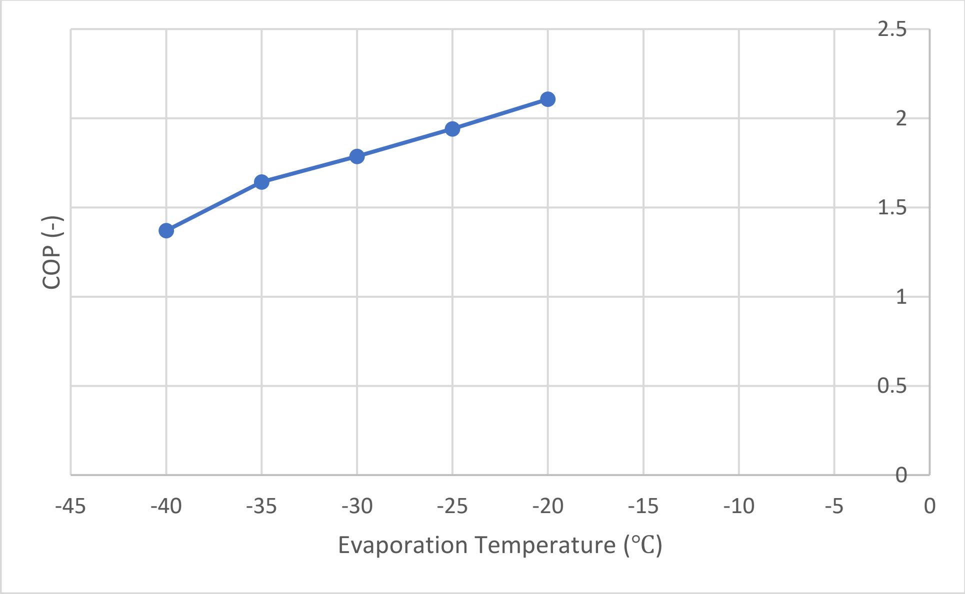

Figure 6.7 COP Vs Evaporation Temperature

6.7 Freeze Concentrator

The coupled equations were solved using Euler method and RK method 4 with the inputs from Dymola simulation with constant mass in crystallizer and results obtained by the simulation are presented below:

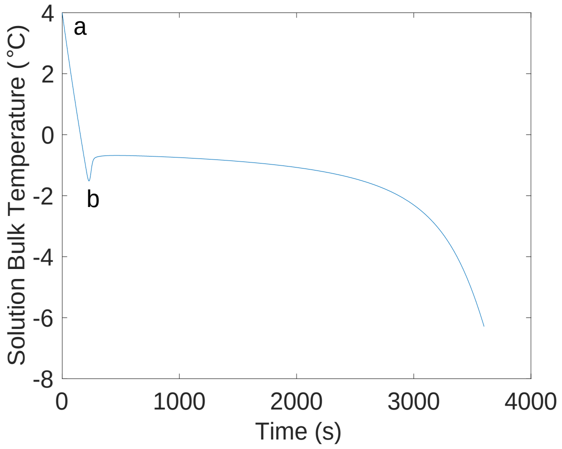

Figure 6.8 Solution Bulk Temperature Vs Time

Figure 6.8 shows the dynamic profile of bulk temperature. Initially the hydrolysates were at 4℃. The temperature goes down to -1.4℃ without any crystallization of water which is known as subcooling process. Point a to b shows subcooling process. Point b is known as seeding point where crystallization starts, and latent heat of fusion is released which increases the temperature till initial freezing point (-0.61 ℃). From b the freezing process starts and because of dissolved solutes in water the freezing point decreases and water crystallizes which is opposite to pure liquid freezes. The bulk temperature decreases till wall temperature of heat exchanger. The equilibrium was not achieved till 3600 seconds because of small surface area of heat exchanger.

Above **Figure 6.8** shows the simulation results when cylinder wall temperature was fixed to -30℃ and to achieve these results effective area of cylinder was reduced. Due to temperature difference of 4℃ of solution and -30℃ of cylinder wall resulted in subcooling as shown in **Figure 6.8**. This can't be achieved if scrubber removes ice from cylinder surface because as ice is removed from cylinder surface the cylinder surface temperature didn't drop to -30℃ rather it drops with solution temperature. This corelation was formulated by performing experiments in lab and was added in the code for correct solution's bulk temperature as shown in **Figure 6.9**.

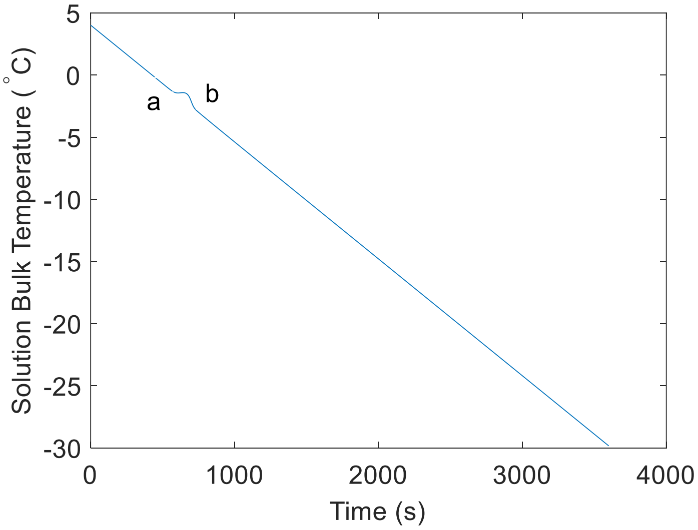

Figure 6.9 Solution Bulk Temperature Vs Time (Cylinder Surface Temperature)

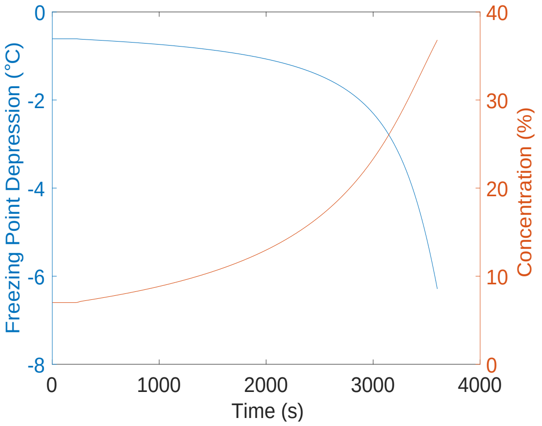

Figure 6.10 Concentration and Freezing point depression Vs Time

Figure 6.10 shows the depression of freezing point of liquid hydrolysates with respect to time. At time zero the freezing point of hydrolysates is -0.61℃ this is the initial freezing point found out experimentally using differential scanning calorimetry (DSC). With progression of time water freezes out which increases the concentration of solutes which further decreases the freezing point of hydrolysates. At the end of simulation, the concentration of solid increased till 36% which resulted in -6.3℃ freezing point depression.

The propagation of ice in the solution is shown in **Figure 6.11**. The seeding time was recorded as 230 seconds meaning that it takes above mentioned time to start the propagation of ice in water. The nucleation of ice starts at 230 seconds which gives the maximum speed of $0.9*10^{-6}$ m/s. Temperature difference between freezing depression point and bulk temperature is the driving force for the propagation of ice as expressed by equation 4.8. Maximum subcooling is achieved during the nucleation which results in maximum propagation of ice after that the subcooling drops to zeros which decreases the propagation of ice. At the end of simulation, the propagation speed was found out $1.182*10^{-9}$ m/s which is approaching zero.

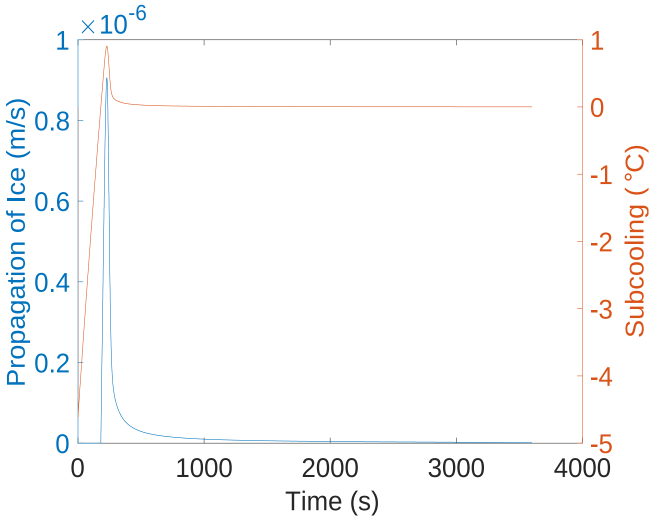

Figure 6.11 Propagation of Ice and Subcooling Vs Time

The simulation can be used to calculate the appropriate crystal size for subsequent washing in wash column. At nucleation the effective diameter of crystals was 0.067 mm while at the end of simulation the mean crystal diameter was found out 0.045mm. This happens because initially the number of crystals is less which results in bigger diameter as temperature drops the number of crystals increases which results in small and fine crystal diameter as shown in **Figure 6.12**.

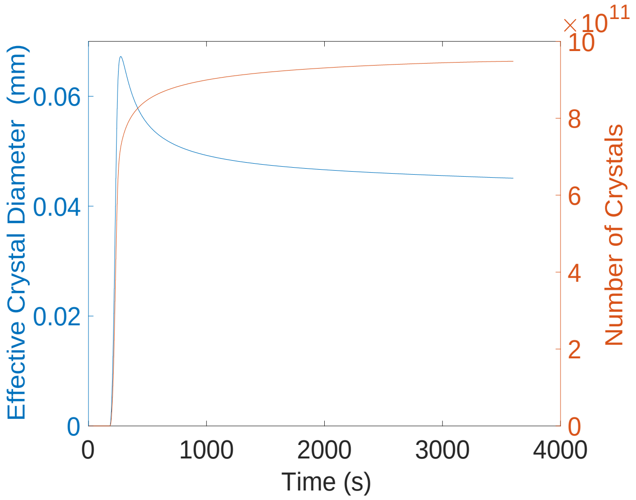

Figure 6.12 Effective Crystal diameter and Number of crystals Vs Time

The below graph (**Figure 6.13**) shows the increase of ice fraction in solution with respect to time. At the end of simulation, it was found out that 86.9 % of water turned into ice. Based on simulation results 36% of concentration was achieved. According to GEA if the viscosity of the concentrated solution increases from 30–50 mm^{2}s^{-1} for smooth operation it is recommended to have multiple stage step crystallizer(van Beek, 2018).

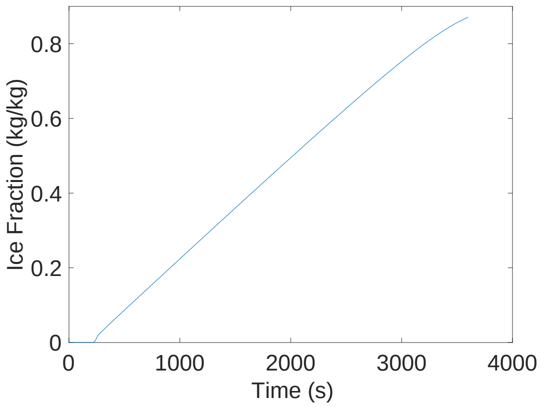

Figure 6.13 Ice fraction Vs Time

6.7.1 Total heat transfer constant (U)

The influence of the total heat transfer coefficient on bulk temperature, ice fraction and the effective crystal diameter are shown below. U value was varied from 200 to 1000 W/m^2.K while keeping other parameters constant. Increasing the total heat transfer constant resulted in less seeding time, more subcooling, high ice fraction and large effective crystal diameter.

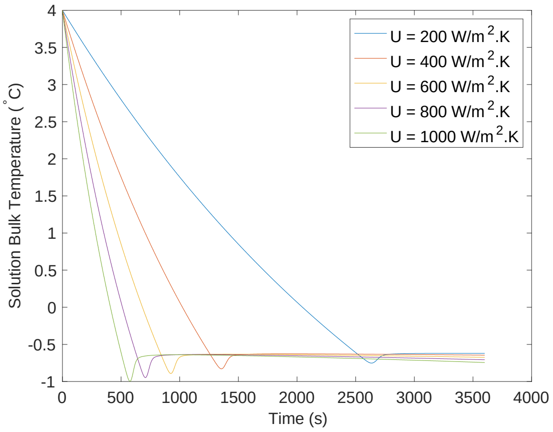

Figure 6.14 Solution's Bulk Temperature Vs Time. U is varied

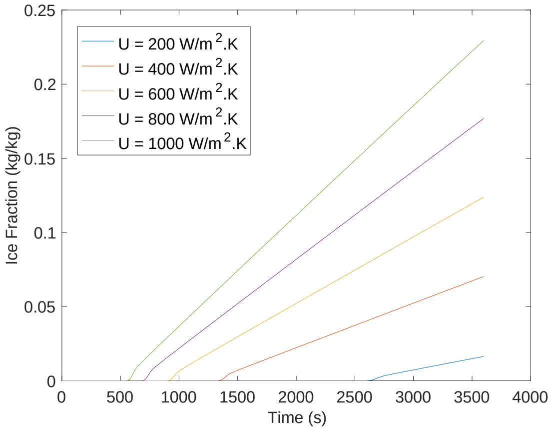

Figure 6.15 Ice fraction Vs Time. U is varied

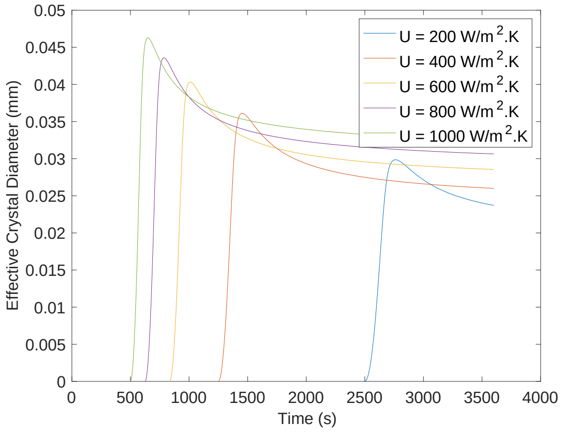

Figure 6.16 Effective Crystal Diameter Vs Time. U is varied

6.7.2 Heat Exchanger Surface Area.

The effect of surface area of evaporator heat exchanger was varied from 0.04 m^2 to 0.2m^2 while keeping U and wall temperature constant at 150 W/m^2K and -5°C respectively. High value of surface area increased the heat transfer which resulted in resulted in less seeding time, more subcooling, high ice fraction and large effective crystal diameter. The influence of surface area of heat exchanger on bulk temperature, ice fraction and the effective crystal diameter is shown below:

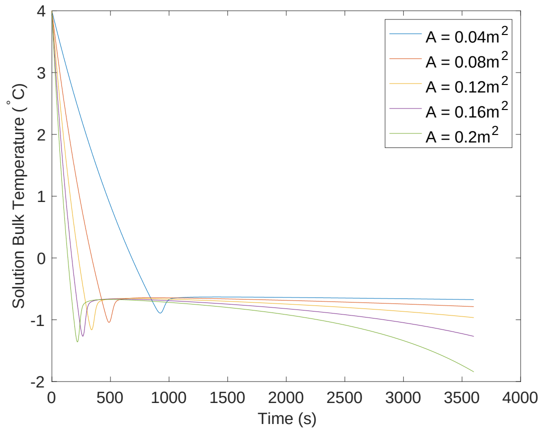

Figure 6.17 Solution's Bulk Temperature Vs Time. Heat Exchanger Surface Area is varied

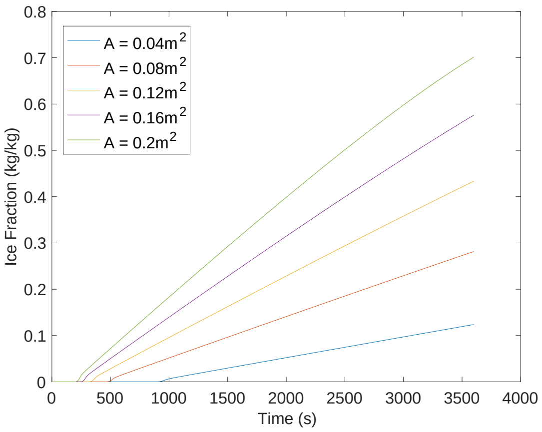

Figure 6.18 Ice fraction Vs Time. Heat Exchanger Surface Area is varied

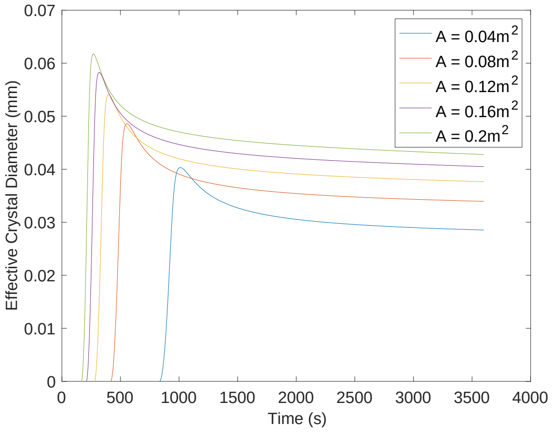

Figure 6.19 Effective Crystal Diameter Vs Time. Heat Exchanger Surface Area is varied

6.7.3 Heat Exchanger Wall Temperature.

The Wall temperature was varied from -5℃ to -35℃ while keeping surface area and U constant at 0.01 m^2 and 150 $W/m^2.K$ respectively. The influence of wall temperature on bulk temperature, ice fraction and the effective crystal diameter is shown in the **Figure 6.20**, **Figure 6.21** and **Figure 6.22**. Low wall temperature results in in less seeding time, more subcooling, high ice fraction and large effective crystal diameter.

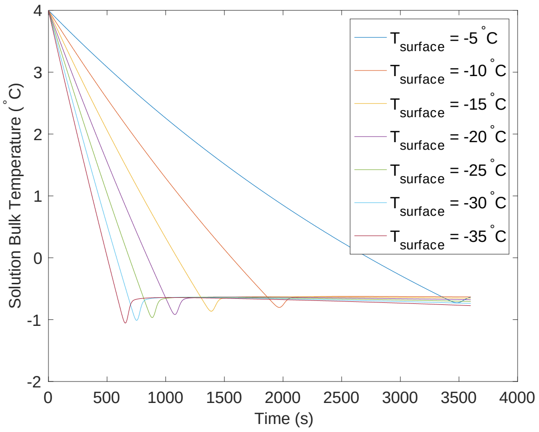

Figure 6.20 Solution's Bulk Temperature Vs Time. Heat Exchanger Wall Temperature is varied

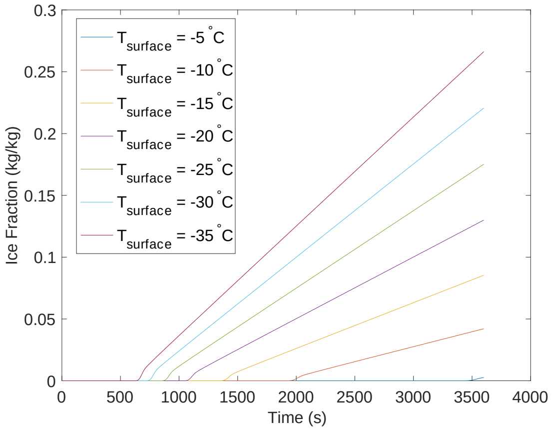

Figure 6.21 Ice fraction Vs Time. Heat Exchanger Wall Temperature is varied

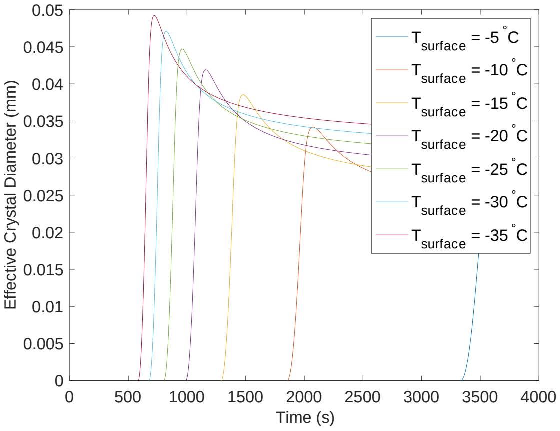

Figure 6.22 Effective Crystal Diameter Vs Time. Heat Exchanger Wall Temperature is varied

The surface area was kept low to slow down the evolution of bulk temperature and capture all graphs in one time frame. These simulations were validated by the results published by ola Fleslad in his PhD thesis.

6.8 Wash Column:

The dynamic model was developed to calculate the length of filtration and wash section. Inputs such as ice fraction and feed mass flow rate were obtained from crystallizer simulation two different approaches were used to calculate the filtration length. The first one uses exponential estimation to calculate filtration length and simulation ends with ice fraction reaches 100%. While the other simulates how the fluid flows and separate by passing through filters. The second one is more accurate as in includes the volume flow rate of slurry and the diameter of wash column. The first simulation results in 1.4 m of filtration length while the second simulation gives 0.74 m. These are the minimum lengths needed to separate concentrate solution from ice, the volume flow rate and wash liquid is controlled with the help of pump. Below graphs show the simulation results.

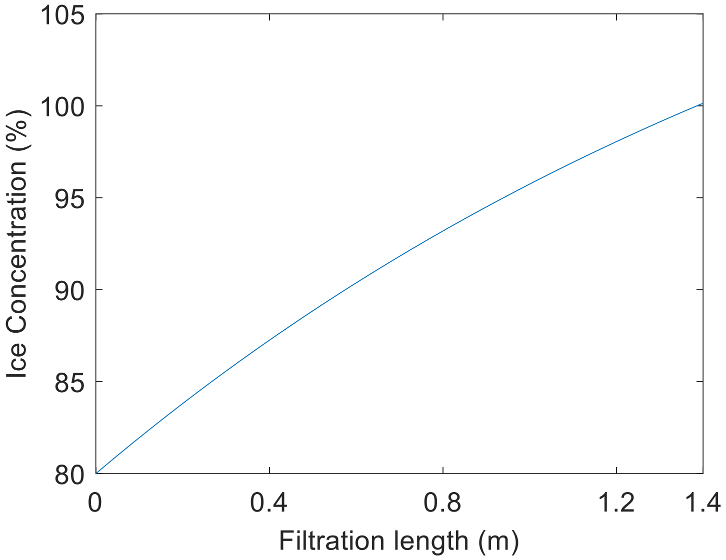

Figure 6.23 Ice Concentration Vs Filtration Length

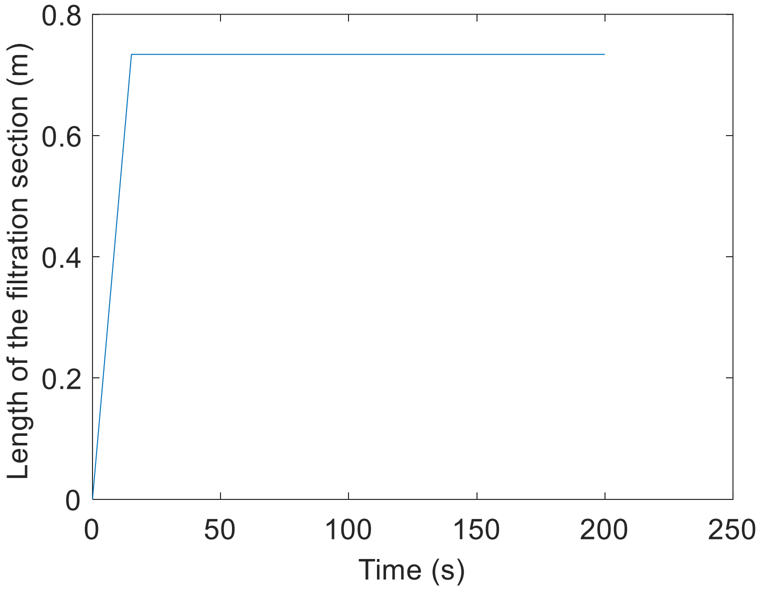

Figure 6.24 Length of the Filtration Section Vs Time

After filtration ice separates from concentrated solution to wash the ice, minimum length was required by wash liquid to easily pick ice from wash column without entering filtration length. **Figure 6.25** Length of wash section Vs Time show the dynamic profile of wash section length.

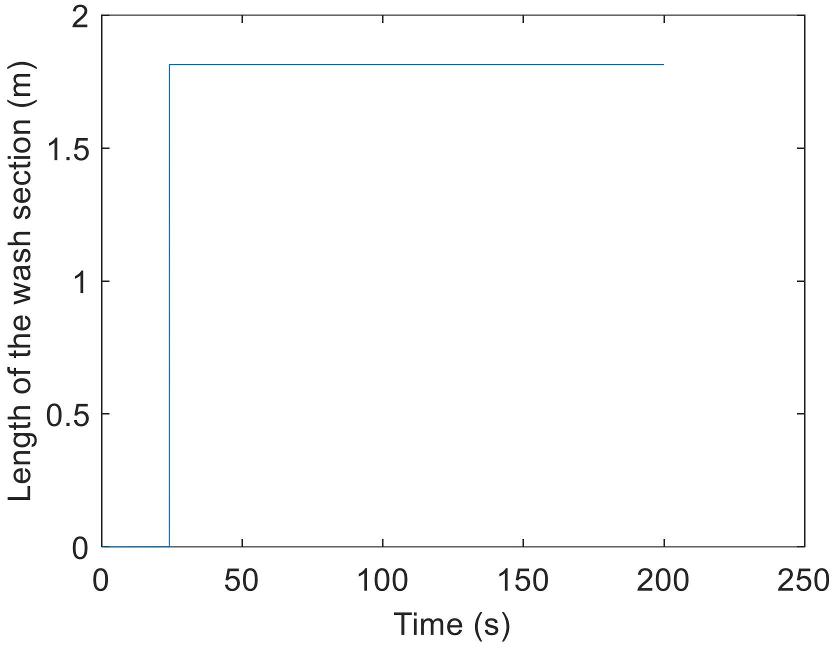

Figure 6.25 Length of wash section Vs Time

The total length of wash column is the sum of filtration and wash section length based on the simulation carried out the total length was calculated as 2.5 to 3.2. The derived PDE's (equation (4.17) and (4.19)) are equal to a constant value which adds on to respective lengths during each time step which is the bases for linearity shown by dynamic model.

Mass flow rate of concentrated solution and ice slurry was calculated. The mass flowrate of concentrated solution can be used to calculate the energy consumption of further drying process while the mass flow rate of ice slurry was used to calculate the energy needed to melt ice. Mass flow rate of concentrated solution and ice slurry were 0.234 kg/s and 0.1 kg/s respectively. Ice in ice slurry was melted by the heat given off by desuperheater.

Based on 1741 kg/hr mass flowrate the dimensions for crystallizer and wash column are shown in **Figure 6.26** and **Figure 6.27** respectively. The filtration and wash section length depends upon ice fraction for this case the ice fraction was taken as 80 percent. Filtration and wash section lengths can vary based upon ice fraction, but the dimensions of wash column would be constant until the mass flowrate remains the same.

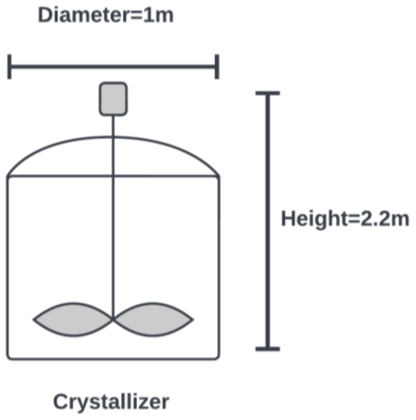

Figure 6.26 Crystallizer Dimensions

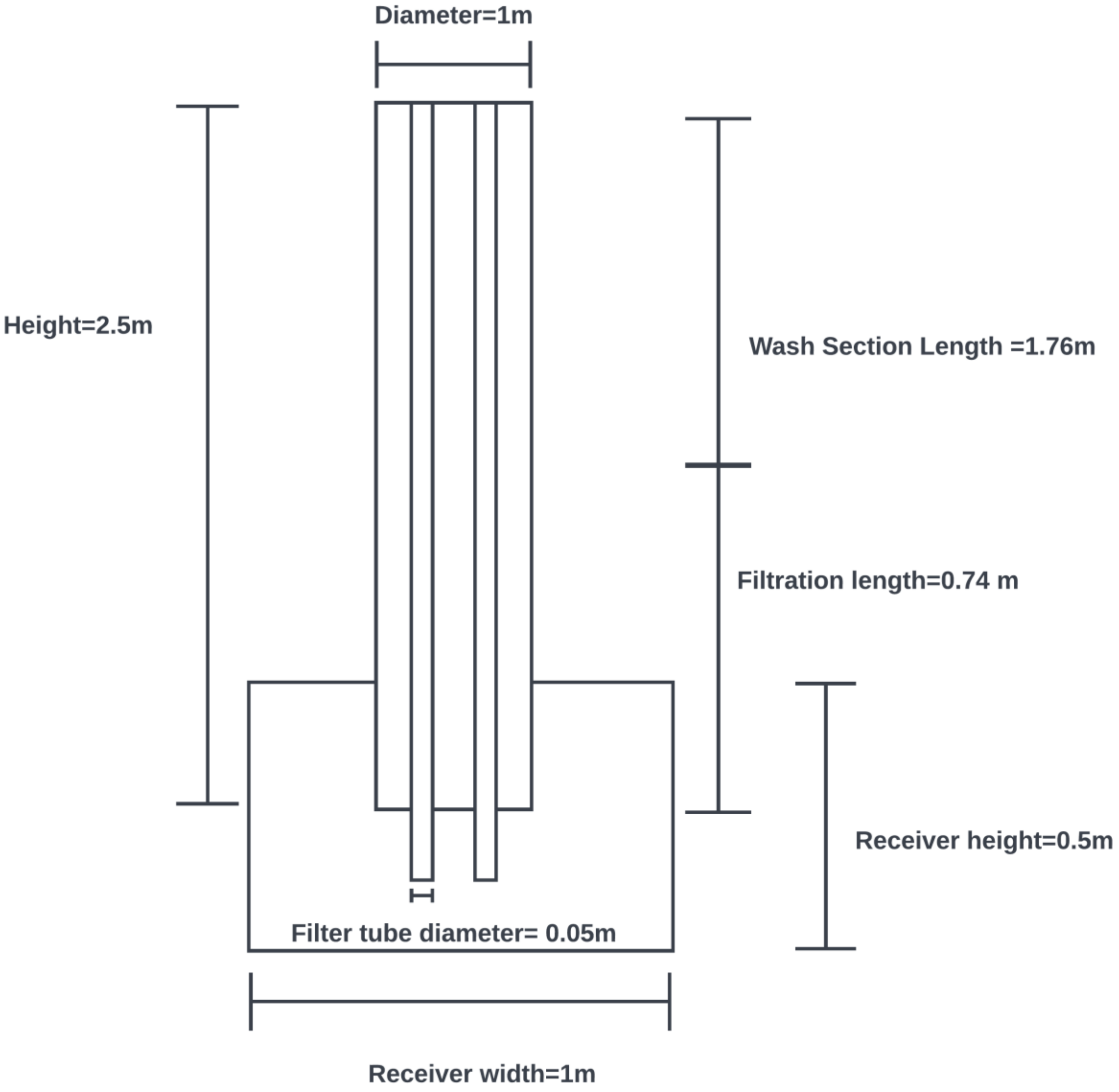

Figure 6.27 Wash Column Dimensions

6.9 Validation:

Experiments were carried out to validate the numerical schemes, initially salt solution was created with a concentration of 7%. Solution bulk temperature was recorded every second with probe and data was transferred to laptop via data logger. Trendline was generated in excel with respect to time step and the equation was inserted in code to compare with numerical results. The extrapolated experiment equation is given below:

$$T(t)=1*10^{-12}*t^{-4}-4*10^{-9}*t^{3}+6*10^{-6}*t^{2}-0.0155*t+20.104 \qquad 6.1$$

The figure below shows the comparison of experiments and numerical results.

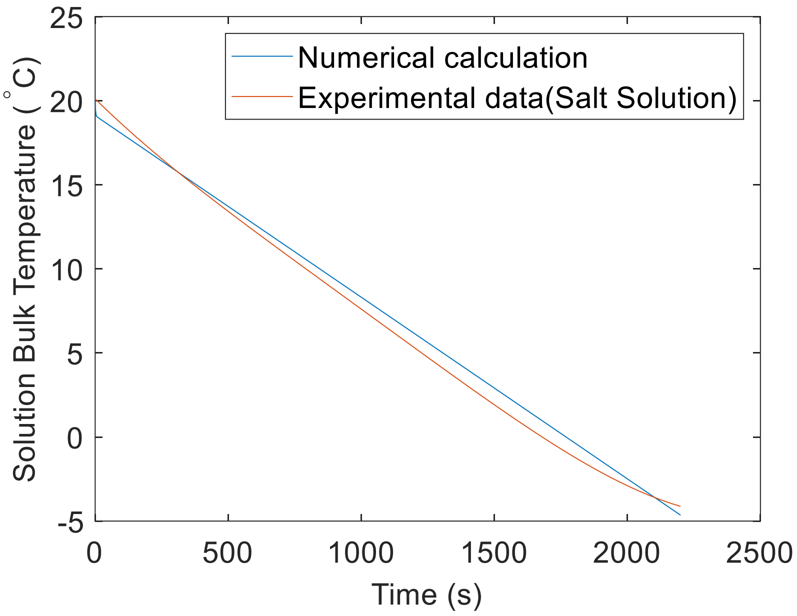

Figure 6.28 Comparison of numerical and experimental data for salt solution

Ice slurry was formed until the bulk temperature reached to -4.5℃. Ice slurry was pumped to wash column to separate ice from concentrated solution. Different parameters were calculated to estimate the error from numerical results.

	Experimental Value	Numerical Value	Error
Solution Bulk Temperature	-4.5℃	-4.1 ℃	8.89%
Ice Formation (% with rest to total mass)	23%	21%	8.7%
Concentration achieved (one cycle)	8.86%	8.672%	2.12%

Table 6.1 Values of Numerical and experimental data for salt solution

Surface temperature plays an important role which was measured experimentally and inserted in numerical scheme to get the desired results.

Chapter 7

7 Discussion

The results were displayed and discussed in chapter 6, but this chapter will discuss the findings and technicalities in a broad perspective. Freeze concentration process contains three components named as refrigeration system, crystallizer, and wash column.

7.1 Refrigeration system

CO_2 trans-critical system was proposed with pressure uplift from 10 bar to 100 bar with an intermediate pressure of 35 bar. This solution is ideal for hydrolysation process and freeze concentration. Results from Two different approaches were explained in the last chapter named as steady state and bulk process. Keeping restricted area considerations in mind its more appropriate to have a steady state process because of low ice content in slurry which is easy to separate using a hydraulic wash column but it's difficult to control the system. Desired concentration after freeze concentration process should be calculated with caution as it might affect the evaporation temperature which might increase or decrease the COP of the system.

High heat recovery from proposed CO_2 system, to store the sensible heat released from hydrolysates a TES system with water storage was proposed. Charging time can be varied based upon the available heat. To minimize the fluctuations in the system it is recommended to have storage tanks after each heat exchangers to store hydrolysates with desired temperature and mass flow rates.

7.2 Crystallizer

Ice formation in crystallizer was numerically solved with the help of coupled equations. For smooth ice formation it is recommended to have high surface area in contact with CO_2 and crystallizer, crystallizer sketch shown below would be the ideal case.

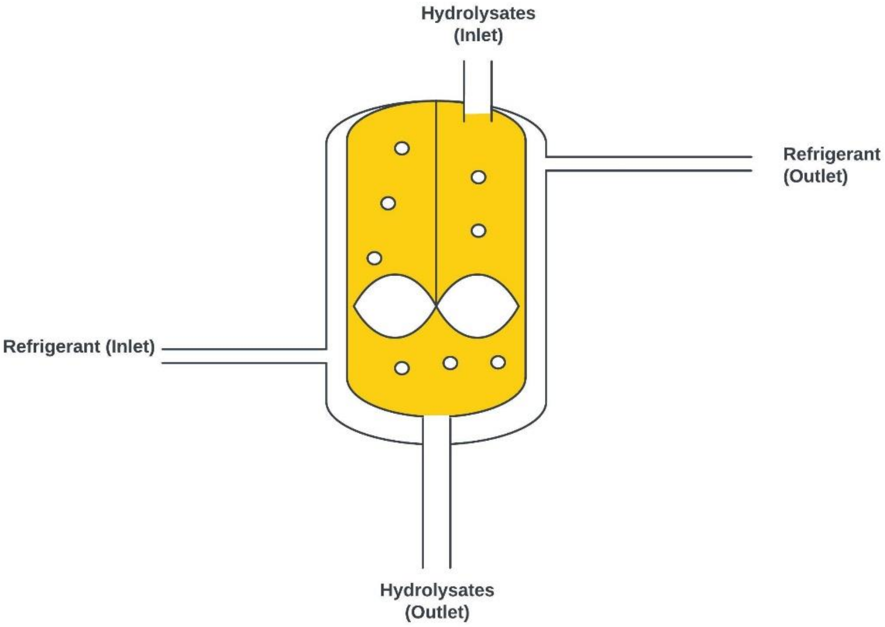

Figure 7.1 Crystallizer Sketch

Large U value and low evaporator temperature can also increase the propagation of ice. With low temperatures more ice can be formed which can result in more concentration. Practically going above 30% concentration two crystallizers with different evaporation temperatures should be used.

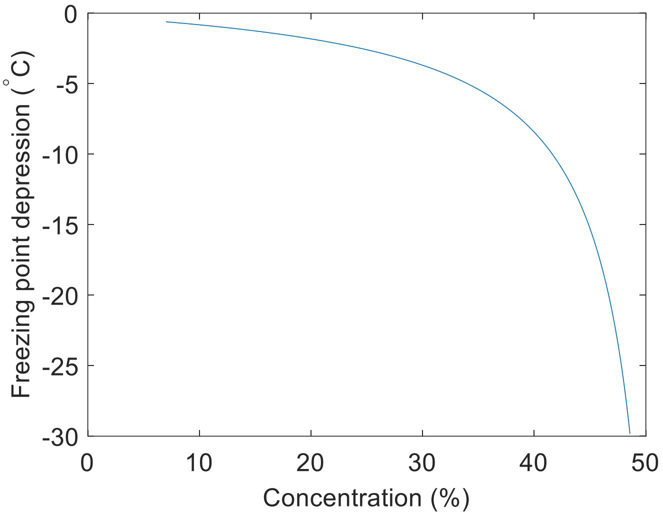

Figure 7.2 Freezing point depression Vs Concentration (%)

More ice formation results in more concentration which could depress the freezing point as shown in **Figure 7.2**. The selection of evaporation temperature depends upon how much concentration is required after freeze concentration process. High concentration obtained from freeze concentration can increase the viscosity of fish protein hydrolysates which may create hindrance in pumping and transportation among equipment.

Size and shape of ice crystals formed in crystallizer have a lot of effect on transport and washing. To acquire a suitable size and shape of ice crystals a good design of scrubber is required which could keep walls of cylinder ice free. Below are two different types of scrubbers which are best for this process.

Figure 7.3 Flake ice scrubber

Figure 7.3 scrubber was also available for experiment it contained bent blades which scraped the ice from cylinder surface in the form of flakes and as time pass these flakes increased in solution which converted solution in slurry. **Figure 7.4** shows experimental shot of this process.

Figure 7.4 Experimental shot of ice scrubber

Figure 7.5 is a conceptual design which will also scrap ice from cylinder surface but because of its round shape round ice crystals can be achieved. The diameter of ice crystal depends upon the scraping speed, higher the speed smaller the diameter for ice crystals.

Figure 7.5 Scrubber design to form spherical ice crystals

7.3 Wash Column

Two different types of wash columns exist which can be used to the separation of ice such as hydraulic and piston wash columns can be used. Hydraulic wash column was used for the separation of ice which suits the steady process and has less complex structure than piston wash column. Wash column comprises of three sections named as filtration, wash section and receiver. Filtration and wash section size depends upon slurry flowrates and ice concentration in slurry. The wash section length can also be controlled by wash fluid flowrate and pressure. Selection of washing fluid flowrate and pressure depends upon the capacity of desuperheater, which is used to melt the ice. Desired vacuum pressure should be maintained in receiver which assists in increasing the suction flowrate of concentrated solution from filter tubes.

2-meter-high hydraulic wash column with a diameter of 0.1 m was constructed to observe the working of wash column. Two crystal bed were prepared vertical and horizontal to observe which one works the best. Due to large gap in filter tubes, vertical bed couldn't maintain stagnation in wash column which resulted in fast separation of ice and concentrated solution. Concentrated solution was recovered from receiver. Then water was added from top to melt ice which was also recovered in receiver.

Good stagnation was achieved with horizontal bed and separation of ice and concentrated solution in wash column was visible, **Figure 7.6** shows this separation. Ice was washed while adding water from the top which created ice slurry and was collected in open tank. To achieve good washing the slurry height in wash column should be maintained. Washing should be quick which will avoid the formation of hard ice, otherwise a knife should be placed at top to grind ice to form ice slurry. Below are some experimental shots for better visualization.

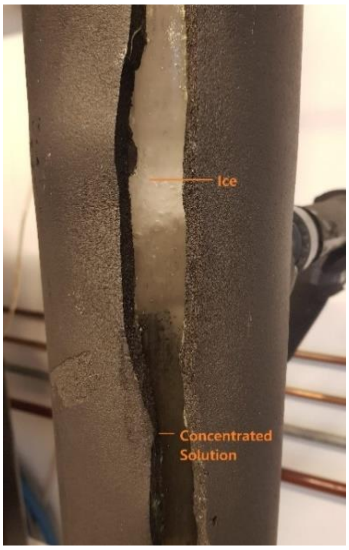

Figure 7.6 Filtration section

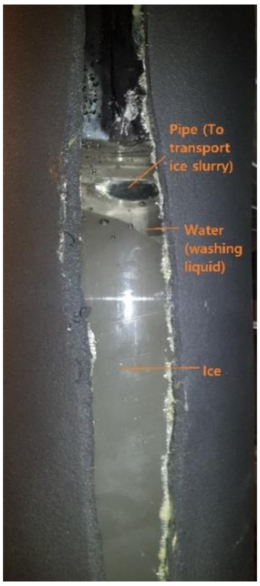

Figure 7.7 Washing section

Length of wash column depends on different parameter such as flow rate of slurry, diameter of wash column and ice content in slurry. Keeping the flow rate of ice slurry and diameter of wash column the height was wash column was calculated which is shown in **Figure 7.8**. To achieve good separation, it is prominent to have the height of wash column greater than 2m irrespective of slurry flow rate, diameter of wash column and ice content in slurry.

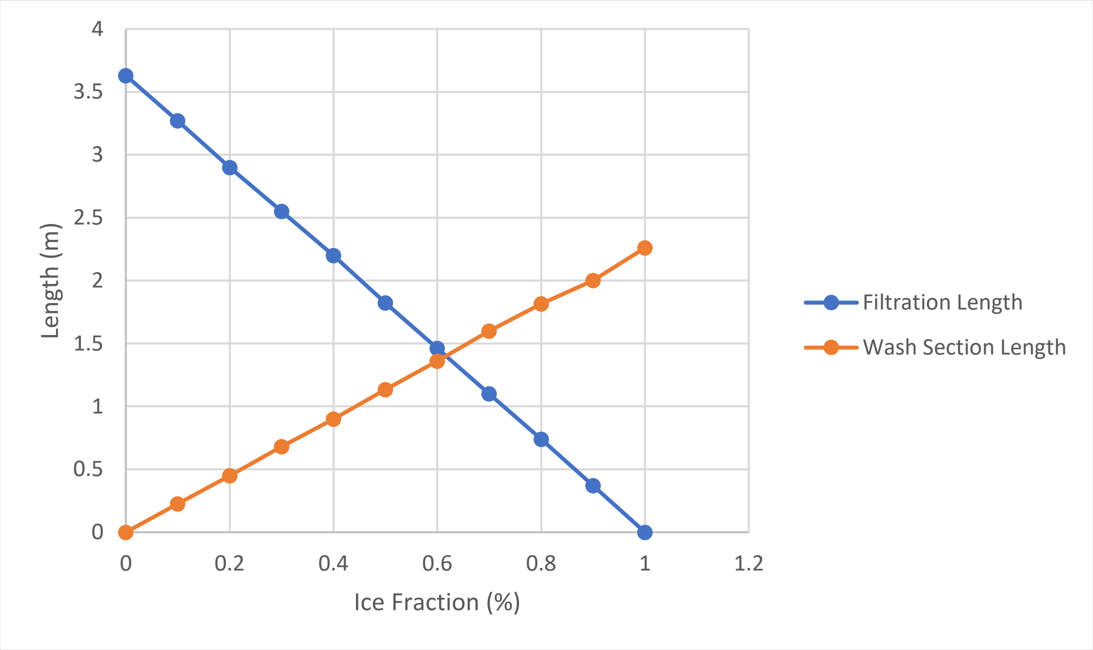

Figure 7.8 Filtration and wash section length vs Ice fraction

Control of crystallizer and wash column for batch and steady state process is very important that's why control system for industrial processes were designed.

7.4 Control system for batch process:

For batch process pumps were controlled as on and off operation. Three sensors were used in the system, One temperature sensor in crystallizer and three height sensors one in wash column, crystallizer, and receiver. When desired temperature reached in crystallizer the first pump was started and all slurry was transferred to wash column. Upon the filling of wash column second pump was started which created ice slurry to remove ice from concentrated solution. Third sensor sensed the height in receiver and started the 3rd pump to pump required concentration solution for further processing. When slurry was pumped out from crystallizer Fourth pump was started which filled crystallizer with fresh hydrolysates **Figure 7.9** shows the respective pumps and sensors.

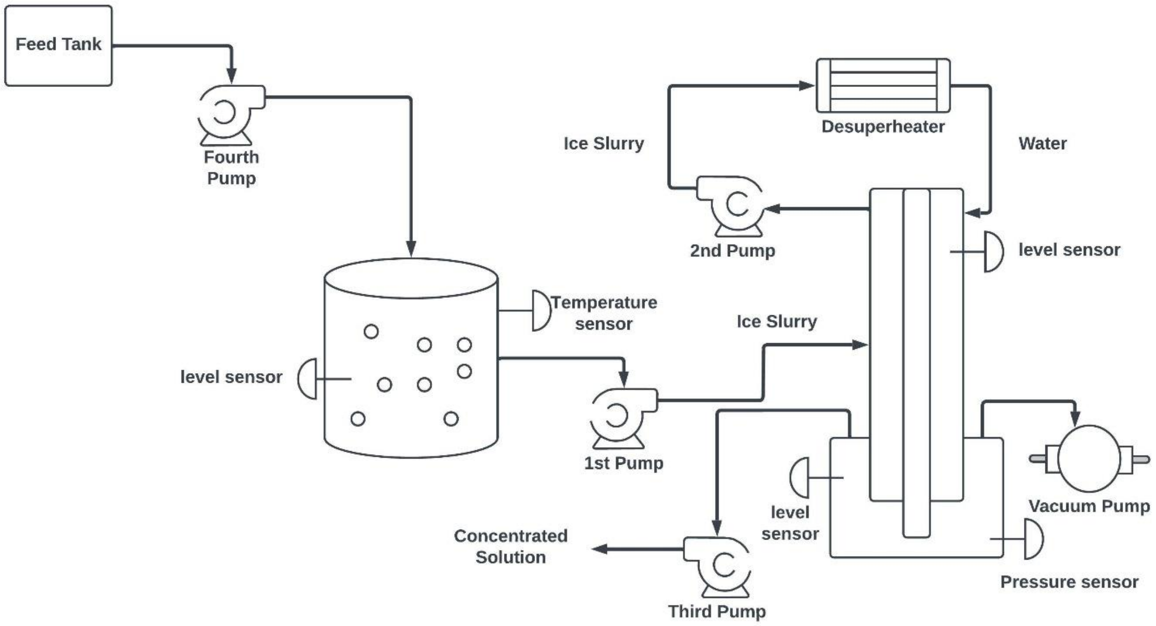

Figure 7.9 Schematic diagram of freeze concentration for batch process

7.5 Steady state process

For steady state, proportional integral (PI) controls were used to control the system until PI controller achieves a steady state solution for freeze concentration process. Below figure shows the respective sensors and pumps for PI control.

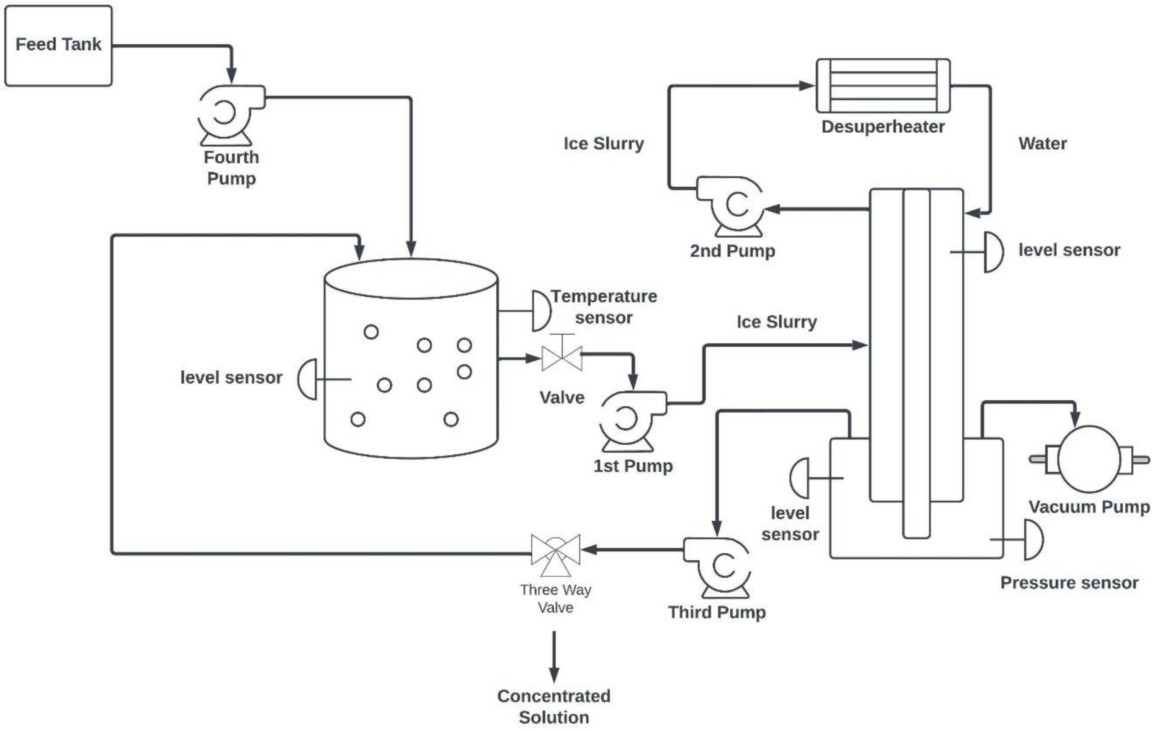

Figure 7.10 Schematic diagram of freeze concentration for steady state process

PI control had two gains named as proportional controller (KP) and Integral controller (KI). KP controller was given 1 value while KI controller was given zero value for simplicity.

A valve was implemented between 1st pump and crystallizer and If statement was implemented by PI control. If desired temperature was achieved which resulted in 15% ice concentration in solution than valve was opened. The 1st pump was controlled by reference height of crystallizer such that pump rpm was reduced when crystallizer height was reduced. The simplified control diagram is given below:

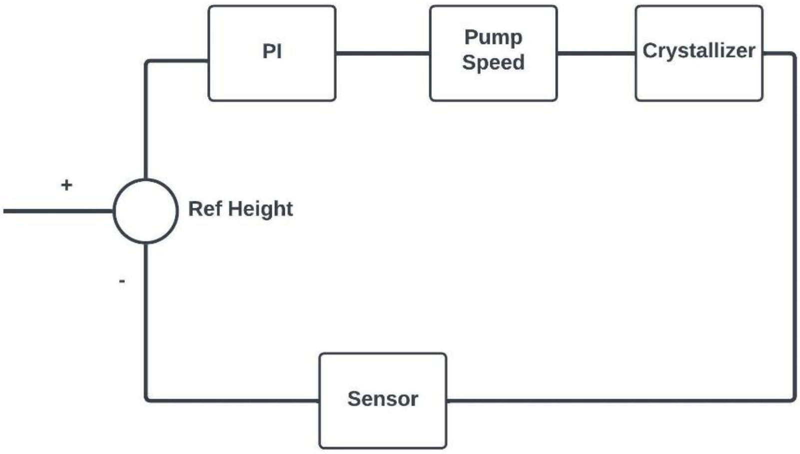

Figure 7.11 Simplified control diagram

PI controls the fourth pump as way as it controls the 1st pump with just one difference that pump rpm was reduced when the fluid height in crystallizer was increased. Similarly, 2nd pump was also controlled was with same logic the rpm of 2nd pump was increased when the fluid level in wash column reaches the maximum level. On and off control was applied to vacuum pump which maintained the 0.5 bar pressure in receiver.

The control of third pump and three-way valve were tricky to control. If statement was used for three-way valve if the desired temperature was achieved in crystallizer solution (in this case -30℃) and certain level was achieved in receiver. The three valve was opened with 80 to 20 ratio. Meaning that 80 % of concentrated solution was recycled while the 20% was final product which can be pumped for further drying. If this statement wasn't true than all concentrated solution was pumped back to crystallizer. PI increased the third pump rpm as the concentrated solution increased from certain level.

A simple control system was designed to control the system. Further study on the controls should be carried out for smooth control.

Chapter 8

8 Economic analysis

Economic analysis essentially enlists the profitability of the project with comparison with a base line process. In this thesis a generic economic analysis was performed to find out the internal rate of interest, pay back and pay off time.

Important profitability parameters are:

- Interest rate (r)
- Lifetime (n)
- Capital cost (I_o)
- Specific Investment cost (\$/kW)
- Net annual Earning/Savings (B)
- Annuity factor (a)

The profitability analysis includes payback time (PB), pay off time (PO) and sensitivity analysis about:

8.1 Payback time

PB is the ratio of additional investment and net annual saving.

$$\mathrm{PB} = \frac{\mathrm{I_o}}{\mathrm{B}} \tag{8.1}$$

PB simply shows how many years are needed to pay back additional investment. Please note that PB method should only be used as a rough estimate because it doesn't contain the real interest rate (r) (Stene, 2021).

8.2 Payoff time

This method is like the pay-back time method, but the interest rate (r) is included. PO is the number of years it takes before the sum of the future net savings/earnings (B) equals the additional investment costs (I_0). The higher the interest rate, the larger the difference between the pay-off method and the pay-back method (Stene, 2021).

$$\mathrm{PO} = \frac{\ln\left[\left(1 - \left(\frac{\mathrm{I_0}}{\mathrm{B}}\right) * \mathrm{r}\right)^{-1}\right]}{\ln\left(1 + \mathrm{r}\right)} \tag{8.2}$$

8.3 Sensitivity analysis

Sensitivity analysis contains two parts named as maximum permissible investment costs (MPI) and minimum permissible earnings/savings (MPS). The formula of MPI and MPS are given below:

$$\mathrm{MPI} = \mathrm{B} * \left(\frac{1 - (1 + \mathrm{r})^{-\mathrm{n}}}{\mathrm{r}}\right) = \left(\frac{\mathrm{B}}{\mathrm{a}}\right) = (\mathrm{I_0} + \mathrm{PV}) \tag{8.3}$$

$$\mathrm{MPS} = \mathrm{I_0} * \left(\frac{\mathrm{r}}{1 - (1 + \mathrm{r})^{-\mathrm{n}}}\right) = \mathrm{I_0} * \mathrm{a} \tag{8.4}$$

The maximum permissible investment costs (MPI) are the maximum additional investment costs (I_0) that gives PV = 0. On the other hand, the minimum permissible earnings/savings (MPS) is the minimum annual savings (B) that gives PV = 0. A profitable project has a relatively large MPI and/or a small MPS. Important factors that determine the additional investment costs (I_0) are the dimensioning and design of the heat pump plant as well as the specific investment costs of the different sub-systems. The interest rate (r) is also an important parameter. On the other hand, the energy prices (e), SCOP (SPF) and the annual heating/cooling demands determines the annual savings/earnings (B) (Stene, 2021).

Economic analysis was carried out to check the feasibility of this system with current industrial practices. Energy consumption for industrial spray drying and freeze concentration assisted spray drying process were 3183 kW and 1245.3 kW respectively. These values were estimated by (Sherman, 2022). Different parameters considered for economic analysis are given below:

Interest rate (r)	5%
Lifetime (n)	15 years
Investment Cost for spray drying	50000 $
Investment Cost for freeze concentration	1.55 million $
Energy prices (e)	0.096 $/kW

Table 8.1 Numerical values used in economic analysis

Economic analysis was carried out with above mentioned parameters and payback and payoff time was calculated. Consequently, a plant size was selected with 400 and 3500 kg h^{-1} of dewatering in the freeze concentration system for a preliminary economic analysis. For drying, both payback of 1.5 years but not for the smaller plant with a payback of around 4 years (van Beek, 2018). The payback time was calculated as 2.8 years which is in accordance with (van Beek, 2018) calculations. While the payoff time came out as 3.1 years.

Sensitivity analysis was carried out to check which parameters have influence on the profitability. MPI was calculated and different parameters were changed, results of those calculations are shown below:

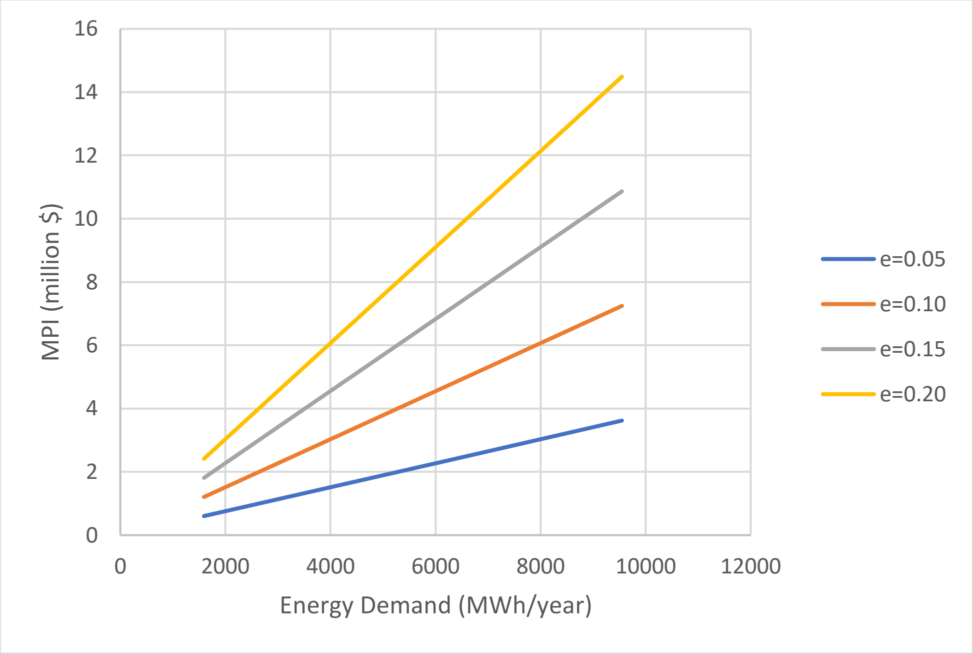

Figure 8.1 MPI vs Energy demand (varying electricity price)

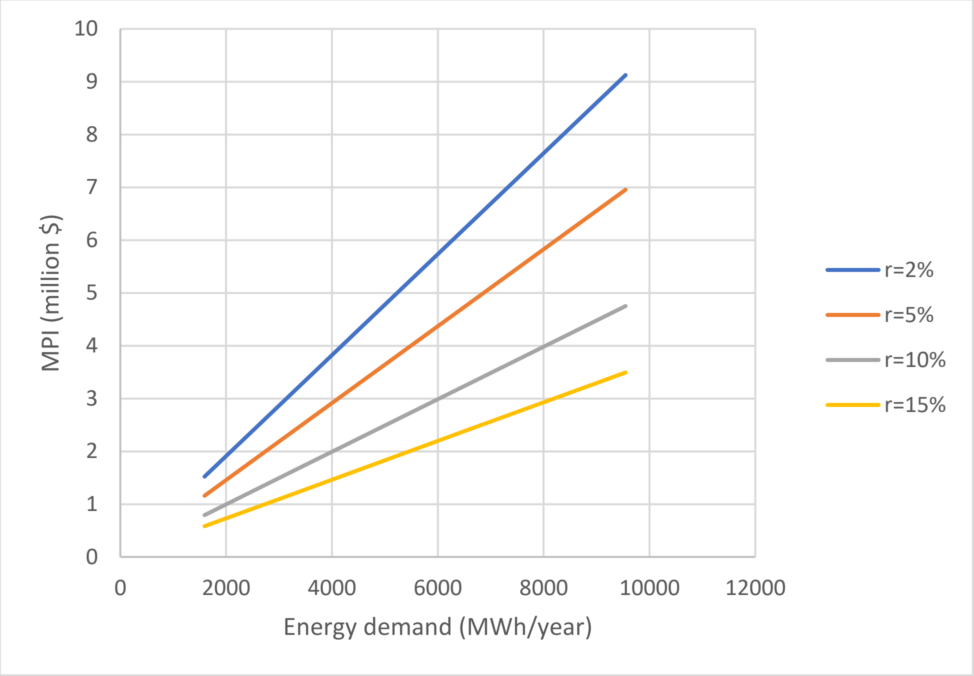

Figure 8.2 MPI vs Energy demand (varying interest rate)

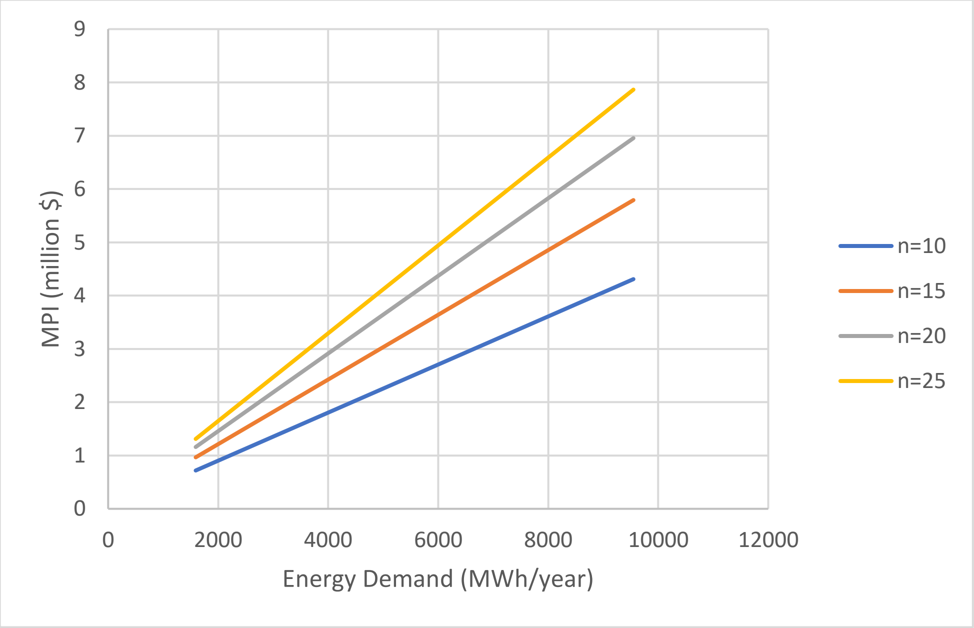

Figure 8.3 MPI vs Energy demand (lifetime of equipment)

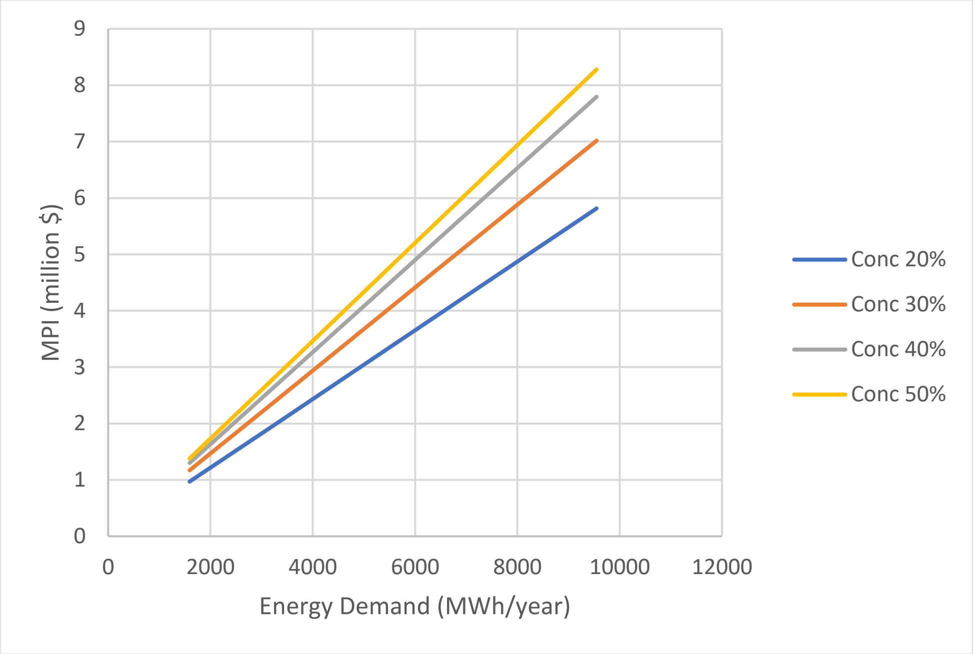

Figure 8.4 MPI vs Energy demand (varying concentration achieved after freeze concentration process)

The following parameters were varied energy price (e), interest rate (r), life of equipment (n) and concentration (conc %) achieved after freeze concentration process. Sensitivity analysis indicated as maximum profit can be achieved with high energy price, low interest rate, long equipment life and more concentration achieved after freeze concentration process. 15 year financial and profitability projection for freeze concentration process was carried out which are given below:

Factors	Freeze Concentration
Setup Cost	1.55 million USD
Maintenance Cost	77500 USD/year
Operational Cost	358647 USD/year
Payback	2 years and 8 months
Profitability in 15 years	6.7 million USD

Table 8.2 Financial and profitability projection

Chapter 9

9 Conclusion

An overview of complete hydrolysation process of 1 ton rest raw material was explained in detail with production of 1741 kg of hydrolysates in result of hydrolysation. Dynamic simulation of freeze concentration and wash column were carried out in MATLAB while the dynamic simulation of refrigeration system was carried out in EES and Dymola.

Two case studies were adopted for freeze concentration, one deals with batch process and other deals with steady state process. In batch process the 36 % concentration is achieved in one go while in steady state process the system is warmed up till 31 % concentration and after that in each cycle with the production of 15% ice 36 % of concentration can be achieved. The freeze concentration process includes two equipment's named as crystallizer and wash column.

Height and diameter for crystallizer was estimated as 2.2 m and 1m respectively. Euler and RK method 4-time discretization was used to solve 6 coupled equations to calculate the dynamic profile of bulk temperature, depression of freezing point, mean diameter of crystals, ice fraction and propagation of ice. At the end of simulation bulk temperature, depression of freezing point, mean diameter of crystals, ice fraction and propagation of ice came out as -6.2℃, -6.3℃, 0.045mm, 0.869 and 1.182*10^-9 m/s respectively. Large U, heat exchanger area and lower wall temperature drastically reduced time for crystallizer process. Maximum concentration of 36% percent was achieved. For smooth operation, it is recommended to have multiple stage step crystallizer. Experiments were carried out to validate the numerical solution of crystallizer and 10 percent error was recorded.

Development of two methods to estimate the filtration length of wash column. Filtration length from exponential and dynamic simulations were 1.4m and 0.74m respectively. Dynamic wash column simulation was also used to calculate the wash section length, mass flow rate of concentrated solution and ice slurry. Wash section length, mass flow rate of concentrated solution and ice slurry were estimated as 1.8 m, 0.234 kg/s and 0.1 kg/s respectively.

To observe the separation, process a hydraulic wash column was constructed. A 2-meter plexiglass tube with a diameter of 0.1 m was used which was insulated to avoid melting of ice in wash column. Vertical and horizontal crystal beds were prepared to observe which one is more suitable for this process. Fast separation of ice and concentrate solution was observed in vertical crystal bed while a good stagnation and separation was achieved with horizontal crystal bed. Length of wash column depends on different parameter such as flow rate of slurry, diameter of wash column and ice content in slurry. To achieve good separation, it is prominent to have the height of wash column greater than 2m irrespective of slurry flow rate, diameter of wash column and ice content in slurry.

Dynamic simulation of refrigeration system was carried out in Dymola for batch and steady state load. Evaporation load in batch and steady state process starts from 8.4 kW to 160.9 kW in batch process and for steady state process it goes till 121.67 kW. For batch process the evaporation load changes every hour but for steady state process, the system takes one hour to achieve steady state. In both the cases, system was able to heat up the hydrolysates to 50℃ and 90℃. TES system can be used to store sensible heat released from hydrolysate when cooled down to 4℃ which can heat up the water till 60 ℃.

Economic and sensitivity analysis were carried out to check the profitability of the system and the payback time was calculated as 2.8 years. Sensitivity analysis indicated as maximum profit can be achieved with high energy price, low interest rate, long equipment life and more concentration achieved after freeze concentration process. This project will be a game-changer in upcoming years for Norwegian fish industries as it is environmentally friendly, innovative, avoid thermal loss and reduction in CO_2 emission from 57.3 tons per year to 22.415 tons per year.

Chapter 10

10 Further Works

This chapter contains suggestions for further work. Some of them are related to improvement in existing work and rest are the extension of work

- Further investigation in freeze concentration and hydrolysation process.
- A solution to constant efficiencies (compressor) in Dymola must figure out to have a real COP analysis.
- Development of pressure model for wash column for the prediction of pump power.
- Improvements in Dymola model to increase the COP of refrigeration system.
- Further improvements in Dymola model.
- Creation of library for crystallizer and wash column in Dymola.
- Developing numerical simulations to estimate the Heat transfer coefficient (U) and surface temperature based on ice propagation on cylinder wall.
- CFD analysis for different crystallizer configuration for further improvements in models.
- Improvement of existing crystallizer and wash column numerical schemes.
- In depth economic and sensitivity analysis.
- Development of control system algorithm for pump control for steady state and batch process.
- Construction of piston wash column for comparison study.
- Study on layer crystallizer and compare with suspension crystallizer.

11 Bibliography

Berk, Z. (2013). *Food process engineering and technology*. Academic press.

Berk, Z. (2016). Chapter 9 - Production of citrus juice concentrates. In Z. Berk (Ed.), *Citrus Fruit Processing* (pp. 187-217). Academic Press. https://doi.org/https://doi.org/10.1016/B978-0-12-803133-9.00009-6

Britannica. (2021). Montreal Protocol. Encyclopedia Britannica. In S. Editors of Encyclopaedia (2021 (Ed.).

Celus, I., Brijs, K., & Delcour, J. A. (2007). Enzymatic Hydrolysis of Brewers’ Spent Grain Proteins and Technofunctional Properties of the Resulting Hydrolysates. *Journal of Agricultural and Food Chemistry*, *55*(21), 8703-8710. https://doi.org/10.1021/jf071793c

Chalamaiah, M., Dinesh kumar, B., Hemalatha, R., & Jyothirmayi, T. (2012). Fish protein hydrolysates: Proximate composition, amino acid composition, antioxidant activities and applications: A review. *Food Chemistry*, *135*(4), 3020-3038. https://doi.org/https://doi.org/10.1016/j.foodchem.2012.06.100

Corp, H. E. (1987). Industrial Applications of Freeze Concentration Technology. In.

D. Verdoes, M. N. (2003). Melt Crystallization: Fundamentals, Equipment, Applications (Eds: J. Ulrich, H. Glaade). *Shaker Verlag*.

Damodaran, S., Parkin, K. L., & Fennema, O. R. (2007). *Fennema's food chemistry*. CRC press.

Dennis R Heldman & Daryl B. Lund, M. D. (1992). *Food Freezing, in Handbook of food engineering*.

Dincer, I. (2017). Refrigeration Systems and Applications. https://public.ebookcentral.proquest.com/choice/publicfullrecord.aspx?p=4833757

Dincer I , K. M. (2010). *Refrigeration systems and applications*.

Eikevik, T. M. (2021a). *Compendium master course, Heat pumping processes and systems, TEP 4255, NTNU.*

Eikevik, T. M. (2021b). *Compendium, Thermal and process engineering of food, TEP 4265.*

Flesland, O. Batch freeze Concentration in a suspension crystallizer.

GEA. https://www.gea.com/en/binaries/crystallization-solution-melt-freeze-biochemicals-wastewater-purification-concentration-gea_tcm11-66133.pdf

Gullo, P., Tsamos, K., Hafner, A., Ge, Y., & Tassou, S. (2017). State-of-the-art technologies for transcritical R744 refrigeration systems – A theoretical assessment of energy advantages for European food retail industry. *Energy Procedia*, *123*, 46-53. https://doi.org/10.1016/j.egypro.2017.07.283

Hartel, R. W. (1987). Ice crystallization in suspension crystallizers.

He, S., Franco, C., & Zhang, W. (2013). Functions, applications and production of protein hydrolysates from fish processing co-products (FPCP). *Food Research International*, *50*(1), 289-297. https://doi.org/https://doi.org/10.1016/j.foodres.2012.10.031

Huige, N. J. J. (1972). *Nucleation and growth of ice crystals from water and sugar solutions in continuous sturred tank crystallizers* Technische Hogeschool Eindhoven]. Eindhoven.

Jenkelunas, P. J., & Li-Chan, E. C. Y. (2018). Production and assessment of Pacific hake (Merluccius productus) hydrolysates as cryoprotectants for frozen fish mince. *Food Chemistry*, *239*, 535-543. https://doi.org/https://doi.org/10.1016/j.foodchem.2017.06.148

Kristinsson, H. G., & Rasco, B. A. (2000). Fish Protein Hydrolysates: Production, Biochemical, and Functional Properties. *Critical Reviews in Food Science and Nutrition*, *40*(1), 43-81. https://doi.org/10.1080/10408690091189266

M.A., R. A. D. L. (1988). Theory of Particulate Processes: Analysis and Techniques of Continuous Crystallization. *Academic Press*, *2nd Edition*.

Makhnatch, P. (2019). *New refrigerants for vapour compression refrigeration and heat pump systems : evaluation in a context of the requirements set by the F-gas Regulation and the Paris Agreement goals* (Publication Number 2019:25) [Doctoral thesis, comprehensive summary, Universitetsservice US-AB]. DiVA. http://urn.kb.se/resolve?urn=urn:nbn:se:kth:diva-257530

Miyawaki, O., Liu, L., Shirai, Y., Sakashita, S., & Kagitani, K. (2005). Tubular ice system for scale-up of progressive freeze-concentration. *Journal of Food Engineering*, *69*(1), 107-113. https://doi.org/https://doi.org/10.1016/j.jfoodeng.2004.07.016

Mujumdar, A. S. (2007). Handbook of industrial drying. http://www.crcnetbase.com/isbn/9781574446685

Muller, B. (2020). *Compendium of Computational Heat and Fluid Flow, TEP4165*.

Oord-Knol, L. v. (2000). *Hydraulic wash columns : solid-liquid separation in melt crystallization* Universal Press Science Publishers]. /z-wcorg/. Veenendaal.

Petrova, I., Tolstorebrov, I., & Eikevik, T. M. (2018). Production of fish protein hydrolysates step by step: technological aspects, equipment used, major energy costs and methods of their minimizing. *International Aquatic Research*, *10*(3), 223-241. https://doi.org/10.1007/s40071-018-0207-4

Saeed, M. Z. (2019). *Energy efficient and climate friendly cooling,freezing and heating on board fishing vessels*.

Sarbu, I., & Sebarchievici, C. (2017). Chapter 4 - Thermal Energy Storage. In I. Sarbu & C. Sebarchievici (Eds.), *Solar Heating and Cooling Systems* (pp. 99-138). Academic Press. https://doi.org/https://doi.org/10.1016/B978-0-12-811662-3.00004-9

Sarmadi, B. H., & Ismail, A. (2010). Antioxidative peptides from food proteins: A review. *Peptides*, *31*(10), 1949-1956. https://doi.org/https://doi.org/10.1016/j.peptides.2010.06.020

Scholz, R. (1993). *Layer crystallization as a thermal separation process* Düsseldorf.

Schwamberger, V., Joshi, C., & Schmidt, F. P. (2011). Second law analysis of a novel cycle concept for adsorption heat pumps. Proceedings of the International Sorption Heat Pump Conference ISHPC,

Sherman, P. K. (2022). *Sustainable production of fish protein hydrolysates: Overall system architecture and footprint* Norwegian University of Science and Technology (NTNU)].

Slizyte R, G. L., Storrø I. (2010). *Processing of secondary raw materials from herring to oil and protein hydrolysate*.

Smith, C. S., H.G. (1985). Ice crystal size changes during ripening in freeze concentration. *Biotechnology Progress*, 111-120.

Stene, J. (2021). *Compendium master course, Heat pumps for heating and cooling of buildings, TEP 4260, NTNU.*

Thijssen, H. A. C., S.A.Goldblith, L.Rey & W.W.Rothmayr. (1975). Current developments in the freeze concentration of liquid foods, in Freeze drying and advanced food technology. *Academic Press*, 481-501.

van Beek, T., Budde, M. and van Esch, J. . (2018). Membrane-Freeze Concentration Hybrid for Temperature-Sensitive Biomolecules. Investigation, Application, and Techno-Economic Benefits. *Chemical engineering and technology*, 2385-2392.

Venugopal, V. (2016). Chapter Three - Enzymes from Seafood Processing Waste and Their Applications in Seafood Processing. In S.-K. Kim & F. Toldrá (Eds.), *Advances in Food and Nutrition Research* (Vol. 78, pp. 47-69). Academic Press. https://doi.org/https://doi.org/10.1016/bs.afnr.2016.06.004

Wey. (1970). *Design of batch crystallization experiments for the ice brine system* Clarcson College of Technology].

Widell, K. N., Nordtvedt, T.S., Eikevik, T.M. (2016). *Natural refrigerants in refrigerated sea water systems on fishing vessels* Gustav Lorentzen natural working fluids, Edinburgh.

A. Appendix A

(Crystallizer MATLAB code)

```
clear all; close all; clc;

inuk=1; % Exponent of nucleation
kn=1*10^10; % Coefficient for ice growth
m=1741; % Mass of solution
rho_l=1000; % Density of solution
rho_ice=917.0; % Density of ice
c_pl=4; % Specific heat of solution
c_pis=2.1; % Specific heat of ice
V=m/rho_l; % Total Volume
d=1.5; % Diameter of vessel
s=(pi*d*d)/4; % Cross section of glass vessel
heff=V/s; % Effective height of glass vessel
U=150; % Heat transfer coefficient
Teq=-1; % Equilibrium temperature
h_is=334; % Heat of freezing for water(KJ/kg)
DH=6008; % Heat of freezing for water (KJ/kmole)
Ms=342*10^-3; % Molar mass of dissolved solutes
Mw=18*10^-3; % molar mass of dissolved water
T0=273; % Reference Temperature
Ts=1; % Initial Temperature
R=8.3143; % Gas Constant (J/molK)
ms=0.07*m; % Mass of solutes
ms0=ms; % Initial mass of solutes
mw0=m-ms; % Initial mass of water
ns=mw0/Mw; % No of moles of solute
nw=mw0/Mw; % No of moles of water
ntot=ns+nw; %Total no of moles
xs=ns/ntot; % Molar fraction of solutes
kv=1*10^-6;
T_inf=-22; % Heat exchanger wall temperature
a=1; % Exponent in ice growth
b=1.25; % Exponent in nucleation equation
T_fb_Cb=-0.61; % Initial freezing point
v_ice=0; % Ice velocity
beta=0; % Nucleation intensity


%%-------------------Simulation
sim_time =3600;
dt = 0.0001;
iter =round(sim_time/dt);

u0 = zeros(1,iter);
u1 = zeros(1,iter);
u2 = zeros(1,iter);
u3 = zeros(1,iter);
Tb = zeros(1,iter);
Tf = zeros(1,iter);
de=zeros(1,iter);
w_ice=zeros(1,iter);

%%% Defining the initial conditions
u0(1)=0;
u1(1) =0;
u2(1) =0;
u3(1)=0;
Tf(1) =-0.61;
Tb(1)=4;
```

```
%  Define colors for the plotted lines and reallocate legend
plotStyle = ['b','k','r','g','m','c'];
legendInfo{5} = [];

for A=0.04:0.04:0.2
     i = A/0.04;

Tc=sol(kn,m,rho_l,rho_ice,c_pl,c_pis,V,d,s,heff,A,U,Teq,h_is,DH,Ms,Mw,T0,Ts
,R,ms,ms0,mw0,ns,nw,ntot,xs,kv,T_inf,a,b,T_fb_Cb,Tb,v_ice,beta,dt,iter,u0,u
1,u2,u3,Tf,de,w_ice);
  figure (1)
  plot((1:iter+1)*(dt),Tc*1000);
  hold on

%   Build legend
    legendInfo{i} = ['A = ' num2str(A)];
end
xlabel('time (s)')
ylabel ('de (mm)')
legend(legendInfo)
hold off


function
icecrystallization=sol(kn,m,rho_l,rho_ice,c_pl,c_pis,V,d,s,heff,A,U,Teq,h_i
s,DH,Ms,Mw,T0,Ts,R,ms,ms0,mw0,ns,nw,ntot,xs,kv,T_inf,a,b,T_fb_Cb,Tb,v_ice,b
eta,dt,iter,u0,u1,u2,u3,Tf,de,w_ice)
for(k=1:iter)
    u0(k+1) = u0(k) + dt*(beta*V); %% First Equation
    u1(k+1) = u1(k) + dt*(u0(k)+v_ice);%% Second Equation
    u2(k+1) = u2(k) + dt*(2*u1(k)*v_ice);%% Third Equation
    u3(k+1) = u3(k) + dt*(3*u2(k)*v_ice); %% Fourth Equation

    %%%Fifth Equation
    num_term1 = U*A*(Tb(k)-T_inf);
    denom_term1 =V*(rho_l*c_pl+(rho_ice*c_pis-rho_l*c_pl)*kv*u3(k));
    term1 = num_term1/denom_term1;
    num_term2 =((rho_ice*c_pis-rho_l*c_pl)*kv*Tb(k)-rho_ice*h_is*kv);
    denom_term2 = rho_l*c_pl + (rho_ice*c_pis-rho_l*c_pl)*kv*u3(k);
    term2=num_term2/denom_term2;
    Tb(k+1) = Tb(k) + dt*(-term1-((u3(k+1)-u3(k))/dt)*term2);

    %%%Sixth Equation
    num_term3 = -R*(Tf(k)+273.15)^2;
    denom_term3 = DH;
    term3 =  num_term3/ denom_term3;
    num_term4 = (ms0/Ms)*((rho_ice*kv*V)/Mw);
    denom_term4 = ((ms0/Ms+mw0/Mw)-((rho_ice*kv*V*u3(k))/Mw));
    denom_tem_4=((mw0/Mw)-((rho_ice*kv*V*u3(k))/Mw));
    term4 = num_term4/(denom_term4*denom_tem_4);
    Tf(k+1) = Tf(k) + dt*(term3*term4)*((u3(k+1)-u3(k))/dt);

    if Tb(k)<Tf(k)
    v_ice=kv*(Tf(k)-Tb(k))^a;
    beta=kn*(Tf(k)-Tb(k))^b;
    end

    v_ice_store(k+1) = v_ice;
    de(k+1)=2*(u3(k+1)/u2(k+1));
    w_ice(k+1)=(rho_ice*V*kv*u3(k))/m;
```

```
end
icecrystallization=de;
end

%%% Plotting
figure (1)
subplot(4,4,1);
plot((1:iter+1)*(dt),u0)
xlabel('time (s)')

subplot(4,4,2);
plot((1:iter+1)*(dt),u1)
xlabel('time (s)')

subplot(4,4,3);
plot((1:iter+1)*(dt),u2)
xlabel('time (s)')

subplot(4,4,4);
plot((1:iter+1)*(dt),u3)
xlabel('time (s)')

subplot(4,4,5);
plot((1:iter+1)*(dt),Tf)
xlabel('time (s)')

subplot(4,4,6);
plot((1:iter+1)*(dt),Tb)
xlabel('time (s)')

subplot(4,4,7);
plot((1:iter+1)*(dt),v_ice_store)
xlabel('time (s)')

subplot(4,4,8);
plot((1:iter+1)*(dt),de*1000)
xlabel('time (s)')

subplot(4,4,9);
plot((1:iter+1)*(dt),w_ice)
xlabel('time (s)')


figure (2)
plot((1:iter+1)*(dt),Tf);
xlabel('time (s)')
ylabel ('Tf (C)')

figure (3)
plot((1:iter+1)*(dt),Tb);
xlabel('time (s)')
ylabel ('Tb (C)')

figure (4)
plot((1:iter+1)*(dt),v_ice_store);
xlabel('time (s)')
ylabel ('Vice (m/s)')
```

```
figure (5)
plot((1:iter+1)*(dt),de*1000);
xlabel('time (s)')
ylabel ('de (mm)')

figure (6)
plot((1:iter+1)*(dt),w_ice);
xlabel('time (s)')
ylabel ('Wice (kg/kg)')
```

B. Appendix B

(Dynamic Wash Column MATLAB code)

```
clear all; close all; clc;

v_feed=0.0005;  % Feed flow, m^3/s
Crystal_concentration=0.8;
v_s=v_feed* Crystal_concentration;
g=9.81; % Gravity
m=1781; % Mass of hydrolysates
r=0.5; % Column radius (m)
density=1000;
volume=m/density;
h=volume/(pi*(r)^2)*(1-Crystal_concentration);
h_ice=volume/(pi*(r)^2)*Crystal_concentration;
velocity_from_filter_tube=sqrt(2*g*h);
r_filter_hole=50*10^-6;
A_filter_hole=pi*(r_filter_hole)^2;
v_ml=A_filter_hole*velocity_from_filter_tube;

d=1;       % Column diameter (m)
Ac=pi*(d^2)/4;  % Open cross-sectional area of the wash column, m^2
e=0.20;        % Porosity in the filtration and stagnant section
alpha_1= Crystal_concentration; % Crystal fraction in the feed slurry
latent_heat=333.5; % Latent heat of fusion
Cp=2.1;        % Specific heat of ice
Tmelt=0;
Tfeed=-2;
density_ice=917; % Density of ice
density_Sol=1132; % Density of solution
density_w=1000; % Density of water
Cs=(Cp*(Tmelt-Tfeed)*v_s)/latent_heat;
Cl=(density_ice/density_Sol)*Cs;
ew=e-(1-e)*((Cp*(Tmelt-Tfeed))/latent_heat);
v_water=0.00001; % Water flow, m^3/s
d_filter_tube=0.1;
d_water_inlet_top=0.03;
Ac_filter_tube=pi*(d_filter_tube^2)/4;
A_water_inlet_top=pi*(d_water_inlet_top^2)/4;

%%--------------------Simulation
sim_time =200;
dt = 0.0001;
iter =round(sim_time/dt);

L_conc_solution=zeros(1,iter);
L_filtration = zeros(1,iter);
L_wash=zeros(1,iter);
v_ml_bottom=zeros(1,iter);
v_product=zeros(1,iter);
v_w_flow=zeros(1,iter);
L_ice_slurry=zeros(1,iter);


%%% Defining the intital conditions
L_conc_solution(1)=h;
L_filtration(1)=0;
L_wash(1)=0;
v_ml_bottom(1)=0;
v_product(1)=0;
v_w_flow(1)=0;
L_ice_slurry(1)=h_ice;
```

```
%%-------------------Simulation
for(k=1:iter)
    L_conc_solution(k+1)=L_conc_solution(k)-v_ml/Ac_filter_tube;
    if L_conc_solution(k+1)<0
       L_filtration(k+1)=L_filtration(k);
    else
        L_filtration(k+1)=L_filtration(k)+dt*(v_feed-v_ml-
(L_conc_solution(k+1)-L_conc_solution(k))/dt)/(Ac*(1-e));
    end
        L_ice_slurry(k+1)=L_ice_slurry(k)-v_water/Ac+Cl/Ac;
   if L_ice_slurry(k+1)<0
        L_wash(k+1)= h_ice;
   else
       L_wash(k+1)=L_wash(k)+dt*((v_water-Cl)/(ew*Ac));
   end

      v_ml_bottom(k)=Ac*e*((L_wash(k+1)-L_wash(k))/dt);
      v_product(k)=v_ml_bottom(k)+v_ml;
      v_w=(density_ice/density_w)*v_s-v_water;
      v_w_flow(k)=v_w+v_water;


end

figure (1)
plot((1:iter+1)*(dt),L_filtration);
xlabel('Time (s)')
ylabel ('Length of the filtration section (m) ')

figure (2)
plot((1:iter+1)*(dt),L_wash);
xlabel('Time (s)')
ylabel (' Length of the wash section (m) ')

figure (3)
plot((1:iter)*(dt),v_product*(1132));
xlabel('Time (s)')
ylabel (' mass flowrate of concentrated solution (kg/s) ')
ylim([0 0.3])

figure (4)
plot((1:iter)*(dt),v_w_flow*(1000));
xlabel('Time (s)')
ylabel (' mass flow rate of ice slurry (kg/s) ')
```

C. Appendix C

(Exponential wash column MATLAB code)

```
clear all; clc;
a=0.5; % Porosity
C=0.2; % Percentage of concentration in slurry
L=0;   % Initial length of filtration
%%-------------------Simulation
sim_L =1.4;
dL = 0.0001;
iter =round(sim_L/dL);

%%% Defining the initial conditions
x = zeros(1,iter);
x(1)=0.8;

for(k=1:iter)
x(k+1)=x(k)+dL*C*exp(-a*L);
L=L+dL;
L_save(k+1)=L;
end
figure (1)
plot(L_save,x*100);
xlabel('L (m)')
ylabel ('Ice Concentration (%)')
```

D. Appendix D

(Experimental campaign for hydrolysates production with SINTEF ocean)

Figure D.1 Grinder

Figure D.2 Heat Exchanger

Figure D.3 Tank

Figure D.4 Tricanter

Figure D.5 Rest Raw Material

Figure D.6 Fish Protein Hydrolysates

E. Appendix E

(EES code for refrigeration system)

```
"Evaporation Pressure"
Pe=10
T1s=temperature(R744,x=1,P=Pe)
"Providing superheat"
T1=T1s+5
h1=enthalpy(R744,T=T1,P=Pe)
s1=entropy(R744,T=T1,P=Pe)
s2=s1
"Intermediate pressure"
Pc=35
"Isentropic efficiency"
eff_is=0.75
h2s=enthalpy(R744,s=s2,P=Pc)
h2=((h2s-h1)/eff_is)+h1
h3=enthalpy(R744,x=1,P=Pc)
h4=enthalpy(R744,x=1,P=Pc)
"Temperature from dymola calculations for validation"
T4=2.698
T5=15.57
h5=enthalpy(R744,T=T5,P=Pc)
"Gas Cooler Pressure"
Pg=100
s5=entropy(R744,T=T5,P=Pc)
h6s=enthalpy(R744,s=s5,P=Pg)
h6=((h6s-h5)/eff_is)+h5
"hydrolysates calculation"
T_1_R=90
T_2_R=4
m_h_R=0.12
T_1h_p=50
T_2h_p=70
P_h=1
h_1_R=enthalpy(Water,T=T_1_R,P=P_h)
h_2_R=enthalpy(Water,T=T_2_R,P=P_h)
h_1h_p=enthalpy(Water,T=T_1h_p,P=P_h)
h_2h_p=enthalpy(Water,T=T_2h_p,P=P_h)
 m_h=0.2259
T_1h=70
T_2h=90
h_1h=enthalpy(Water,T=T_1h,P=P_h)
h_2h=enthalpy(Water,T=T_2h,P=P_h)
h11=enthalpy(R744,x=0,P=Pc)
T8=30.22
h8=enthalpy(R744,T=T8,P=Pg)
"Vessel calculation"
h9=h8+h4-h5
h10=h9
h12=h11
Qe=150
"Calculation of mass flow rate from low to intermediate pressure side"
m_R_low=Qe/(h1-h12)
```

```
"Calculation of mass flow rate from intermediate to high pressure side"
m_R_high=(m_R_low*(h3-h11))/(h4-h10)
h7=h6-(m_h*(h_2h-h_1h))/m_R_high
T7=temperature(R744,P=Pg,h=h7)
T_h_20=20
T_h_50=50
h_h_20=enthalpy(Water,T=T_h_20,P=P_h)
h_h_50=enthalpy(Water,T=T_h_50,P=P_h)
m_h_50=(m_R_high*(h7-h8))/(h_h_50-h_h_20)
"Compressor work"
W_Comp_1=m_R_low*(h2-h1)
"Desuperheater capacity"
Q_desuper_heater=m_R_low*(h2-h3)
"Compressor work"
W_Comp_2=m_R_high*(h6-h5)
"COP calculation"
COP=Qe/(W_Comp_1+W_Comp_2)
"Gas cooler capacity"
Qgas_cooler_1=m_R_high*(h6-h7)
Qgas_cooler_2=m_R_high*(h7-h8)
```

F. Appendix F

(Lab scale freeze concentration process)

Figure F.1 Lab scale freeze concentration process (Insulated)

Figure F.2 Filtration section

Figure F.3 Wash Section

Figure F.4 Insulation

Figure F.5 Receiver

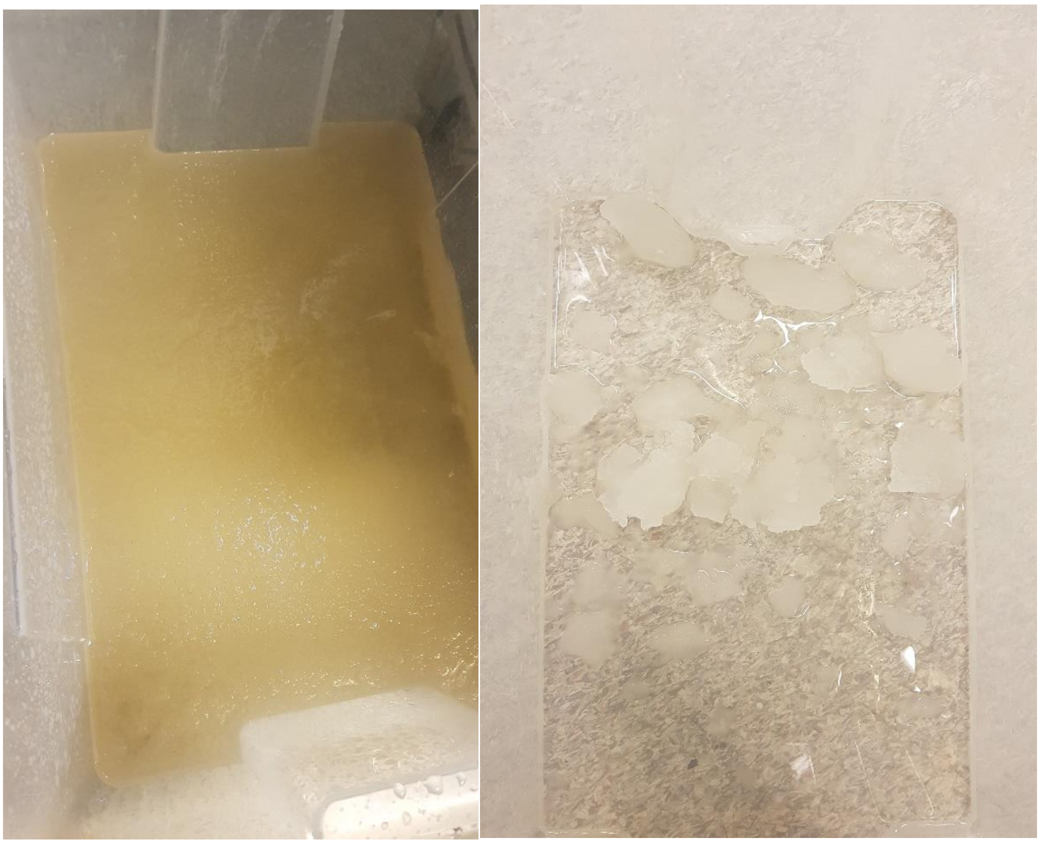

Figure F.6 Washed Ice

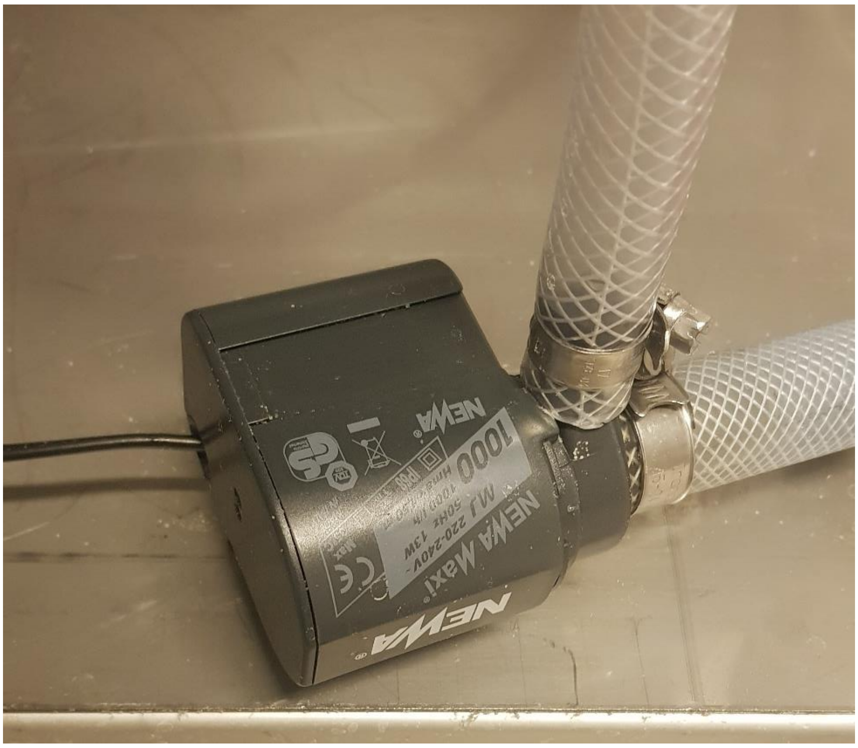

Figure F.7 Pump to transport concentration solution to crystallizer

Figure F.8 Pump to transport slurry to wash column

Figure F.9 Vacuum Pump

G. Appendix G

(Dymola simulation including temperature glides log Ph and Ts diagram)

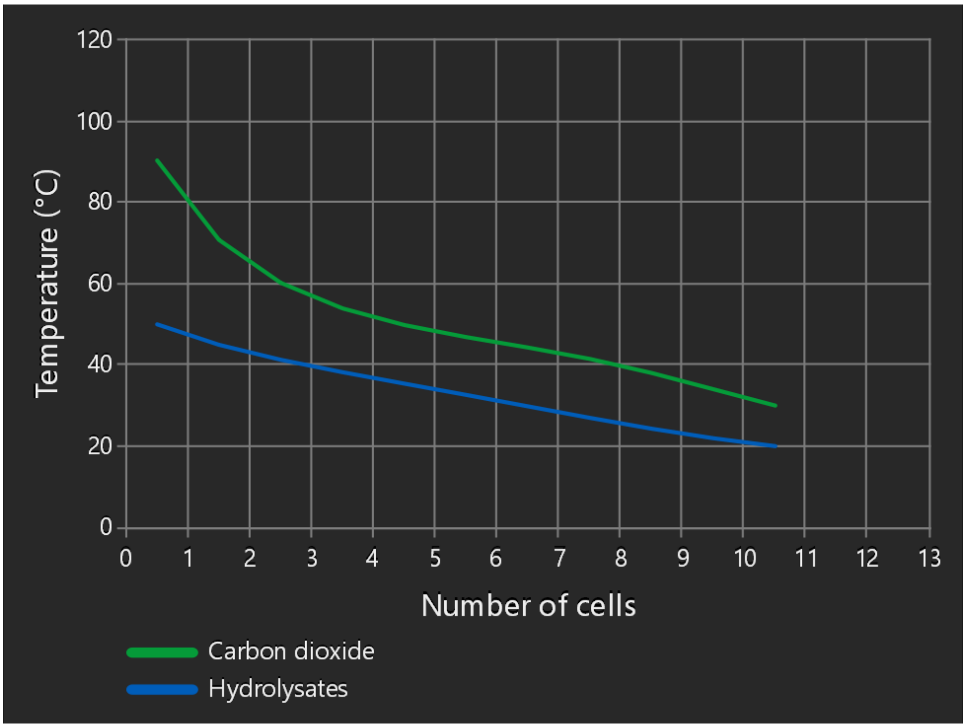

Figure G.1 Temperature glide of 1st gas cooler

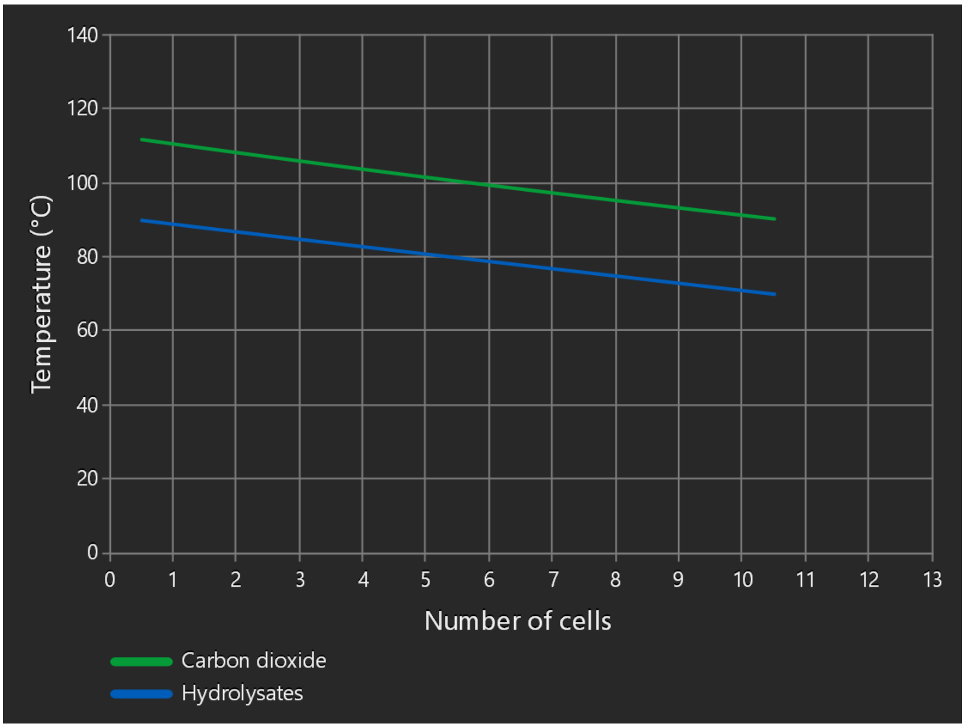

Figure G.2 Temperature glide of 2nd gas cooler

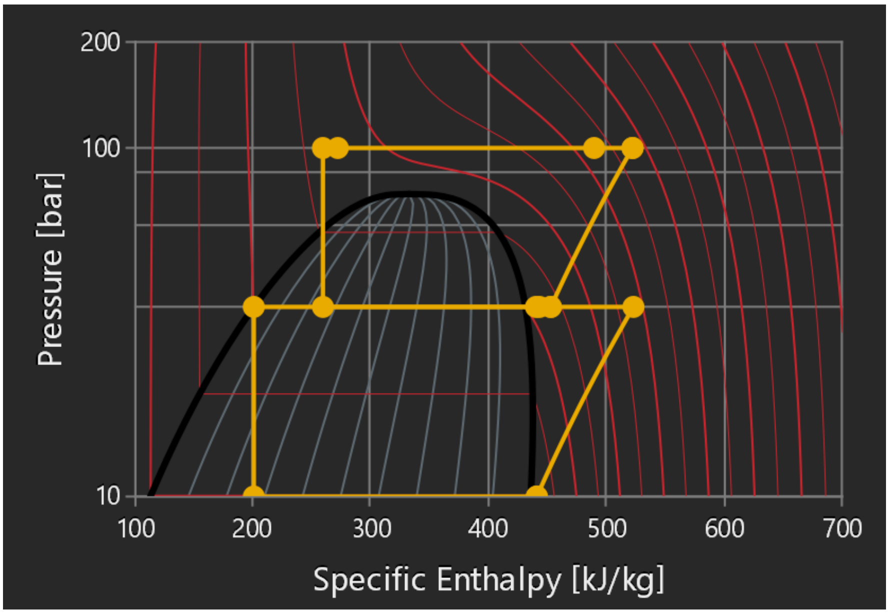

Figure G.3 log Ph diagram for prescribed refrigeration system

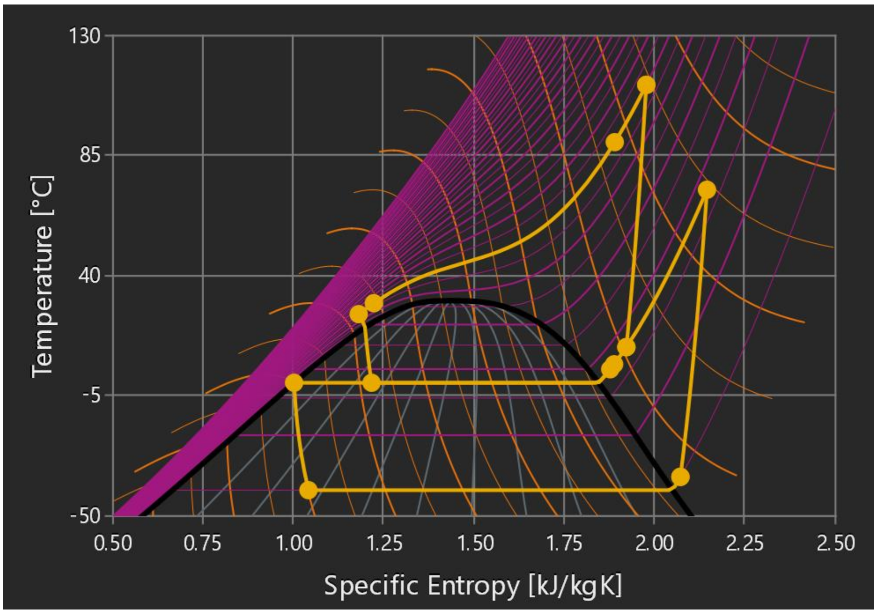

Figure G.4 T-S diagram for prescribed refrigeration system

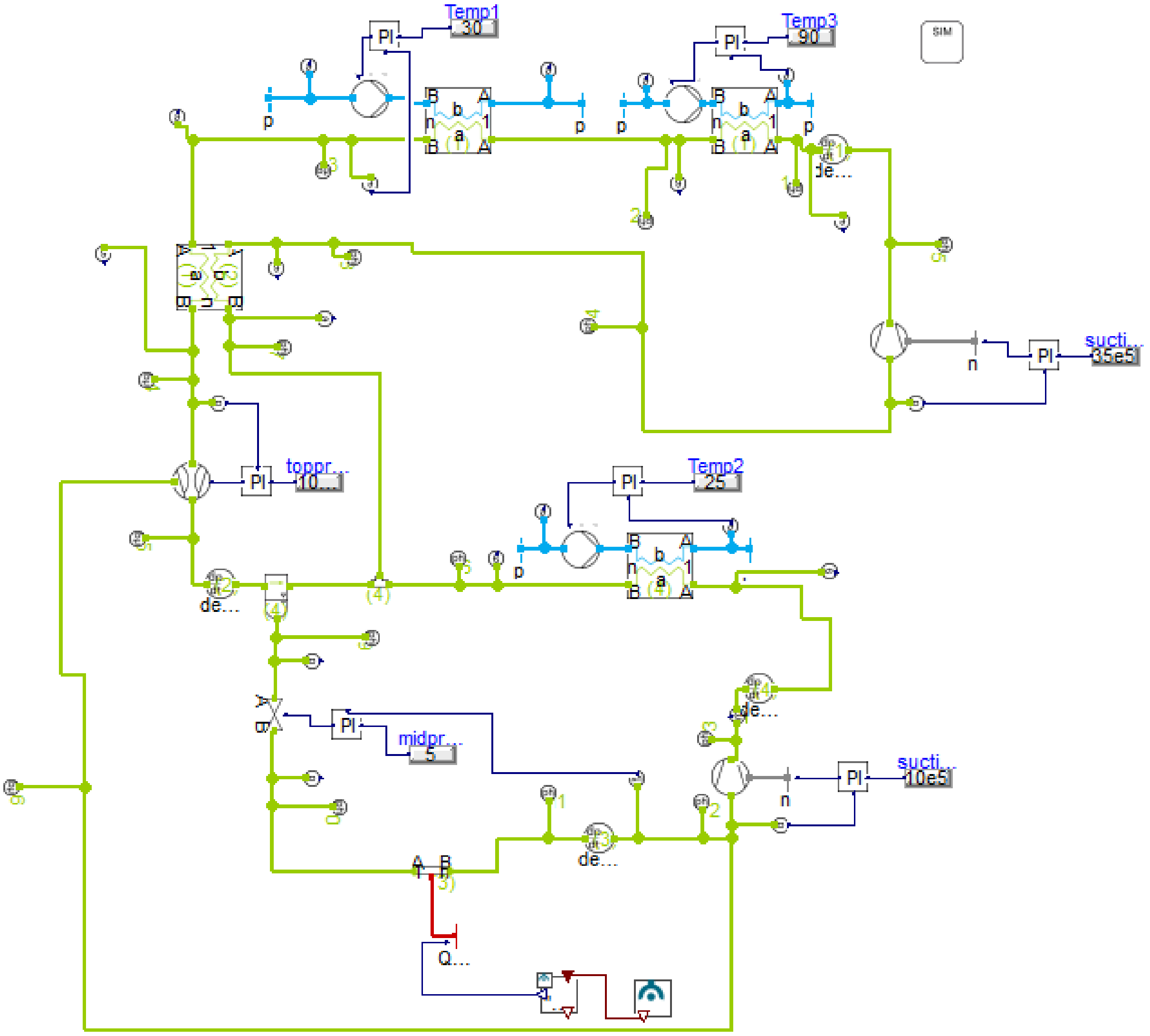

Figure G.5 Dymola simulation with ejector

H. Appendix H

Research Paper

DOI: 10.18462/iir.iccc2022.1131

Modelling of crystallization during freeze-concentration of hydrolysates

Muhammad Umar KHAN[a], Ignat TOLSTOREBROV [a], Kristina N. WIDELL[b], Armin Hafner[a],Tom Ståle NORDTVEDT[b]

[a] Norwegian University of Science and Technology, Department of Energy and Process Engineering
Trondheim, 7491, Norway, ignat.tolstorebrov@ntnu.no
[b] SINTEF Ocean
Trondheim, 7465, Norway kristina.widell@sintef.no

ABSTRACT

Dewatering of fish protein hydrolysates is energy intensive process. The freeze concentration is one of the solutions, which provide high quality of concentrate, energy efficiency and sustainability of the hydrolysate production. This study investigates two important aspects: crystallization of water in fish protein hydrolysates and separation of the ice from the concentrate. The processes were modelled using Modelica tools and MATLAB. The models were validated via experimental campaign and literature review. When the influence of the following factors were taken into account: refrigeration temperature, fluid flow, concentration of solids and ice fraction.

Keywords: fish protein hydrolysates, freeze-concentration, separation, crystallization

1. INTRODUCTION

Fish and marine products are one of the most used protein sources for human consumption. However, a big part of the catch is utilized for production of cheap by-products such as fish meal and oil. At the same time, a growing amount of fishery and, consequently, fishing waste demands efficient solutions for their utilization since they have good nutritional source, which is highly underestimated (Petrova et al., 2018).

Fish protein hydrolysates (FPH) are produced form hydrolysation technique which involves breakdown of proteins and fats present in internal tissues of fish into smaller parts (Damodaran et al., 2007). The reaction usually takes place in a controlled condition, enzymatic hydrolysis and chemical hydrolysis were found to be the widely used hydrolysation techniques. However the enzymatic hydrolysis is more sustainable process. (Slizyte R, 2010).

An improved functional properties was reported by He et al., (2013) and Kristinsson & Rasco., (2000) when comparing the FPH to the origin protein due to breakdown of larger proteins into finer ones. The other important properties like anti-oxidative, anti-hypertensive behaviour of FPH was found to be improved as reported in several studies (Chalamaiah et al., 2012; He et al., 2013; Sarmadi & Ismail, 2010).Jenkelunas & Li-Chan., (2018) investigated and reported that FPH can be used in cryoprotectants application for fish products which are in frozen state.

Liquid FPH is a water mixture of hydrolysed proteins, the original product, which contains up to 95% of moisture. FPH in a liquid form is highly unstable moreover the transportation costs are high due to strict requirements of cold chain. Thus, dried FPH is preferable due to long shelf-life, cheap storage, and transportation. Nevertheless, at the same time, the removal of such a big amount of water from liquid FPH is a difficult and costly task, which is one of the challenges of dried FPH production (Petrova et al., 2018). Conventionally, spray dryers were widely used to remove the moisture content and convert it into final powder state. However, the industrial spray dryers are the major energy consumers of around 4 500 and 11 500 kJ/kg of moisture removed (Mujumdar, 2007).

As an alternative technique, freeze concentration and evaporation methods can be adopted before drying, which reduces the overall energy consumption rate. Freeze concentration technique is a novel method for dewatering of food products. Concentration is to stabilize the quality of food, increase shelf-life and decrease energy costs for further processing. The multistage evaporation of 1 kg of water requires energy less than 2,700 kJ/kg and for freeze concentrators ~ 330 kJ/kg of water as reported in studies by Miyawaki et al., (2005). These dewatering methods can reduce the moisture content significantly down 50-70%. This makes drying methods like freeze drying applicable due to significant decreasing of raw product flow.

The aim of this paper is to design an energy efficient freeze concentration process for fish protein hydrolysates. Dynamic modelling of crystallizer and wash column was carried out in MATLAB while simulation of refrigeration system was carried out in Dymola. Simulations were carried out to study the dynamic profile of solution's bulk temperature, diameter of crystals, ice fraction, propagation of ice, bulk cooling, calculation of freezing capacity and heat recovery.

2. SYSTEM DESIGN

2.1. Hydrolysation process

The hydrolysation process starts with the mincing of rest raw material (RRM), after the mincing process, the minced RRM is pumped to a tank. In the tank the required amount of water and enzymes are added usually 50 % of water and 0.1% of enzymes are added. The tank is heated to 50℃ and this temperature is maintained for 1 hour, which is the ideal temperature for enzymes to breakdown minced RRM to smaller peptides and amino acids. After the hydrolysation process the tank is maintained at 90℃ to terminate all enzyme activities. At the end the filtration process is carried out to separate FPH from ash and slug. The crystallizer forms a slurry of ice and concentrated hydrolysates and with the help of hydraulic wash column ice and concentrated hydrolysates solution is separated.

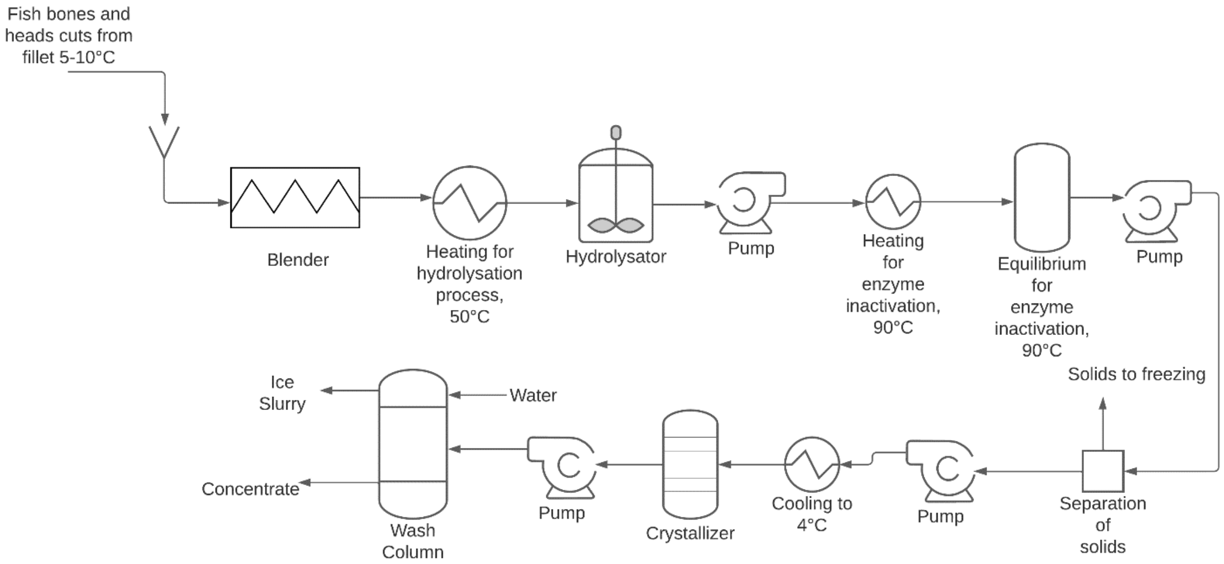

Figure 1 Systematic diagram of complete process

2.2. Simulation software

The following simulation of crystallizer and wash column were carried out in MATLAB R2018a, and refrigeration system simulation was carried out in Dymola. This software contains components and refrigerant libraries from TLK-Thermo GmbH which were used for dynamic simulations. Three libraries were used, TIL 3.90 for components such as compressors, heat exchanger and vales. TIL 3.90 was used for refrigerants and secondary fluid while TIL 3.9.2 to read and input refrigeration load files. Dave is a software from TLK which can be used to plot Dymola results. Ph and Ts diagrams can also be visualized with the help of TLK Dave. The software can read two inputs load formats MATLAB(.mat) and Excel(.csv). The software has a built-in control of different parameters and boundary conditions.

2.3. Model description

To simulate crystallizer, six coupled partial differential equations were solved, and the time discretization of those partial differential equation (PDE's) is given below:

$$\mu_0{}^{n+1} = \mu_0{}^{n} + dt * (B_0 * V) \qquad \text{Eq (1)}$$

$$\mu_1{}^{n+1} = \mu_1{}^{n} + dt * (\mu_0{}^{n} * v_{ice}) \qquad \text{Eq (2)}$$

$$\mu_2{}^{n+1} = \mu_2{}^{n} + dt * (2 * \mu_1{}^{n} * v_{ice}) \qquad \text{Eq (3)}$$

$$\mu_3{}^{n+1} = \mu_3{}^{n} + dt * (3 * \mu_2{}^{n} * v_{ice}) \qquad \text{Eq (4)}$$

$$T_b{}^{n+1} = T_b{}^{n} + dt * (-\frac{U * A * (T_b - T_\infty)}{V * (\rho_l * Cp_l + (\rho_{ice} * Cp_{ice} - \rho_l * Cp_l) * k_v * \mu_3{}^{n})} - \frac{\mu_3{}^{n+1} - \mu_3{}^{n}}{dt} * \frac{((\rho_{ice} * Cp_{ice} - \rho_l * Cp_l) * k_v * T_b - \rho_{ice} * h_{ice} * k_v))}{\rho_l * Cp_l + (\rho_{ice} * Cp_{ice} - \rho_l * Cp_l) * k_v * \mu_3{}^{n}}) \qquad \text{Eq (5)}$$

$$T_f{}^{n+1} = T_f{}^{n} + dt * (\frac{R * T^2}{\Delta_f * H} * \frac{-\frac{m_{s,0}}{M_s} * \frac{\rho_{ice} * k_v * V}{M_w}}{\left(\frac{m_{s,0}}{M_s} + \frac{m_{w,0}}{M_w} - \frac{\rho_{ice} * k_v * V * \mu_3{}^{n}}{M_w}\right) * \left(\frac{m_{w,0}}{M_w} - \frac{\rho_{ice} * k_v * V * \mu_3{}^{n}}{M_w}\right)} * \frac{\mu_3{}^{n+1} - \mu_3{}^{n}}{dt}) \qquad \text{Eq (6)}$$

$$v_{ice} = k_v * \left(T_f{}^{n} - T_b{}^{n}\right)^a \qquad \text{Eq (7)}$$

$$B_0 = k_n * \left(T_f{}^{n} - T_b{}^{n}\right)^b \qquad \text{Eq (8)}$$

The first four moments (Eq (1)-Eq (4)) which are used in this study, describes total number crystals, total length of crystals, total area, and total volume of crystallized material. Density multiplied by the third moment gives the total mass of crystalized material per volume of the suspension. The initial conditions are the moments of the size distribution of the seeds, the initial bulk temperature (4°C), and the initial freezing point (-0.61°C). It is assumed that the seeds are of size zero which means that the moments μ_0, μ_1, μ_2 and μ_3= 0. The total mass of hydrolysates in crystallizer were 1741 kg with 7% solids. Fish protein hydrolysates comprise of 93% of water,6.3% of protein, 0.35% of fat and 0.35% of ash, the estimation of solution was carried out to predict the properties of FPH and will be validated by experiments.

All these six equations were solved simultaneously in one time step. The simulation was run for 3600 seconds with a time step of 0.0001 seconds. The constant values used in calculation are given in nomenclature.

K_n, K_v, a and b are coefficients that are generally determined experimentally. For now, these parameters were taken from literature. Similarly, it goes of molar weight of protein but for this project molar weight of sucrose was used.

Two different approaches were used to calculate the filtration length of the wash column and the simulation to find the length was carried out in MATLAB. The time discretization of those partial differential equation (PDE's) is given below:

$$L_f^{n+1} = L_f^{n} + dt * (\frac{\emptyset_{feed} - \emptyset_s}{A_c * (1 - \varepsilon)}) \qquad \text{Eq (9)}$$

$$L_f^{n+1} = L_f^{n} + dt * (\frac{\emptyset_{feed} - \emptyset_s}{A_c * (1 - \varepsilon)}) \qquad \text{Eq (10)}$$

$$X^{n+1} = X^{n} + dl * C * e^{-a*L} \qquad \text{Eq (11)}$$

$$L_w^{n+1} = L_w^{n} + dt * (\frac{\emptyset_{w,l} - C_l}{\varepsilon_w * A_c}) \qquad \text{Eq (12)}$$

$$\emptyset_{ml,bottom} = A_c * \varepsilon * (\frac{L_w^{n+1} - L_w^{n}}{dt}) \qquad \text{Eq (13)}$$

The refrigeration system was simulated using Dymola software with some simplifications. A simple sub critical CO_2 system was developed, with the addition of desuperheater and subcooler to increase the COP of the refrigeration system. Plate heat exchangers (heat exchanger type in Dymola) were used for condenser, desuperheater and subcooler while tube and tube heat exchanger (heat exchanger type in Dymola) were used for evaporator.

Five PI controllers were used to control the refrigeration system, the first PI controller was used to control the opening of throttling valve which senses the condenser pressure which was fixed 50 bar while the other PI controller controls the frequency of efficient compressor (compressor type in Dymola) to maintain the required suction pressure of 10 bar. Outlet temperature from the desuperheater is controlled by the mass flow of pump with PI controller, which takes outlet temperature of desuperheater as input. Inlet and outlet temperature of desuperheater is fixed to 0℃ and 25℃ respectively. The outlet temperature of condenser is controlled by adjusting the water flow in condenser with PI controller such as the refrigerant condenses completely. To remove the condenser heat, ice, and water slurry at 0℃ is used. To increase the COP of system a subcooler was used and the outlet temperature of subcooler is controlled by adjusting the water flow to subcooler with PI controller such that the refrigerant is cooled down to 5℃.

To increase the COP of the system flooded evaporator was used and to ensure no liquid enters compressor a phase separator was included. Isentropic efficiency of compressor is fixed to 70%. Dymola doesn't contain any crystallizer library so to visualize this heat exchanger named as "evaporator" was used which cooled down hydrolysates. Due to limitation of Dymola water was used instead of hydrolysates and ice slurry.

3. RESULTS AND DISCUSSION

Based on refrigeration load subcooler, condenser and desuperheater capacities were 15.35 kW,101.65 kW and 68.5 kW respectively. After wash column the ice is washed by water which forms an ice water slurry at 0℃, the slurry was pumped through sub-cooler and condenser and the mass flow rate of this slurry was controlled by the capacity of subcooler and condenser. The requirement to melt the ice from the slurry was 111.2 kW which was covered by subcooler and condenser.

The COP was calculated by evaporation load and a constant evaporation load was maintained during the simulation by PI controller which resulted in constant COP of 2.16. There are couple of reasons why the COP of the refrigeration system is low. Single compression was used to achieve a 55-K temperature difference which increased the discharge gas temperature of CO_2 and increased the compressor work. Secondly the condenser temperature is close to critical temperature which reduces the evaporation capacity drastically.

Figure 2 shows the dynamic profile of bulk temperature. Initially the hydrolysates were at 4℃. The temperature goes down to -1.4℃ without any crystallization of water which is known as subcooling process. Point a to b shows subcooling process. Point b is known as seeding point where crystallization starts, and latent heat of fusion is released which increases the temperature till initial freezing point (-0.61 ℃). From b the freezing process starts and because of dissolved solutes in water the freezing point decreases and water crystallizes which is opposite to pure liquid freezes. The bulk temperature decreases till wall temperature of heat exchanger. The equilibrium was not achieved till 3600 seconds because of small surface area of heat exchanger.

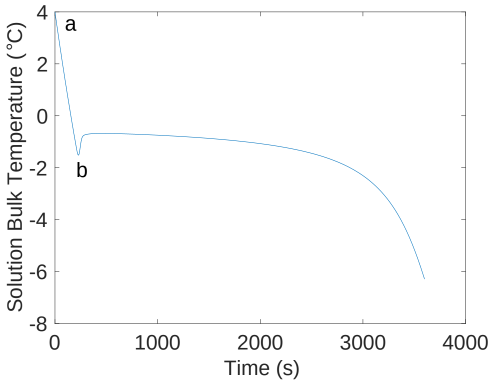

Figure 2 Bulk Temperature Vs Time

Figure 3 shows the depression of freezing point of liquid hydrolysates with respect to time. At time zero the freezing point of hydrolysates is -0.61℃ this is the initial freezing point found out experimentally using differential scanning calorimetry (DSC). With progression of time water freezes out which increases the concentration of solutes which further decreases the freezing point of hydrolysates. At the end of simulation, the concentration of solid increased till 36% which resulted in -6.3℃ freezing point depression.

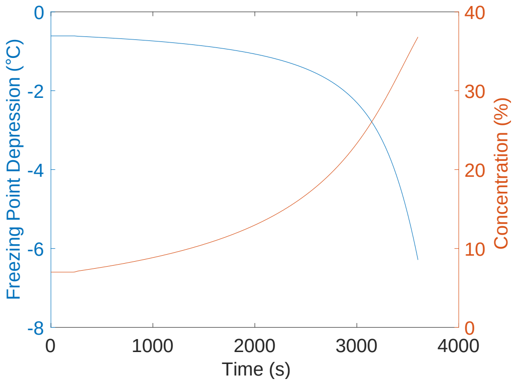

Figure 3 Concentration and Freezing point depression Vs Time

The propagation of ice in the solution is shown in ***Figure 4***. The seeding time was recorded as 230 seconds meaning that it takes above mentioned time to start the propagation of ice in water. The nucleation of ice starts at 230 seconds which gives the maximum speed of 0.9*10^{-6} m/s. Temperature difference between freezing depression point and bulk temperature is the driving force for the propagation of ice as expressed by Eq (7). Maximum subcooling is achieved during the nucleation which results in maximum propagation of ice after that the subcooling drops to zeros which decreases the propagation of ice. At the end of simulation, the propagation speed was found out 1.182*10^{-9} m/s which is approaching zero.

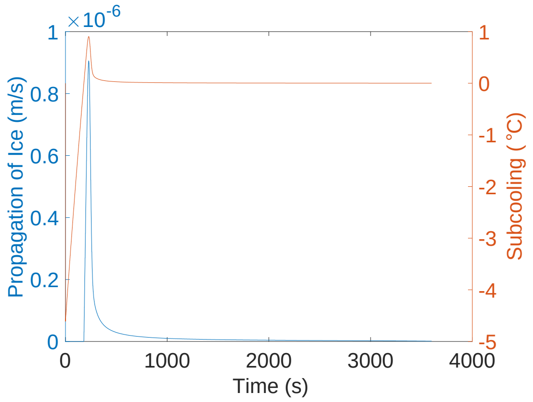

Figure 4 Propagation of Ice and Subcooling Vs Time

The simulation can be used to calculate the appropriate crystal size for subsequent washing in wash column. At nucleation the effective diameter of crystals was 0.067 mm while at the end of simulation the mean crystal diameter was found out 0.045mm. This happens because initially the number of crystals is less which results in bigger diameter as temperature drops the number of crystals increases which results in small and fine crystal diameter as shown in ***Figure 5***.

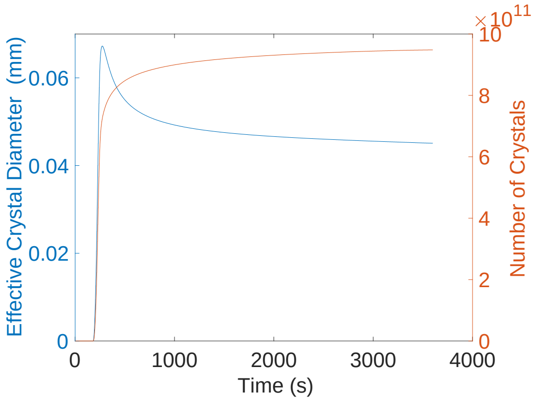

Figure 5 Effective Crystal diameter and Number of crystals Vs Time

The below graph (***Figure 6***) shows the increase of ice fraction in solution with respect to time. At the end of simulation, it was found out that 86.9 % of water turned into ice. Based on simulation results 36% of concentration was achieved. According to GEA if the viscosity of the concentrated solution increases from 30–50 mm^{2}s^{-1} for smooth operation it is recommended to have multiple stage step crystallizer(van Beek, 2018).

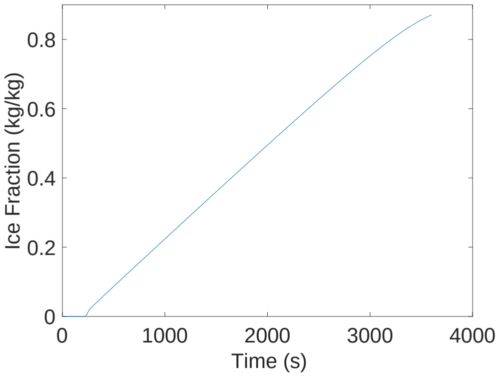

Figure 6 Ice Fraction Vs Time

The dynamic model was developed to calculate the length of filtration and wash section. Inputs such as ice fraction and feed mass flow rate were obtained from crystallizer simulation Two different approaches were used to calculate the filtration length. The first one uses exponential estimation to calculate filtration length and simulation ends with ice fraction reaches 100%. While the other simulation shows how the fluid flows and separate by passing through filters. The second one is more accurate as in includes the volume flow rate of slurry and the diameter of wash column. The first simulation results in 1.4 m of filtration length while the second simulation gives 1.3 m. These are the minimum lengths needed to separate concentrate solution from ice, the volume flow rate and wash liquid is controlled with the help of pump. Below graph (***Figure 7***) shows the simulation result.

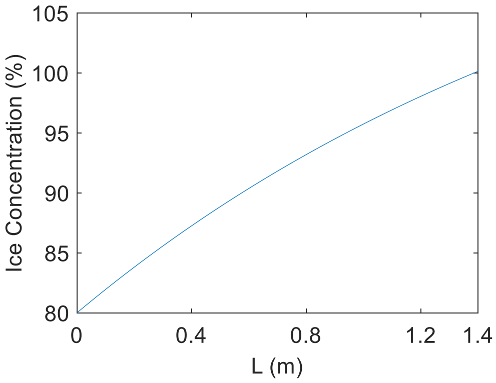

Figure 7 Ice Concentration Vs Filtration Length

After filtration ice separates from concentrated solution to wash the ice, minimum length was required by wash liquid to easily pick ice from wash column without entering filtration length was 1.1m. The total length of wash column is the sum of filtration and wash section length based on the simulation carried out the total length was calculated as 2.4 to 2.5 m. Mass flow rate of concentrated solution and ice slurry was calculated. The mass flowrate of concentrated solution can be used to calculate the energy consumption of further drying process while the mass flow rate of ice slurry was used to calculate the energy needed to melt ice. Mass flow rate of concentrated solution and ice slurry were 0.1457 kg/s and 0.3668 kg/s respectively. The mass flowrate of ice in ice slurry was 0.3328 kg/s and 111.2 kW is the required energy to melt ice. The mass flowrate of ice was calculated by subtracting the makeup water for the creation of slurry.

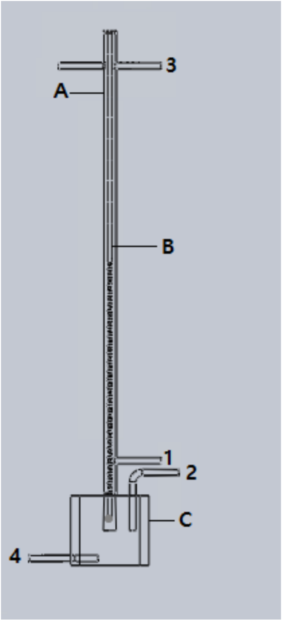

Figure 8 Front View of designed Wash column

Wash columns contains three parts named as tower(A), filter tube (B) and tank (C) as shown in ***Figure 8***. Slurry enters the wash column from (1) it fills the wash column till top, due to density differences the ice floats at top while concentrated solution settles down. Filter tube contains pores of 150µm with the help of vacuum pump attached at (2) all concentrated solution is sucked in and collected in tank. Another pump attached at (4) pumps all the concentrated solution for further drying while water enters from (3) and washes all wash column for next batch.

4. CONCLUSION

In this paper a freeze concentration process was analysed with CO_2 as a refrigerant. MATLAB and Dymola software were used to carry out dynamic simulations. Refrigeration system was designed with a maximum capacity of 127 kW, the heat recovery based on subcooler, condenser and desuperheater were 15.35 kW,101.65 kW and 68.5 kW respectively. The heat capacity of condenser and subcooler were enough to melt the ice from ice slurry and desuperheater was able to heat the recovered water up to 25℃ and the COP of the refrigeration system was 2.16.

Height and diameter for crystallizer was estimated as 2.5 m and 1m respectively. Euler time discretization was used to solve 6 coupled equations. At the end of simulation bulk temperature, depression of freezing point, mean diameter of crystals, ice fraction and propagation of ice came out as -6.2℃, -6.3℃, 0.045mm, 0.869 and $1.182*10^{-9}$ m/s respectively. Large U, heat exchanger area and lower wall temperature drastically reduced time for crystallization process. Maximum concentration of 36 percent was achieved, for smooth operation it is recommended to have multiple stage step crystallizer.

The two methods were developed to estimate the filtration length of wash column. Filtration length from exponential and dynamic simulations were 1.4m and 1.3m respectively. Dynamic wash column simulation was also used to calculate the wash section length, mass flow rate of concentrated solution and ice slurry. Wash section length, mass flow rate of concentrated solution and ice slurry were estimated as 1.1 m, 0.1457 kg/s and 0.3668 kg/s respectively.

ACKNOWLEDGEMENTS

The authors gratefully acknowledge the Research Council of Norway and industrial project partners for the financial support for carrying out the present research [NFR project No. 294662, CoolFish].

NOMENCLATURE

T_b	Bulk temperature (K or°C)	v_{ice}	Ice velocity (linear ice growth rate) (m/s)
T_{fp}	Freezing point of solution (K or°C)	B^o	Nucleation intensity (numbers/s*volume)
a	Exponent in ice growth equation (1)	b	Exponent in nucleation equation (1.25)
k_n	Nucleation constant ($1*10^{10}$)	k_v	Volume form factor ($1*10^{-6}$)
Cp	Specific heat capacity (kJ/kg.K)	U	Total heat transfer coefficient (W/m^{2}k)
M	Molar weight (kg/mole)	$Ø_{feed}$	Feed flow (0.0005 m^3/s)
L_f	Filtration Length (m)	Øs	Crystal flow (m^3/s)
A_c	Cross sectional area (m^2)	ε	Porosity in the filtration and stagnant section (0.2)
L_w	Wash section length (m)	ε_w	Porosity in the wash section
$Ø_{ml,bottom}$	Mother liquor flow (m^3/s)	α	Crystal fraction in feed (0.8)

REFERENCES

Chalamaiah, M., Dinesh kumar, B., Hemalatha, R., & Jyothirmayi, T. (2012). Fish protein hydrolysates: Proximate composition, amino acid composition, antioxidant activities and applications: A review. *Food Chemistry*, *135*(4), 3020-3038. https://doi.org/https://doi.org/10.1016/j.foodchem.2012.06.100

Damodaran, S., Parkin, K. L., & Fennema, O. R. (2007). *Fennema's food chemistry*. CRC press.

He, S., Franco, C., & Zhang, W. (2013). Functions, applications and production of protein hydrolysates from fish processing co-products (FPCP). *Food Research International*, *50*(1), 289-297. https://doi.org/https://doi.org/10.1016/j.foodres.2012.10.031

Jenkelunas, P. J., & Li-Chan, E. C. Y. (2018). Production and assessment of Pacific hake (Merluccius productus) hydrolysates as cryoprotectants for frozen fish mince. *Food Chemistry*, *239*, 535-543. https://doi.org/https://doi.org/10.1016/j.foodchem.2017.06.148

Kristinsson, H. G., & Rasco, B. A. (2000). Fish Protein Hydrolysates: Production, Biochemical, and Functional Properties. *Critical Reviews in Food Science and Nutrition*, *40*(1), 43-81. https://doi.org/10.1080/10408690091189266

Miyawaki, O., Liu, L., Shirai, Y., Sakashita, S., & Kagitani, K. (2005). Tubular ice system for scale-up of progressive freeze-concentration. *Journal of Food Engineering*, *69*(1), 107-113. https://doi.org/https://doi.org/10.1016/j.jfoodeng.2004.07.016

Mujumdar, A. S. (2007). Handbook of industrial drying. http://www.crcnetbase.com/isbn/9781574446685

Petrova, I., Tolstorebrov, I., & Eikevik, T. M. (2018). Production of fish protein hydrolysates step by step: technological aspects, equipment used, major energy costs and methods of their minimizing. *International Aquatic Research*, *10*(3), 223-241. https://doi.org/10.1007/s40071-018-0207-4

Sarmadi, B. H., & Ismail, A. (2010). Antioxidative peptides from food proteins: A review. *Peptides*, *31*(10), 1949-1956. https://doi.org/https://doi.org/10.1016/j.peptides.2010.06.020

Slizyte R, G. L., Storrø I. (2010). *Processing of secondary raw materials from herring to oil and protein hydrolysate*.

van Beek, T., Budde, M. and van Esch, J. . (2018). Membrane-Freeze Concentration Hybrid for Temperature-Sensitive Biomolecules. Investigation, Application, and Techno-Economic Benefits. *Chemical engineering and technology*, 2385-2392.